The Institute of Paper Chemistry

Appleton, Wisconsin

Doctor's Dissertation

Adsorption Kinetics in the Polyethylenimine-Cellulose Fiber System

W. A. Kindler, Jr.

January, 1971

ADSORPTION KINETICS IN THE POLYETHYLENIMINE-CELLULOSE FIBER SYSTEM

A thesis submitted by

W. A. Kindler, Jr.

B.A. 1965, Western Washington State College
M.S. 1967, Lawrence University

in partial fulfillment of the requirements
of The Institute of Paper Chemistry
for the degree of Doctor of Philosophy
from Lawrence University,
Appleton, Wisconsin

January, 1971

TABLE OF CONTENTS

SUMMARY

The rate of adsorption of polyethylenimine (PEI) onto regenerated cellulose fibers can be described as a mass-transport process. The application of simple mass-transfer theory led to the conclusion that diffusion into the internal porous structure of the fiber represents the predominant barrier to rapid adsorption. Under suitable conditions, mass transfer as a result of electrostatic interactions between polymer and fiber may play a role in determining the sorption rate. Adsorption rate curves were measured as a function of polymer molecular weight, initial polymer concentration, ionic strength, and pH.

A rate equation based on diffusion control with Langmuirian adsorption in stirred solution was developed. The equation predicted that the initial rate should depend linearly on initial polymer concentration and on the adsorbate diffusion coefficient to the 0.66 power. This equation served to aid in the design and interpretation of experiments.

Fractionated PEI was sorbed onto regenerated cellulose fibers from aqueous solution. This system was chosen to facilitate characterization and control of variables. The polymer was fractionated by means of gel permeation chromatography to limit the effects of polymolecularity.

Equilibrium adsorption measurements showed that, over a molecular weight range of from 8,000 to 20,000, the smaller molecules were sorbed to a greater extent than the larger ones. For all molecular weight fractions studied, a maximum in retention was observed at pH 10.9. It was shown that the pH dependence is due primarily to an ion-exchange reaction involving ionized hydroxyls on the fibers. Differences in polymer size greatly affected accessibility to reactive sites.

The diffusion coefficient was found to decrease with increasing ionic strength, pH, and molecular weight. The sensitivity to pH and salt concentration can be explained by means of an electrophoretic effect.

Adsorption equilibrium was achieved after six to eight hours for most cases. The initial rate was found to increase with initial polymer concentration and to decrease with ~~increasing~~ decreasing pH, ionic strength, and molecular weight. With some exceptions, the magnitude of these effects is in accord with simple mass-transfer theory. The deviations from theory are shown to be a result of electrostatic interactions between the fiber and the polymer. The electrostatic interactions are reflected, in general, by an accelerated initial rate and a retarded approach to equilibrium as compared with simple diffusion alone.

An effective diffusional film thickness was defined as the distance over which the polymer must diffuse to produce the observed rate. This quantity was calculated from the rate data and found to be on the order of four centimeters. This physically impossible magnitude was interpreted as an indication of the presence of a physical barrier to mass transfer. It was concluded that this barrier is a result of the necessity of the polymer to penetrate the porous structure of the fiber.

Electron micrographs of fiber cross sections treated with PEI and copper acetate indicate that the polymer causes changes in the appearance of microtomed sections of the fiber wall. This observation may be related to an effect of internally sorbed polymer on the response of the cellulosic material to the microtoming procedure.

INTRODUCTION

The adsorption of polymers at solid-liquid interfaces is a phenomenon which has generated considerable interest both academically and industrially over the past several years. To the molecular biologist, polymer adsorption concepts are pertinent to such poorly understood phenomena as enzyme activity and colloidal stability. Adsorption characteristics have been put to practical use in the laboratory as a means of fractionating polymer samples with respect to molecular weight. The rubber industry relies heavily on the use of carbon black as an adsorbent for high polymers. The effects of adsorbed polymer on colloidal stability play a major role in the operation of municipal and industrial waste-treatment systems as well as in the handling of various pigments.

The adsorption of high polymers onto cellulose surfaces has long provided the papermaker with a means of extending the useful range of his product. Suitable polymers can be employed to enhance the wet and dry strength of the product, to provide for more rapid machine speeds through accelerated drainage rates, and to increase the amount of retained fines, pigments, and other additives. A large and growing fraction of these polymers contain cationic groups which significantly affect their behavior in aqueous systems.

Our current knowledge of retention behavior is particularly weak in the area of adsorption kinetics. Since many applications involve very short contact times, it is likely that true equilibrium is never attained. In addition, kinetic data may provide valuable information relating to the overall adsorption process. For these reasons it is felt that a study of the adsorption kinetics would contribute greatly to the general understanding of the behavior of polyelectrolyte-cellulose systems. It is to this goal that this thesis is devoted. Although this study deals with a cellulose system, the concepts to be developed are important to many other sorption systems.

LITERATURE REVIEW

The extensive literature pertaining to experimental and theoretical investigations of polymer adsorption has been reviewed by Hughes and von Frankenburg (1), Silberberg (2), and Patat, Killman, and Schliebener (3). Discussions of the literature pertaining to the adsorption of polymers by cellulose are given in monograph form (4) and by Swanson (5). Due to the availability of these reviews, no attempt will be made to present a comprehensive review of the literature. A brief summary of these reviews will be included, however, to acquaint the reader with some of the general features of polymer adsorption. In addition, there are several papers which present concepts essential to the analysis of the thesis topic and warrant brief discussion.

Nearly any statement concerning the behavior of polymer adsorption may be contradicted by results obtained with some specific system. The following facts appear to be fairly general for most systems.

The amount of polymer adsorbed per unit surface area increases with the concentration of polymer in solution up to some saturation value at which point the curve levels off. In most cases, this equilibrium sorption curve can be empirically described by the Langmuir isotherm equation.

Only a fraction of the segments of the sorbed chain are in direct contact with the surface. Remaining sequences of segments are looped into the solution phase. The actual configuration of the adsorbed chain is difficult to determine experimentally and depends on the particular adsorbate-solvent-adsorbent system. Recent work indicates that the configuration of the sorbed polymer is closely related to the configuration of the polymer in solution.

The amount of polymer adsorbed at equilibrium is usually only slightly dependent on temperature. Depending on the system, the temperature coefficient can be either negative or positive. The amount adsorbed is very sensitive to solvent power; less polymer is adsorbed out of a good solvent than a poor one. The observations with respect to temperature and solvent power indicate that the sorption energies are quite low, usually in the range of Van der Waals interactions. Ionic bonds appear to play a major role in the specific cases of the adsorption of a cationic polyelectrolyte onto cellulose.

Although low-energy bonding is involved, most systems exhibit an apparent irreversibility with respect to solution concentration. Even washing with pure solvent will often remove only a small fraction of adsorbed polymer. It has been shown (2) that this problem is only a practical one and does not imply that adsorption cannot be treated by equilibrium thermodynamics.

On the basis of previous work (6-9) the following generalization can be made about the kinetics of polymer adsorption. A fairly rapid initial rise in adsorption is followed by a slow asymptotic approach to equilibrium. Most systems reach equilibrium after several hours but in some cases the time required is as short as fifteen minutes or as long as thirty hours.

Claesson and Claesson (6) studied the adsorption of nitrocellulose onto active carbon out of acetone in one of the earliest polymer adsorption investigations. It was found that the amount adsorbed and the rate of adsorption increased as the molecular weight decreased. The same results were reported by Hobden and Jellinek (7) for the system polystyrene-butanone-charcoal. Binford and Gessler (8) measured the rate of adsorption of polyisobutylene onto carbon black out of a number of organic solvents. Equilibrium was attained in several hours except for the highest molecular weight (325,000) which required twenty-four hours. Similar results were

obtained for polyacrylamide sorbed onto calcium phosphate by Jankovics (9). The effect of molecular weight is generally interpreted in terms of a diffusion-controlled adsorption process. The more slowly diffusing high molecular weight species require more time to arrive at the reaction sites than do the smaller, more mobile molecules.

One of the most direct illustrations of the importance of diffusion to polymer adsorption is given in the works of Emery (10) and Farrar (11). These authors verified the existence of a time-dependent partitioning with respect to molecular weight between the polymer in solution and that on the surface for the polystyrene-dichloroethane-carbon black system. This could be interpreted as being due to the early adsorption of the more rapidly diffusing low molecular weight species followed by later displacement by the larger macromolecules. Evidence of this phenomenon occurring in the polyethylenimine-cellulose fiber system has been given (12).

If the rate of adsorption on the external substrate surface is diffusion-controlled, the adsorption rate would be expected to increase with the degree of agitation. This has been observed experimentally by Jankovics (9), Russo and Thode (13), and by Becher, et al. (14).

The relationship between temperature and rate should provide additional information relating to the mechanism of the rate-controlling step. An apparent activation energy for the reaction can be calculated from the temperature-dependence of the initial rate. For a diffusion-controlled process this value should be in reasonable agreement with the apparent activation energy for a physical process which is of the order of five kilocalories per mole or less. Thode, et al. (15) determined an activation energy of 5600 calories per mole for the adsorption of melamine-formaldehyde resin on sulfite pulp fibers. For the sorption of partially methylated locust bean gum, Russo and Thode (13) measured an activation energy of 4400 calories per mole. A similar investigation of the adsorption of a cationic urea-formaldehyde resin by

Kurath, et al. (16) resulted in an activation energy of 5200 calories per mole. These values are all compatible with the concept of a diffusion-controlled reaction.

The porous nature of many substrates indicates that surface structure may also be an important consideration in diffusion-controlled reactions. The observation of increasing equilibrium adsorption with decreasing molecular weight is consistent with the adsorption of solute in pores. The larger macromolecules would be excluded from some areas accessible to the smaller polymer molecules. Theoretical analyses for nonporous substrates predict that the adsorption of higher molecular weight polymers is thermodynamically preferred over the smaller molecules (17-19). This has been verified experimentally for a number of systems (3).

Howard and McConnell (20) provide substantiating evidence for the importance of diffusion into pores in a study of the adsorption of polyethers onto silica, porous and nonporous carbon black, and nylon powder. In all cases the rate increased with decreasing molecular weight. Little molecular weight-dependence was observed for the equilibrium adsorption onto porous charcoal but the sorption increased significantly with molecular weight on nonporous charcoal. Sorption onto powdered nylon was found to decrease with increasing molecular weight up to an intermediate molecular weight and then subsequently increased with polymer size. The molecular weight at which this change in behavior occurred might be associated with the limiting molecular size excluded from the porous structure.

The accessibility of the internal porous structure of cellulose to high polymers has been observed directly and indirectly by a number of different methods. Thode, et al. (15) found that the sorption rate of melamine-formaldehyde resin onto fines-free sulfite pulp increased with the degree of beating. On the basis of a small amount of data, it was observed that the increase in rate was more closely related to swollen volume rather than to the increase of specific surface area. Russo and

Thode (13) on the other hand, found a linear relationship between the hydrodynamic surface area of bleached sulfite pulp and the initial rate of adsorption of a partially methylated locust bean gum. Allen, et al. (21) claim that the penetration of polyethylenimine into the porous structure of cellulose is responsible for the apparent irreversibility of adsorption.

Stone, et al. (22) measured the accessibility of regenerated cellulose to various sized dextran molecules by a solute exclusion technique. A sample of the cellulose is mixed with a dextran solution of known concentration. The change in the bulk phase concentration of the solute is attributed to dilution by accessible water within the cellulose structure. For textile rayon the authors found a maximum pore size of 100 A. and a median pore size of about 25 A. It was estimated that the fibers contained 1.2 ml. of water per gram of cellulose.

Becher, et al. (14) measured the penetration of melamine formaldehyde into the cell wall of bleached sulfite fibers by a dye-tracing technique. At addition levels of less than 5% the resin appeared to be uniformly distributed on the fiber surface with little penetration into the wall. However, the sensitivity of the test may not have been sufficient to detect small amounts of resin in the internal structure. At higher addition levels the resin was observed to penetrate all the way to the lumen. In a similar experiment, Bates (23) found that he could follow the penetration of polyamide-epichlorohydrin into the cell wall by electron microscopy. This was made possible by the reduction and deposition of osmium tetroxide by the resin. The author concluded that even resin which would not pass through dialysis tubing (average pore size 48 A.) was small enough to penetrate the cell wall of wood pulp fibers.

All of the observations cited above may be taken as evidence that diffusion to the surface of the adsorbent, or into the pores, is the rate-determining

step in adsorption. The evidence is certainly not conclusive in this respect, however.

Peterson and Kwei (24) explained the sorption of polymers at the solid-liquid interface as a three-step process. The polymer coil in solution moves to the interface and is transferred into a polymer coil on the solid surface with only a few segment-surface contacts. Finally, the adsorbed polymer flattens out with nearly all segments in contact with the surface.

Steinberg (25) used a similar model to explain a curious maximum observed in the rate of adsorption of some polymethacrylates onto iron powder. The author concluded that when the polymers begin to uncoil on the surface, a number of neighboring molecules are displaced resulting in a decrease in sorption with time.

Diffusion control has been noted in other processes occurring in heterogeneous systems. For example, Bircumshaw and Riddiford (26) reviewed the literature and concluded that the rate of dissolution of a wide variety of systems was diffusion-controlled. It was observed that all of the rate data could be expressed by means of a first order equation:

$$dC/dt = k(C_{sa} - C) \qquad (1)$$

where C is the solution concentration at time t, C_{sa} is the saturation concentration, and k is the rate constant. According to Nernst (27) the rate constant for a diffusion-controlled process in an agitated system is given by

$$k = DA/V\delta \qquad (2)$$

where D is the diffusion coefficient of the solute, A is the area of the surface at which the reaction occurs, V is the total volume of the system, and δ is the distance over which the solute must diffuse in order for the reaction to occur. A number of

systems were tested and found to fit Equation (1). For every case δ was calculated from Equation (2) and found to be between 0.02 and 0.04 mm. Further, it was found that δ could be decreased by increasing the rate of agitation (26).

Moelwyn-Hughes (28) discussed the observations on the thickness of the diffusion film and made the following comment. "For a number of reactions in water at 20°C., δ is about 3×10^{-3} cm. This is a physically improbable result, but the fact that it is roughly the same for many reactions of a wholly different chemical nature is consistent with the view that the rates are determined by the process of diffusion."

Frank-Kamenetskii (29) gives a detailed development and discussion of the concept of a diffusional film from a hydrodynamic point of view. It is shown that δ represents the zone in which the transfer of solute can be considered as purely molecular. In other words, δ is defined as the thickness of the film over which molecular diffusion must occur to account for the actual intensity of mass transfer. Thus, the thickness of the film stands in no relation to the true physical structure of the flow. Accordingly, the film thickness so calculated should show a dependence on the diffusion coefficient of the solute. It has been shown that δ depends on $D^{0.25}$ for turbulent flow conditions and on $D^{0.34}$ for laminar flow (26, 30, 31). This exponential relationship has been shown theoretically for heat transfer and observed experimentally for mass transfer.

ANALYSIS OF THE PROBLEM

It can be seen from the brief review of the literature that the experimental evidence from a variety of systems is compatible with the theory of a diffusion-controlled adsorption rate. Unfortunately, there has been no previous attempt to quantitatively relate the polymer diffusion coefficient to the rate of adsorption. The availability of even an elementary theoretical rate equation would be a great aid to the design of experiments as well as to the interpretation of results. Such an expression was developed during the course of this work. The derivation is based on the Nernst diffusional film concept with Langmuirian adsorption and is described in the Results and Discussion section. An expression was derived for the overall rate curve and also for the initial adsorption rate.

The expression for the initial rate takes the following form:

$$\left(\frac{dC^*}{dt}\right)_{t\to o} = \frac{D^{0.66} A_o C_o}{V g_i} \qquad (3)$$

where $(dC^*/dt)_{t\to o}$ is the initial rate, D is the diffusion coefficient, A_o is the fiber surface area, V is the volume of the system, g_1 is a constant depending only on the hydrodynamic conditions of the system, and C_o is the initial polymer concentration. Equation (3) provided a framework for a discussion of the system variables which might influence the sorption rate.

An increase in the rate of agitation would produce a decrease in the hydrodynamic film constant, g_1, which would result in a more rapid adsorption process. The effect of agitation on adsorption rate for cellulose fiber systems has already been reported (13, 14) and is qualitatively in agreement with the predicted behavior.

According to the simple mass-transfer theory, the molecular weight of the polymer should affect the adsorption rate only through the diffusion coefficient.

In the absence of other effects, the diffusion coefficient should decrease with increasing molecular size. The molecular weight-dependence of adsorption rate has been exhibited previously for noncellulosic systems (6-9). There has been no attempt, however, to show that the increasing rate with decreasing molecular weight is due to changes in the diffusion coefficient and not some other mechanism. Also, most of the previous work was performed with polymer samples possessing broad molecular-weight distributions which makes interpretation of results difficult. For the case of a porous substrate, differences in polymer molecular weight might affect the magnitude of the accessible surface area which would, in turn, affect the rate.

Equation (3) predicts a first-order rate curve with respect to both accessible substrate surface area and polymer concentration. Russo and Thode (13) noted a linear dependence between fiber surface area and initial rate. The same authors found that the initial rate depended on the initial polymer concentration to the 0.61 power instead of the predicted linear relationship. It should be noted that the partially methylated locust bean gum used by the authors had a broad molecular weight distribution which could explain the deviation from the predicted behavior. Verification of the linear concentration-dependence should be performed with a carefully fractionated polymer.

The presence of charge groups on the polymer chain might be expected to affect the adsorption rate by at least two different mechanisms. The most apparent charge effect is a result of electrostatic interactions between the charge groups on the fibers and those on the polymer. For the adsorption of a cationic polymer onto a cellulose fiber, a net electrostatic attraction would be predicted. If this interaction is significant, the mass-transfer process would be accelerated and the rate would be more rapid than predicted by mass transfer theory. It has been shown by Kenaga, et al. (32) that sufficient cationic polymer can be deposited on the fiber

surface to produce a fiber having a net positive charge. When this is the case, the mass-transfer process will be retarded and the rate of adsorption will be slower than predicted by mass transfer theory. Thus, if electrostatic interactions between the fiber and polymer are significant, the initial rate would be accelerated. At later times, after the isoelectric point of the fiber has been surpassed, the rate will be retarded by electrostatic repulsions.

The second possible charge-related mechanism is due to the effect of charged groups on the diffusion coefficient of the polymer. According to Nagasawa and Fujita (33) there are three charge-related factors which could affect the diffusion of a polyelectrolyte: (1) changes in molecular configuration; (2) electrophoretic interactions between polyion, counterions, and solvent; (3) changes in the osmotic or second virial coefficient. The term counterion refers to the simple ionic species of opposite charge held within the domain of the polyelectrolyte to maintain electroneutrality. Depending on the system and the conditions of measurement, all three effects have been shown to apply (34-36).

The analysis of a diffusion-controlled rate process involving a cationic polymer and an anionic fiber leads to the following previously unverified predictions:

1. The effect of polymer molecular weight operates on the diffusion coefficient and possibly the accessible surface area.
2. The initial rate depends linearly on the initial polymer concentration and the accessible surface area of the fiber.
3. Significant electrostatic interactions between the polymer and fiber will result in an accelerated initial rate and a retarded overall approach to equilibrium. These effects cannot be predicted by mass transfer theory.

4. Changes in the ionic conditions of the polymer may affect the diffusion coefficient. The effect on the overall adsorption rate can be predicted by mass-transfer theory provided the diffusion coefficient is known for the ionic conditions of adsorption.
5. Calculation of the effective film thickness from the experimental data and Equation (3) will provide additional information concerning the magnitude of the resistance to mass transfer.
6. If the adsorption rate is not controlled by a mass-transfer process, the above statements will not all apply.

OBJECTIVES OF THE THESIS

The objective of this thesis is to investigate the kinetics of adsorption of a cationic polyelectrolyte by cellulose fibers. It is necessary to provide more substantial evidence than is currently available in the literature for the importance of a mass-transfer process as the rate-controlling step. This objective is to be accomplished by measuring the effect of a number of system variables on experimental rate curves. These results will be compared with predictions based on a simple mass-transfer model.

It is especially important to demonstrate the effect of polymer charge on the adsorption rate. An analysis of the problem indicates that two charge-related mechanisms are possible. The first is a result of electrostatic interactions between the polymer and the fiber. The second reflects the effect of polymer charge on the diffusion coefficient. Elucidation of the relative importance of each mechanism is sought.

EXPERIMENTAL EQUIPMENT, MATERIAL, AND PROCEDURES

SUMMARY OF EXPERIMENTAL PROCEDURES

Unequivocal analysis of the rate process requires experimental data from a well-characterized system. An adsorbate-solvent-adsorbent system was chosen to permit the most complete description of components and control of variables within the limits of the problem. The adsorbate polymer used is considered to be the simplest representative of a cationic polyelectrolyte available. The polymer was fractionated with respect to molecular weight to limit the effects of polymolecularity. The molecular weight of the fractions used was determined by means of sedimentation equilibrium analysis.

The polymer was adsorbed onto regenerated cellulose fibers from aqueous solution. The adsorption experiments were performed by mildly agitating a suspension of the fibers in a polymer solution and examining the liquid phase for a decrease in polymer concentration. The rate experiments were performed by a batch method to eliminate dilution errors. A sampling technique was devised which would permit the withdrawal of an aliquot of solution with a minimum of hydrodynamic disturbance. Equilibrium isotherms were determined for each set of conditions at which the rate data were taken. The quantitative analysis of the polymer was performed by means of a colorimetric technique based on the formation of a copper complex with the polymer.

Diffusion coefficients were measured under the same solution conditions as the rate experiments. These measurements were made on a Beckman Spinco Model E ultracentrifuge by a free-diffusion method.

SELECTION AND DESCRIPTION OF ADSORBATE

Polyethylenimine (PEI) was chosen as a representative cationic polyelectrolyte. This polymer is readily available, has been previously studied in similar systems (12, 32, 37-38), and is amenable to quantitative analysis in dilute solution. The polymer shows no tendency to form colloidal aggregates and, in the absence of additives, should have an indefinite shelf life.

PEI is commercially valuable to the pulp and paper industry as a drainage and retention aid.

As a result of branching, PEI contains primary, secondary, and tertiary amines. Its structure might be given nominally by the following representation:

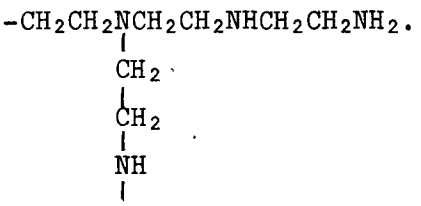

The PEI used in this study was a laboratory sample (control number SA1117-633974) provided by The Dow Chemical Company. This sample is reputedly of very high purity and contains no cross-linking agents. According to the supplier, the molecular weight is the highest obtainable without resorting to some means of artificially induced cross-linking and is reported to be about 5000. This polymer sample will be referred to as PEI-63 in the future.

Some early work was done with higher molecular weight PEI preparations containing dichloroethane or a diepoxide as a cross-linking agent. These samples were observed to undergo a change which reduced the reactivity with cellulose fibers after six to twelve months of receipt. The loss of adsorptivity was usually accompanied by a yellowing of the polymer solution and an apparent increase in molecular

weight. It was theorized that the change was due either to oxidation or additional cross-linking during storage. In any event, the instability of these solutions rendered them useless for further work and they were abandoned. PEI-63 was guaranteed by the supplier to have an indefinite shelf life. As an added precaution, this sample was stored in polyethylene containers in a nitrogen atmosphere. Comparisons of results obtained over long time intervals indicated that there was no change in the polymer over the course of the study.

SELECTION AND DESCRIPTION OF SOLVENT

Water was chosen as the solvent since the observation of charge effects requires a polar solvent. In commercial applications, sorption almost always occurs from aqueous solution.

The water used in all phases of this study was usually deionized and distilled in one of the service stills. When the water from this source failed to meet acceptable limits, a double-distillation process was used. The water was first distilled out of a solution consisting of 0.02% potassium permanganate and 0.05% sodium hydroxide. In the second stage, the once-distilled water was distilled out of dilute sulfuric acid. All components of the still were constructed of Pyrex. The conductivity of the doubly-distilled water was always less than 1.2×10^{-6} mhos.-cm.$^{-1}$ and the pH when freshly boiled was about 6.8. In all cases, a conductivity of 1.5×10^{-6} mhos.-cm.$^{-1}$ was arbitrarily set as the maximum allowable.

SELECTION AND DESCRIPTION OF ADSORBENT

Regenerated viscose fibers were chosen as the substrate. The use of synthetic fibers eliminates problems due to fines and helps to assure a more reproducible, homogeneous surface.

The adsorbent used in this study was the RD-101 product supplied by the American Viscose Division of FMC Corporation. These fibers are 1.5 denier in thickness and 0.25 inch in length. The fibers are characterized by a particularly high surface area for synthetic fibers. This material was subjected to six, four-hour soaks in distilled water to remove any occluded impurities which might have been introduced during manufacture. The fibers were then dewatered on a Buchner funnel to a solids content of about 35% and were stored at 6°C. The porous nature of these fibers is illustrated in Fig. 1. The very small amount of material inside the fiber wall indicates that these fibers have a nearly hollow core analogous to the lumen in wood pulp fibers.

QUANTITATIVE ANALYSIS OF POLYMER SOLUTIONS

SPECTROPHOTOMETRIC ANALYSIS

A spectrophotometric method of determining the dilute solution concentration of PEI was developed. The technique is based on a color-forming reaction between cupric ion and the amine groups on the polymer chain. A similar technique has been used to study the structure of PEI (39).

The experimental technique may be described as follows. One ml. of 0.01M cupric acetate was added to 5 ml. of the unknown solution and the mixture was thoroughly agitated. The absorbance was measured on a Beckman Model DU spectrophotometer at a wavelength of 269 nm. The spectrophotometer was zeroed against a blank consisting of 1 ml. of 0.01M cupric acetate in 5 ml. of distilled water. The concentration was determined by comparing the absorbance with a standard curve. Best results were obtained with PEI concentrations between 5 and 50 mg./liter. A typical calibration curve is shown in Fig. 2. The concentration of PEI in the standard solutions is based on the total nitrogen content determined from a modified Dumas method.

Figure 1. Electron Micrograph of Cross Section of RD-101 Fiber

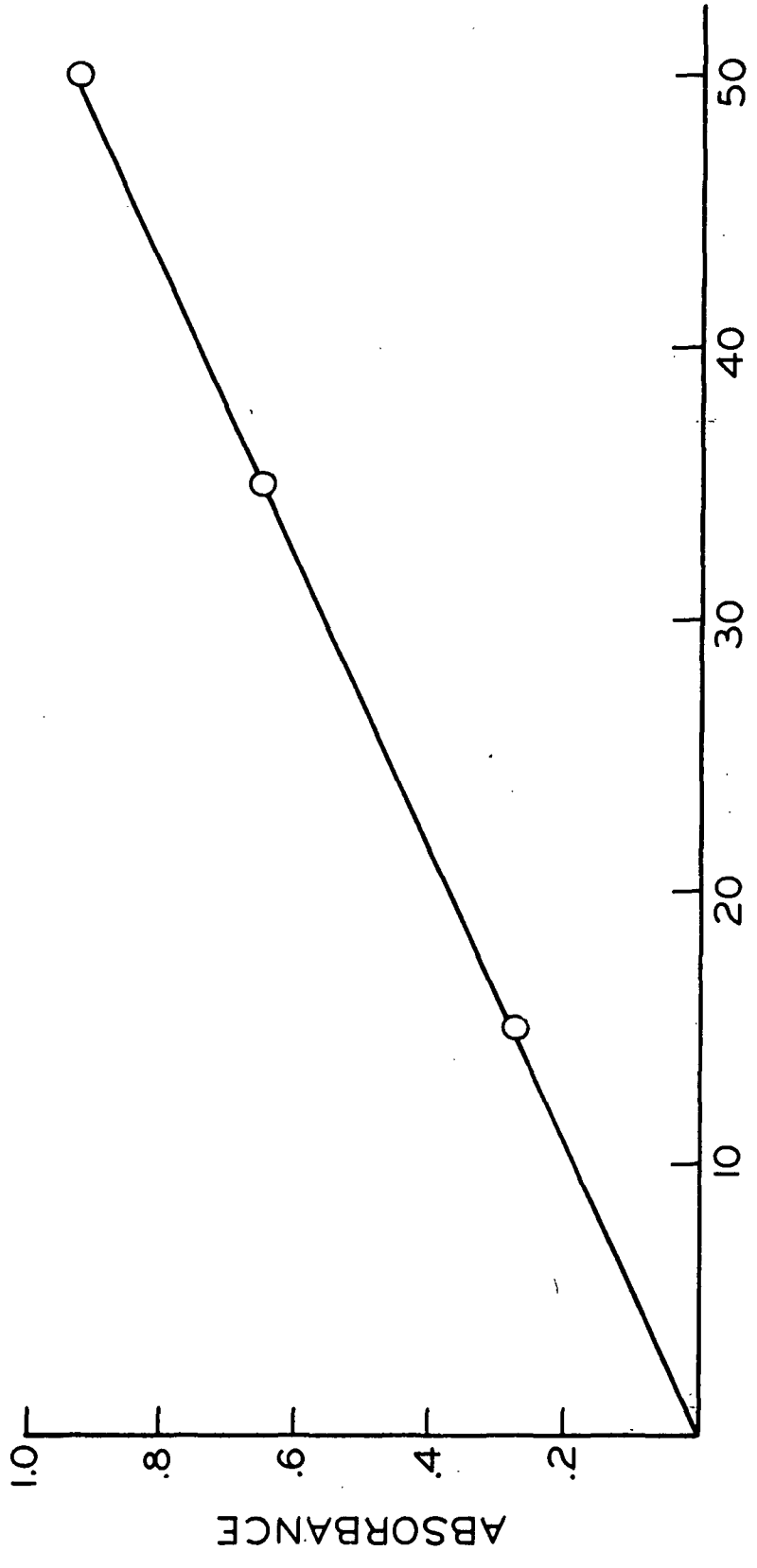

Figure 2. Colorimetric Analysis of 63-5: Standard Curve

Between pH 4 and 9, the color reaction is almost independent of pH. Above pH 9, however, the absorptivity is very sensitive to changes in the pH. For the purposes of this discussion, the absorptivity is defined as the measured absorbance divided by the concentration in grams per liter when measured in a cell of one centimeter path length. Figure 3 was prepared by mixing 1 ml. of 0.01M copper acetate with 5 ml. of Fraction 63-6 at a concentration of 0.0864 g. per liter and measuring the absorbance. The pH is that of the polymer solution adjusted with sodium hydroxide prior to the addition of the copper acetate. No attempt was made to correct the pH readings for sodium error so they must be considered to be relative above pH 10.0. Since the copper ion apparently forms the amine complex only with ~~un~~ionized amine groups, the shape of Fig. 3 may, in part, reflect the effect of pH on the degree of polymer ionization. For the purpose of quantitative solution analysis at high pH, it is necessary to reduce the extreme sensitivity to pH. It was found that the buffering action of the copper acetate could be extended by adding one mole of hydrochloric acid for every two moles of acetate ion. Thus, if the color reagent consists of a mixture of 0.01M cupric acetate and 0.01M hydrochloric acid, the absorptivity is essentially independent of pH up to about pH 11.5. A standard of approximately the same pH as the unknown solution was used to ascertain the absorptivity for every analysis of an unknown solution.

The absorbance depends slightly on the molecular weight of the polymer. This is probably a reflection of differences in branching. Again, an appropriate standard was used to eliminate this effect.

NITROGEN ANALYSIS OF PEI SOLUTIONS

Fractions 63-5 through 63-8 were analyzed for nitrogen concentration to permit the determination of the absolute PEI concentration. This analysis was accomplished

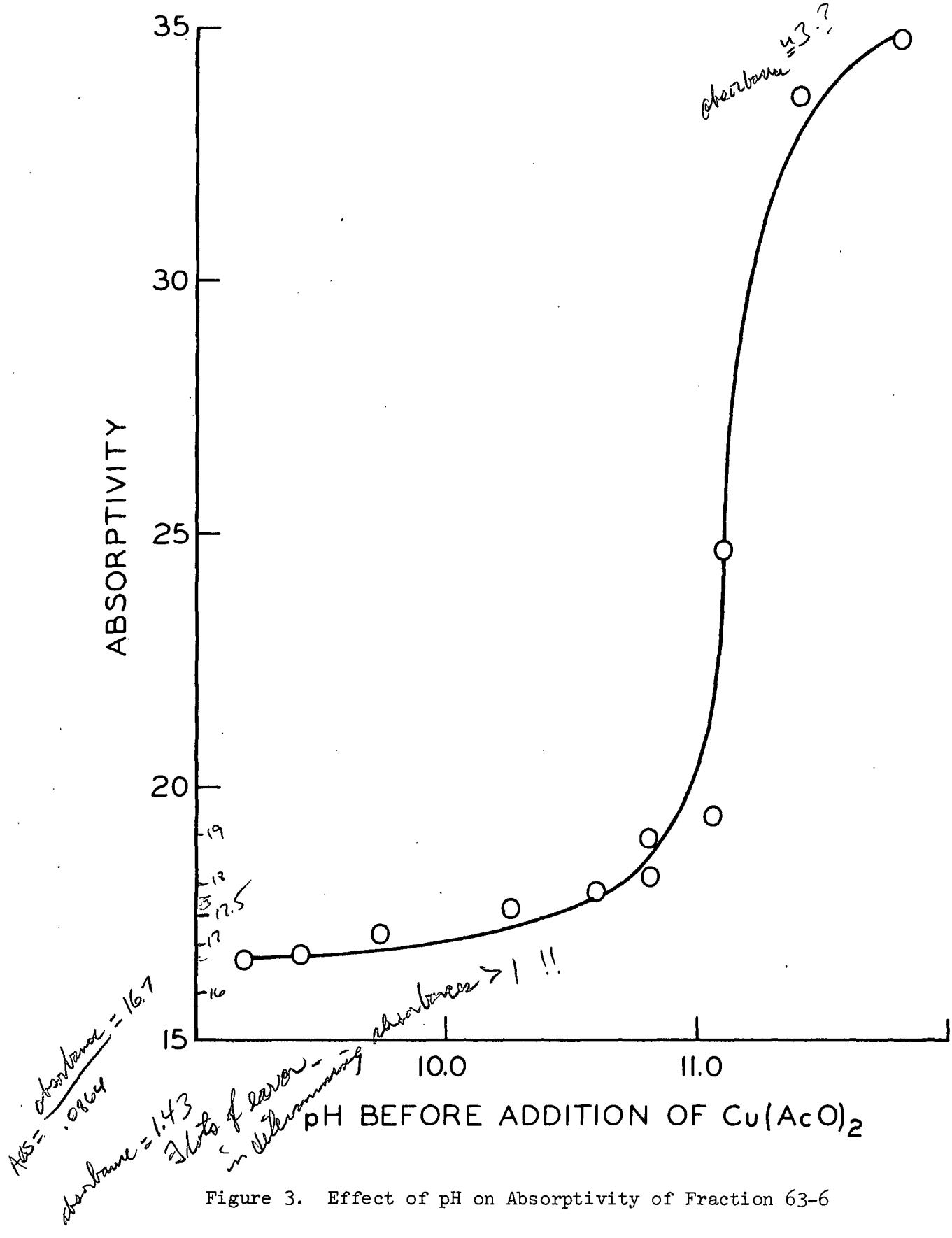

Figure 3. Effect of pH on Absorptivity of Fraction 63-6

with the use of a Coleman Nitrogen Analyzer which operates on the basis of a micro-Dumas technique. The results of these analyses are given in Appendix I.

POLYMER FRACTIONATION PROCEDURES

It was necessary to prepare narrow molecular-weight fractions of the polymer in order to reduce the effect of polydispersity on the adsorption data. Gel permeation chromatography (GPC) was chosen as the method of fractionation for several reasons. This method is capable of providing very narrow fractions. Once the proper operating conditions have been chosen, large quantities of fractionated polymer can be prepared in a relatively short time. Good reproducibility from run to run is easier to attain with this method than with other techniques.

In simplest terms, the operating principle of GPC is thought to be based on the retardation to elution due to lateral diffusion into a porous network. The smaller solute molecules can diffuse more deeply into the porous structure and get farther away from the main flow channels. Thus, the lower molecular weight fractions will be eluted after the larger, partially excluded species. Aliquots possessing narrow molecular-weight distributions can be obtained by isolating portions of the eluting stream. Other factors being equal, smaller portions will provide narrower distributions.

The physical equipment for GPC experiments must perform several functions. A means of supporting a porous gel medium to permit flow of polymer solution and eluting solvent must be provided. The flow rate through the gel must be reproducible and homogeneous through the entire bed. A monitoring device for the eluting solute is required to determine the elution behavior of the polymer sample. Finally, some means of separating the elution stream into individual fractions must be provided.

The selection of an appropriate gel material depends on the nature of the polymer sample to be fractionated. The most important criterion is that there be no interactions between the gel and the polymer which might lead to sorption. The equilibrium partitioning of molecular weight due to adsorption favors the retention of the higher molecular weight species. Thus, if sorption occurred in the GPC process there would be two partitioning mechanisms operating against one another. The solute exclusion mechanism would favor the early elution of high molecular weights while the sorption process would cause the low molecular-weight material to be eluted first. The result would be an imperfect fractionation. If the interactions between gel and polymer are very strong, apparent irreversible adsorption would result in poor yields and unstable gel behavior. Adsorption problems can often be eliminated by the proper choice of gel material and eluting solvent.

Another criterion of the gel is pore size. Most gels are prepared in a wide variety of pore sizes so as to cover applications to a wide range of molecular weights. Specifications supplied by the manufacturers are helpful in determining the best gel for a given application.

The final consideration is the size of the gel beads. Smaller beads provide better resolution at the expense of requiring much lower flow rates. For preparative work, higher flow rates are desirable since it may be necessary to perform a number of runs to prepare a sufficient quantity of material.

The gel chosen as best meeting these criteria for this application is Bio Gel P. This gel is a cross-linked copolymer of acrylamide and methylene bisacrylamide produced by Bio-Rad Laboratories. It is supplied in the form of spherical beads which can be readily hydrated in aqueous solution. The P-10 gel with a bead size of 50-100 mesh offered the best combination of resolution and flow rate. Initial experiments

showed that there was no adsorption of PEI onto the gel when a solvent of 0.64% sodium acetate in water was used for loading and elution.

DESCRIPTION OF SYSTEM

The gel was supported in a precision bore, glass chromatographic tube which is 2.5 cm. in diameter and 100 cm. in height. Upper fittings are supplied for the eluent inlet and sample application port. The bottom end of the column is designed to have a minimum of dead space at the outlet port. The sample applicator consists of a one centimeter high Lucite cylinder with a disk of Teflon mesh bonded across one end. This device fits snugly inside the column and is supported by the gel. The applicator allows the sample solution to be evenly distributed over the area of the column without disrupting the upper surface of the gel bed. The entire column is fitted with an outer jacket through which water controlled at 25.0°C. is pumped from an adjacent bath. The column and fittings are manufactured commercially by Sephadex.

The eluting solvent is supplied to the head of the column at a constant flow rate by a variable speed peristaltic pump. A surge tank was placed on stream just below the pump to reduce flow pulsations due to the peristaltic action. This device consists of a vertically mounted 18-cm. drying tube with a screw clamp on the outlet tubing. The drying tube is kept approximately half full of solvent. A positive pressure in the tube is maintained by proper adjustment of the screw clamp. In this manner, periodic pulsations in the flow rate are reduced to less than ± 2% of the average flow rate.

The eluent flowing out of the column passes through the measuring head of a differential refractometer for the detection of eluting polymer. This instrument is the Model 404 Refractive Index Monitor made by the Nester/Faust Manufacturing Corporation. The measuring head of the refractometer is immersed in the constant

temperature water bath controlled at 25.0°C. The operating principle of the refractometer is based on the Fresnel equations. In brief, the Fresnel principle states that the fraction of the incident light which is reflected at the interface of two different media is dependent upon the angle of incidence and the refractive indexes of the media. An optical interface is created between the flowing stream and the measuring cell of the instrument. By holding the angle of incidence constant, the intensity of the reflected beam is proportional to the refractive index of the stream. The reflected light is monitored continuously with a photocell and compared with the output from a photocell measuring the reflected light from the standard cell. In this work, the standard cell always contains pure solvent so that the differential refractive index of the stream is zero until the polymer begins to elute from the column. The differential output between the standard and measuring cells is recorded on a Sargent Model MR recorder.

After passing through the refractometer the stream is collected in a Technicon fraction collector. The collector operates on a constant time basis and is set to collect samples in fifteen-minute increments.

All components on the stream are connected by Teflon tubing (0.031 inch I.D.) with the exception of a short length of pure gum rubber tubing (0.125 inch I.D.) passing through the peristaltic pump. There is no evidence of water extractives present in the gum rubber tubing which would affect the refractometer readings. Polymer solutions are injected downstream from the gum rubber tubing so that there is no chance of PEI sorbing on the wall. In order to assure complete equilibration of the eluent, the stream passes through a three-foot coil of tubing immersed in the water bath just ahead of the refractometer head. All joints and connections are made air tight to prevent the formation of air bubbles in the system. A diagram of the entire system is shown in Fig. 4.

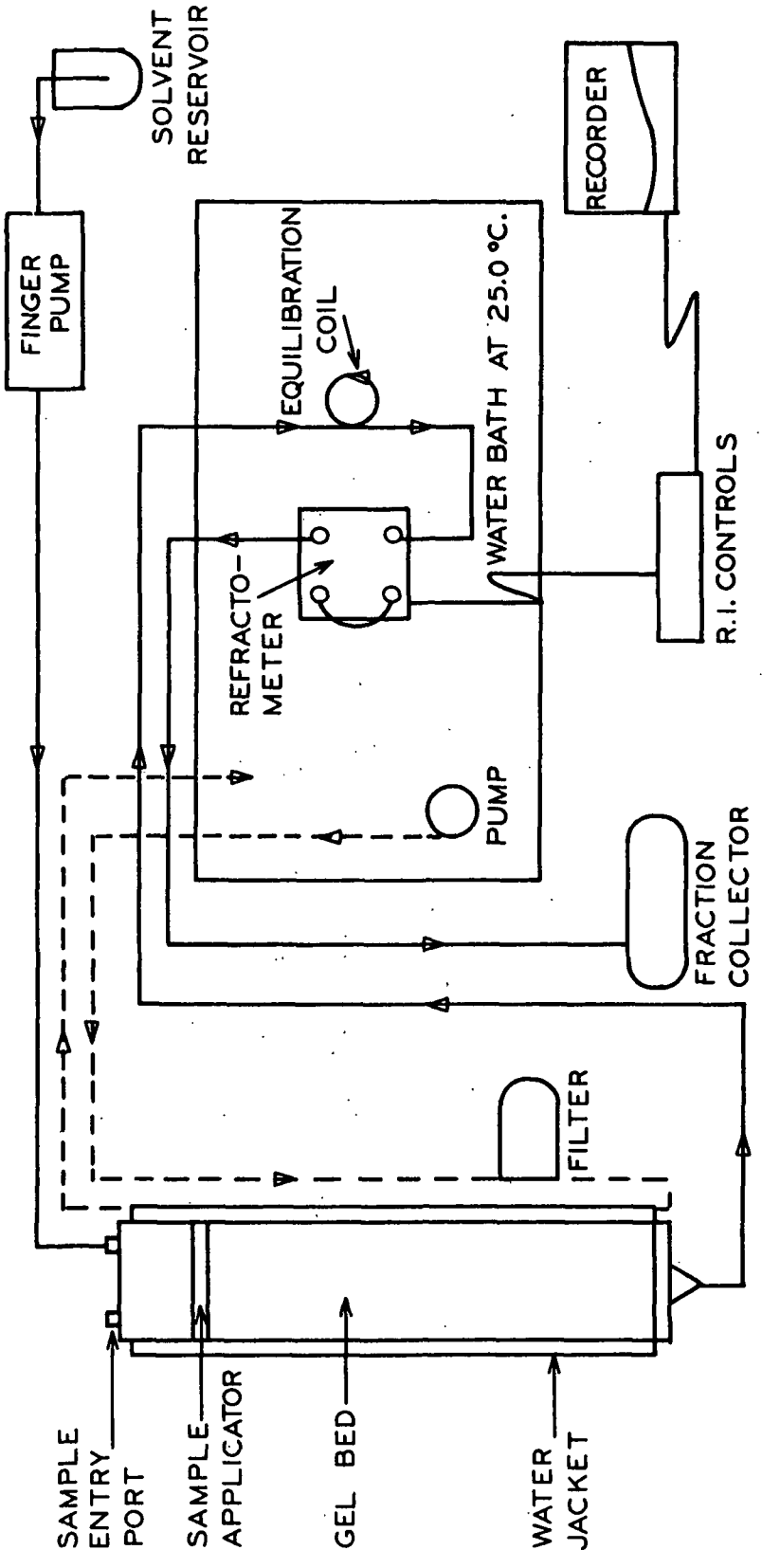

Figure 4. Schematic Diagram of GPC Equipment

CALIBRATION OF REFRACTOMETER

The response of the refractometer to a solution of known refractive index was measured in order to determine the absolute sensitivity. An aqueous solution of sucrose was chosen as a standard since the refractive indexes of sucrose solutions are readily available (40). A 10.00% solution of sucrose (AR grade) was prepared fresh and injected into the measuring cell of the refractometer. The reference cell was filled with distilled water. For this experiment the detector head was thermostatted at 20.0°C. Using Cell A as the measuring cell, a response of 56 mv. was observed. The refractive index of a 10% solution of sucrose is given as 1.3479 at 20.0°C. and that of water at the same temperature is given as 1.3330. The difference (as measured by a differential refractometer) is 0.0149. The sensitivity of Cell A is thus 0.000266 RI units/mv.

Cell A was also calibrated with respect to PEI concentration by the same method. The response of the instrument was 1.46 ± 0.09 mv.-liter/g. at 25.0°C. Since the recorded output can be estimated to about 0.01 mv., concentrations as low as around 10 mg. of polymer per liter should be detectable. Problems with inadequate voltage and temperature control make this sensitivity difficult to realize, however.

COLUMN PREPARATION

Fifty grams of Bio-Gel P-10 was dispersed in one liter of 0.64% sodium acetate and agitated for five hours with a magnetic stirrer. The slurry was then transferred to a large filter flask and evacuated with an aspirator for about four hours to remove as much dissolved air as possible. Following deaeration, the column is filled with 0.64% sodium acetate and a large funnel is fitted to the top with a rubber stopper. The gel slurry is poured into the funnel in one batch and allowed to settle into the column. The slurry in the funnel is stirred gently to prevent

plugging in the neck. After about five centimeters of gel have settled into the bottom of the column a slow flow rate is begun to help assure that the gel is well packed. When the column has filled with the gel, the funnel and stirrer are removed and the sample applicator is inserted into the column. The upper inlet fittings are replaced and the column is pumped through for a couple of days with the elution solvent. The flow rate for this pretreatment is slightly above that to be used for the actual fractionation experiments. Throughout the loading procedure and the ensuing fractionations, the column is maintained in vertical alignment with the aid of a plumb bob. The void volume of this column was estimated from the elution volume of the highest molecular weight species to be about 126 milliliters.

FRACTIONATION PROCEDURES

The polymer loading process was begun by draining the solvent down to the level of the Teflon mesh sample applicator. Twenty milliliters of 7.74% PEI-63 in 0.64% sodium acetate was loaded into the column with a syringe. The solution is then drawn into the bed by allowing the solvent to drain slowly from the column outlet. The sides of the column are washed down with solvent and the injection port is sealed. The polymer was eluted at a flow rate of 0.98 ± 0.02 ml./min. at 25.0°C. Collection was begun 6.0 minutes after the refractometer response showed that the polymer had begun to emerge from the column. A total of eighteen fractions each having a volume of 14.7 ml. was collected from each run.

An aliquot of each fraction of the first run was analyzed colorimetrically for PEI content. The elution curve determined in this manner is shown in Fig. 5 along with a reproduction of a refractometer trace for the same run. It can be seen that the refractometer gives a response which is qualitatively similar to the actual elution curve. An attempt was made to utilize the refractometer trace

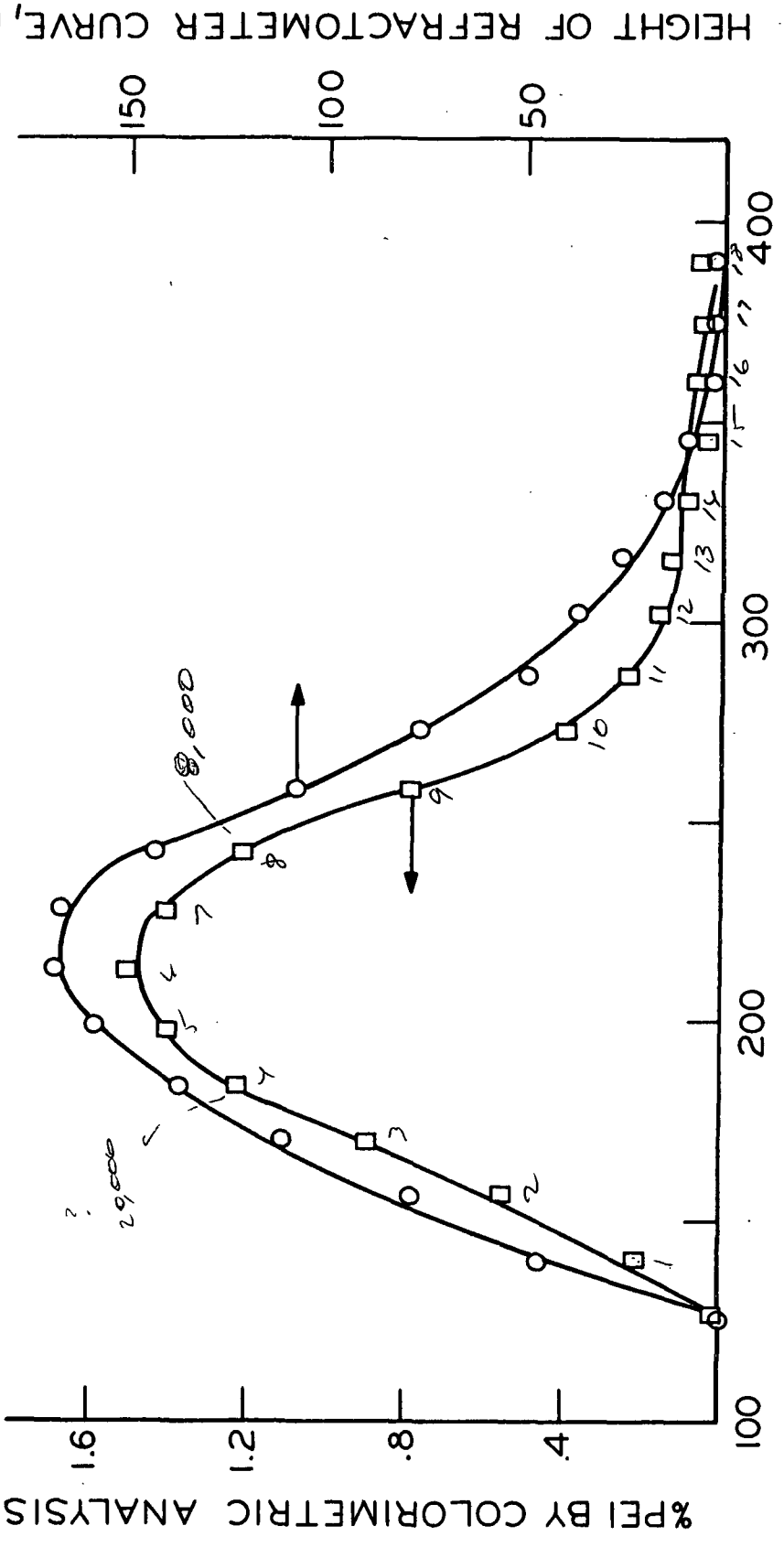

Figure 5. Elution Curve for PEI-63

as a means of quantitatively analyzing the eluting polymer. The area under the curve was integrated numerically and converted to the total amount of eluted polymer with the aid of the refractometer calibration data. Results obtained by this method differed from the colorimetric analysis by a factor of about 30%. The inability of the instrument to give quantitative results may be due to a couple of reasons. One, the refractive index of the polymer may depend significantly on molecular weight. A second possibility is due to the fact that this refractometer operates on the principle of reflection from the interface between the cell wall and the solution. Any abnormality in the flow pattern and/or polymer distribution along the wall of the cell would influence the reading. The latter phenomenon has been observed before and could possibly be alleviated by packing the cell with small silica spheres to disrupt the flow pattern (41). In all ensuing runs, the refractometer was used to provide qualitative information on the fractionation process.

The total amount of eluted polymer as calculated from the colorimetric analysis shows that 1.529 grams of polymer were collected. This value is well within experimental error of the 1.548 grams of polymer which were added to the column. A total of seven runs was made on the column under these same conditions. The refractometer traces were the same for each run. Corresponding fractions from each run were combined to give a total of about 100 ml. of solution for each fraction. The fractions were stored in polyethylene bottles. The bottles were kept in a dry box under nitrogen. The solutions were labelled according to the source solution and fraction number. Thus, Solution 63-4 refers to the fourth fraction of PEI-63.

REMOVAL OF ACETATE BUFFER

The acetate buffer was removed from the aqueous polymer fractions by dialysis against distilled water. Early attempts to remove the sodium acetate by means of

ion exchange columns were unsuccessful. Problems due to sorption of PEI on the resin beads and contamination from a soluble portion of the beads could not be overcome.

The dialysis bags were constructed of cellulose acetate having an average pore size of 48 A. It was necessary to wash the bags free of glycerin which was present as plasticizer. This was accomplished by soaking the film in distilled water for several days with frequent changes of the water. The polymer fractions were of fairly low molecular weight and there was some danger of polymer diffusion through the bag. It was found that the loss of polymer to the dialyzate could be reduced to a negligible level by conducting the dialysis under conditions of no agitation. Solution 63-8 was the highest fraction (lowest molecular weight) that could be treated this way.

The dialyzate was monitored continuously with a conductivity cell to determine the rate of sodium acetate removal. In addition, colorimetric spot tests were performed periodically on the dialyzate to ascertain the extent of polymer diffusion through the bag. Equilibrium for the sodium acetate removal process was attained in four hours. In this time period, the appearance of PEI in the dialyzate was negligible. Estimates of sodium acetate concentration in the dialyzate obtained from potentiometric titrations indicate that the sodium acetate is completely removed.

All dialyses were performed with 500 ml. of distilled water as dialyzate and 100 ml. of polymer solution inside the bag. After six such steps, the concentration of acetate remaining in the bag is estimated to be about 10^{-7} molar, or less than one mole of acetate per one million moles of monomer units.

Each fraction was analyzed for total nitrogen content by the Dumas method and the PEI concentration was calculated from these data. The results of these tests are given in Appendix I.

MOLECULAR WEIGHT OF FRACTIONS

The molecular weight of Fractions 63-4 through 63-8 was measured by a sedimentation equilibrium technique. The experimental details and results of the method are given in Appendix II.

Figure 6 shows the ratio of the elution volume to the void volume as a function of molecular weight for PEI-63. This curve is shifted to higher molecular weights compared to the calibration curve supplied by the manufacturer. The suppliers curve was determined using globular proteins as the eluting solute.

DIFFUSION COEFFICIENT DETERMINATIONS

The diffusion coefficients of solutes are most conveniently calculated with data obtained from free-diffusion experiments. This type of experiment is initiated by creating a boundary between two solutions having different concentrations of the solute species under investigation. Observation of the solute concentration as a function of distance from the initial boundary and elapsed time permits the calculation of the diffusion coefficient. A comprehensive review of the analysis of diffusion coefficients is given by Gosting (42).

The use of a Rayleigh optical system is an appropriate method of following the solute concentration with respect to distance and time. The difference in refractive index between solute and solvent produces an interference fringe pattern which is related to the distribution of solute within the cell. The relative positions of interference fringes are the primary information required for diffusion measurements.

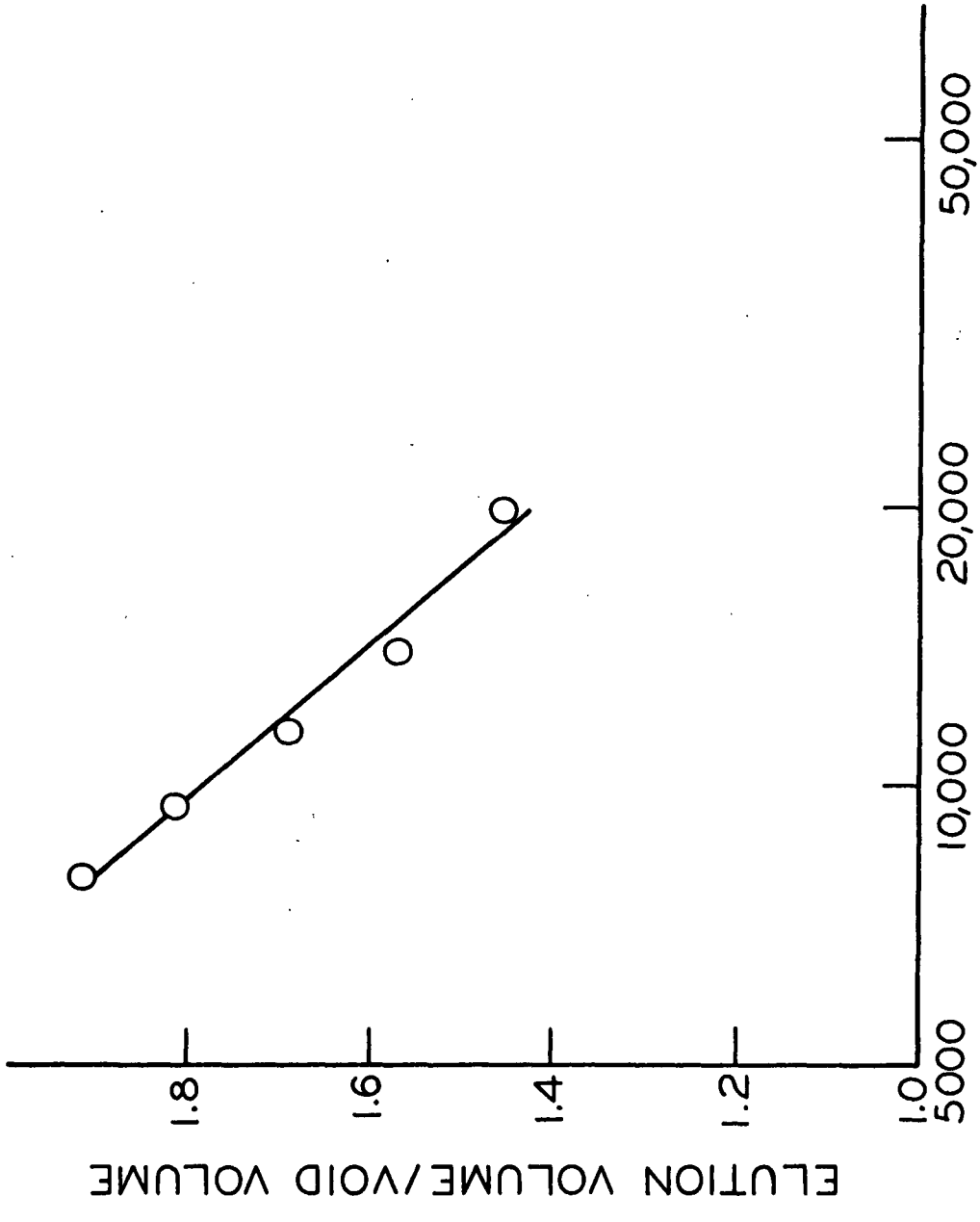

Figure 6. Molecular Weight Versus Elution Volume for PEI-63

EXPERIMENTAL

The Beckman Spinco Model E ultracentrifuge was chosen for diffusion measurements since this instrument requires only a small volume of the polymer solutions. Solvent conditions of the solutions were chosen so as to duplicate those used in the adsorption experiments. Thus, the solutions had to be prepared at a variety of concentrations of sodium hydroxide and sodium chloride. In order to assure that the concentrations of the simple ionic species in the solvent were equal to those in the polymer solutions, the two were dialyzed against one another prior to the boundary formations.

The double-sector synthetic boundary cells were used for the diffusion measurements. A 0.15-ml. aliquot of polymer solution was placed in one sector and 0.45 ml. of solvent was placed in the other sector. The cell was placed in an aluminum An-D rotor, aligned, counterbalanced and mounted in the ultracentrifuge. The vacuum chamber was then evacuated and brought to temperature (25.0°C.). The rotor was accelerated to 5227 r.p.m. to transfer 0.15 ml. of the solvent to the solution side. The remaining 0.30 ml. of solvent served as the reference cell for the formation of the interference fringes. Timing was begun at the onset of the boundary formation. The first photograph was taken as soon as the fringes in the boundary region became resolved. Thereafter, five photographs were taken at intervals of two minutes, followed by three at four minutes and one at eight minutes. At this point, the boundary was usually approaching the bottom of the cell so the experiment was terminated. The rotor was then removed and shaken thoroughly to destroy the gradient. After reassembly the rotor was again accelerated to 5227 r.p.m. and a final picture was taken to permit correction for any curvature in the optics and to assure that there was no sedimentation of polymer under the conditions of measurement.

In order to conserve on the number of photographic plates consumed, a minor change in the usual procedure was adopted. The Rayleigh optical system ordinarily permits the recording of only five consecutive patterns on a single plate. Since the Rayleigh patterns only occupy the upper half of the plate, the lower half is usually unexposed unless schlieren pictures are also recorded. For these experiments, after the first five exposures were taken the plate holder was removed and taken into the dark room where the plate was flipped end for end. The plate holder was then returned to the instrument for the final five exposures. In this way, an entire run could be recorded on a single plate.

Each solution was measured at five concentrations, the highest being approximately 1% and the most dilute at about 0.2%. It is not possible to make measurements much lower than 0.2% for this material since there are not enough fringes for sufficient analysis.

A detailed description of the ultracentrifuge and its operation is given elsewhere (43).

The information which was measured from each plate included the total number of fringes, the horizontal position of each fringe, and the suitable base-line correction. The recording of these data was facilitated through the use of a microcomparator which provides both digital and punched card output. This device is fitted with an x-y traversing stage and a means of aligning the plate.

After a plate was aligned with respect to the microcomparator, a single well-defined fringe was chosen as the horizontal line of sight and the y position was recorded. As the pattern was traversed in the x direction each fringe position was recorded. Finally, at a point very near the bottom of the cell, the y positions of the fringes immediately above and below the horizontal line of sight were measured.

These latter data were used for interpolation to determine the fractional fringe number. The x and y positions of a selected fringe from the base-line photograph were measured at the top and bottom of the cell and applied to the calculation of the fractional fringe.

METHOD OF DATA ANALYSIS

The solution to Fick's second law for free diffusion experiments may be given by

$$\frac{2j - J}{J} = \frac{2}{\sqrt{\pi}} \int_0^Z \exp(-\beta^2)\, d\beta \qquad (4)$$

where j is the fringe number, J is the total number of fringes, β is the variable of integration and Z is the upper integration limit given by

$$Z = \frac{x}{2\sqrt{Dt}} \qquad (5)$$

where x is the distance from the initial boundary, D is the diffusion coefficient, and t is the time elapsed from the boundary formation (42). The quantity on the left side of Equation (4) is referred to as the reduced cell coordinate and may be determined directly from the fringe patterns. The right side of Equation (4) is nothing more than the error function. The magnitude of the error function is tabulated for values of Z to a high degree of accuracy (44). The diffusion coefficient can be calculated from the experimental quantities x and t and the value of Z determined from the reduced cell coordinate and the error function tables.

The applicability of Equations (4) and (5) to the diffusion of PEI can be assured by testing the dependence of fringe position on the square root of time. According to Equation (5) this dependence should be linear. Figure 7 confirms the validity of application.

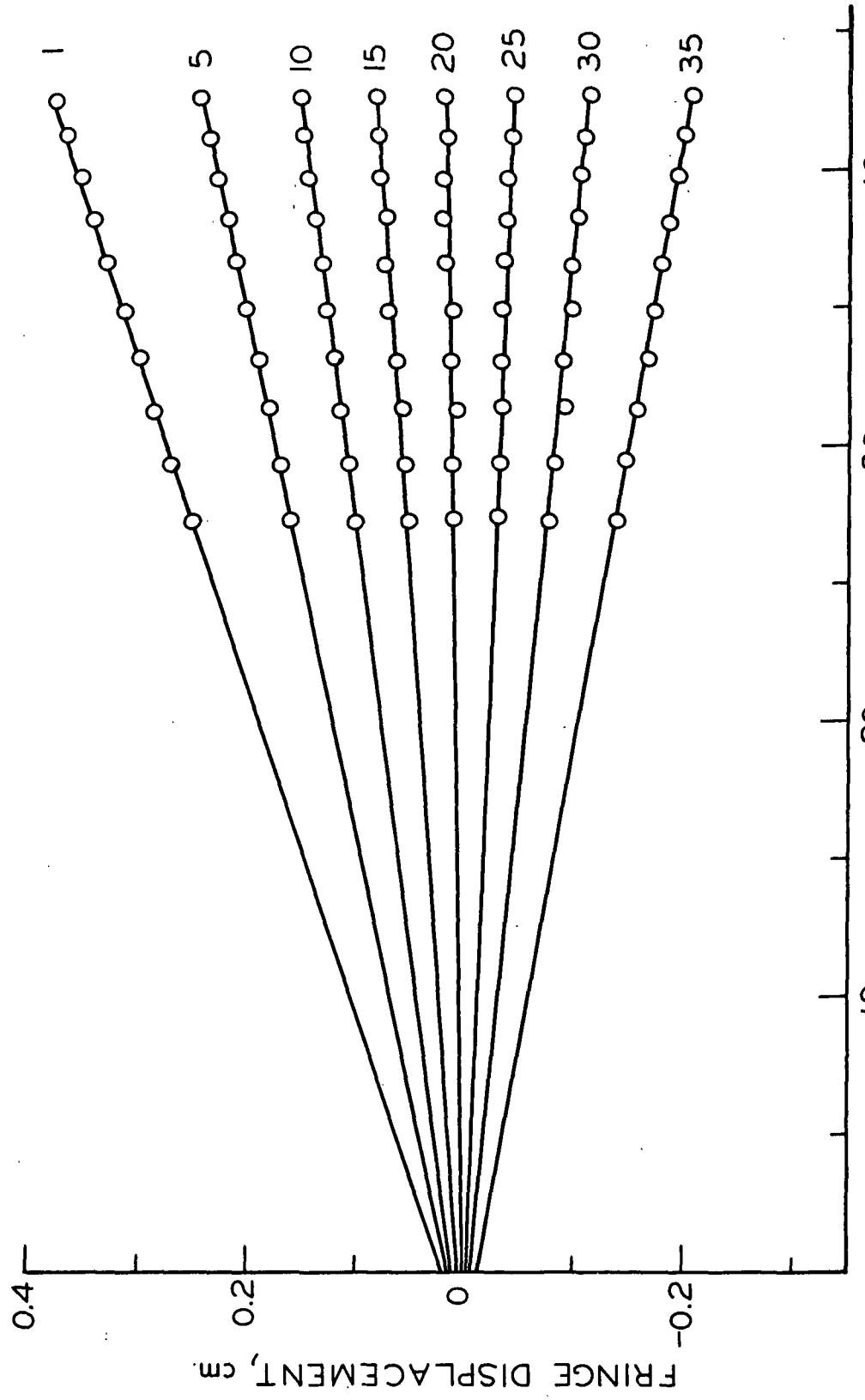

Figure 7. Fringe Position as a Function of Root Time, Numbers Refer to Fringes

The use of the reduced cell coordinate in terms of fringe number requires that the total number of fringes be a linear function of solute concentration. Figure 8 shows that this requirement is met for three different samples. The highest concentration given (relative dilution equal to one) is approximately one percent for each of the samples. All solutions tested showed a good linear relationship over the range of concentrations studied.

In order to avoid the rather difficult determination of the initial boundary position ($Z = 0$), the calculations are based on the separation between fringe pairs. There are essentially two different methods of forming fringe pairs. Longsworth (45) suggests holding Δj constant so that fringe j is paired with fringe $(J/2) + j$. In other words, the first fringe is paired with the first fringe past the center of the pattern, etc. When fringes are paired in this way, each fringe pair corresponds to a different solute concentration. If the diffusion coefficient is independent of concentration, the diffusion coefficient for each fringe pair can be averaged to give a very accurate value. For a concentration-dependent diffusion coefficient this treatment yields information on the dependence within the limits of error of a single pair of fringe position measurements.

The other method of pairing is that given by Creeth (46) in which fringes are paired symmetrically about $J/2$. That is, the first fringe is paired with the last fringe, the second with the next to last, etc. This author has shown that the first-order concentration effects are symmetrical about the midpoint and cancel out when the fringes are paired symmetrically. By this method, the diffusion coefficients calculated from all fringe pairs can be averaged to give a coefficient corresponding to the average cell concentration.

A comparison of the Creeth and Longsworth methods given in Fig. 9 shows that both methods yield the same results. All data presented in the remainder of the thesis will be based on the Creeth method.

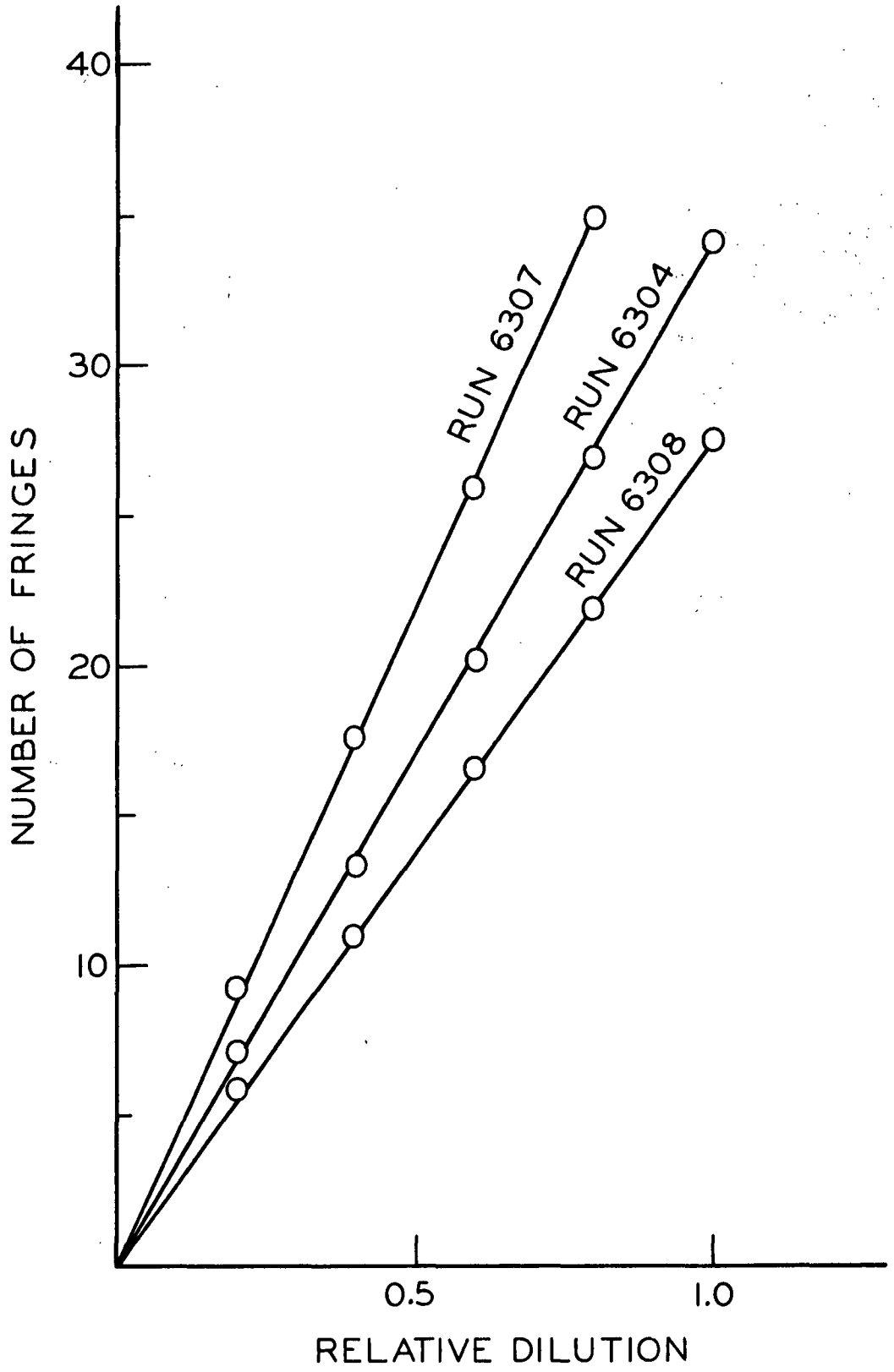

Figure 8. Verification of Linear Concentration-Refractive Index Dependence

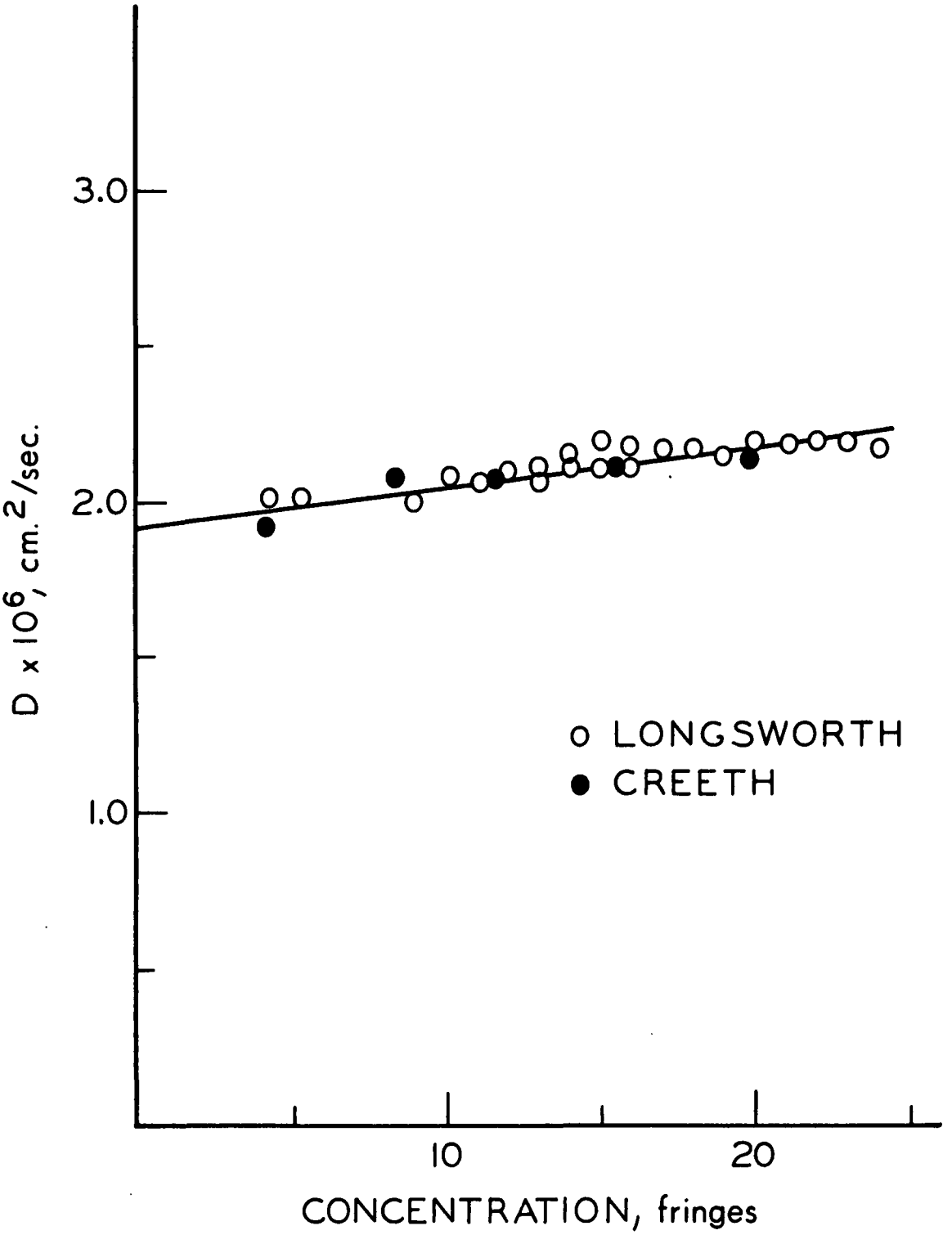

Figure 9. Comparison of Creeth and Longsworth Methods of Fringe Pairings for 63-6

Since it is not possible to form a perfect boundary, a time correction is required to account for initial mixing in the boundary region. This is accomplished by use of the following equation:

$$D' = D(1 + \Delta t/t'), \qquad (6)$$

where D' and t' are the experimentally observed diffusion coefficient and time, D is the true diffusion coefficient, and Δt is the time correction which must be added to t' to obtain the true time. A plot of D' versus $1/t'$ gives a straight line from which D can be determined.

Calculation of the diffusion coefficients was greatly facilitated through the use of the IBM 360 computer. A polynomial approximation to the error function (47) was used in the program. The program is given in Appendix III. All of the photographic plates from which the diffusion data are derived are stored in the Calder Biochemistry Laboratory at The Institute of Paper Chemistry.

POLYMER ADSORPTION EXPERIMENTS

The experimental procedure for determining sorption behavior was basically the same for the equilibrium tests and for the kinetic experiments. In essence, a predetermined amount of polymer was exposed to a known quantity of fibers under a preselected set of conditions. A portion of the solution phase was removed after an appropriate time interval for the quantitative analysis for PEI and the remaining slurry was discarded. The quantity of PEI adsorbed by the fibers was calculated from the change in the solution phase concentration. The procedure will be outlined in detail below and variations from the basic plan will be described where pertinent.

The adsorption experiments were conducted in screw-top centrifuge tubes of 50-ml. capacity. The centrifuge tube caps are lined with rubber inserts which are

covered with fresh Parafilm disks prior to each run. This provides a good tight seal and prevents any of the solution from running under the rubber inserts. After the tubes were loaded, they were fastened to the periphery of two notched twelve-inch wheels mounted on a common axis. The wheels were mounted in a manner which permitted varying the angle between the tubes and the axis. The wheels could be rotated at various speeds up to about 60 r.p.m. Unless otherwise noted, all experiments were performed at a rotation speed of 4.5 r.p.m. and an angle of 15°. These conditions provide very little agitation within the tube but allow for no settling of the fibers. The entire agitation assembly was immersed in a water bath controlled at 25.0°C.

The viscose fibers of known moisture content were weighed directly into the tubes. A quantity of 0.130 ± 0.002 g. of fibers was added to each tube to give a consistency of 0.29% unless specified otherwise. A given amount of the appropriate solvent was added to the tubes by buret. The solvent was an aqueous solution made up to the conditions of the adsorption test in terms of sodium hydroxide and sodium chloride concentration. The quantity of solvent added at this stage varied depending on the amount of polymer solution to be added but was always at least 25 ml. The fiber-solvent slurry was agitated in the water bath for at least twelve hours prior to the addition of the polymer. This was to assure complete equilibrium of the fibers with respect to temperature, swelling, dispersion, and the ionic distribution of the solvent.

A stock polymer solution was also prepared under the conditions of the sorption experiment in terms of ionic strength and pH. The concentration of this solution is chosen such that when a convenient volume is added to the slurry, the desired initial polymer concentration is approximated. The volume of the solvent initially added to the fibers was chosen to result in a total system volume of 45.0 ml. after the addition of the appropriate quantity of polymer.

The appropriate volume of polymer solution was added to the slurry with a pipet. The pipet tip was moved through the slurry during addition to assure a uniform initial distribution. Tests with the blue copper-PEI complex indicated that this method of polymer addition produced immediate dispersion of the polymer in the slurry. The tubes were then resealed and returned to the agitation assembly. It required approximately thirty seconds to load the polymer solution and begin agitation.

After agitation for a predetermined time interval, the tubes were removed from the agitation apparatus for analysis. When making kinetic measurements, it is undesirable to separate the fibers from the solution phase by means of filtration. The shear conditions about the fibers produced by the solution streaming through the forming mat would be considerably different from the conditions during agitation. According to the theory of a diffusion-controlled rate process, any change in the shear conditions would produce a change in the rate and would make proper interpretation of the kinetics data impossible. To eliminate this problem, a 5-ml. aliquot of the solution phase is removed from each tube without forming a mat. This is accomplished with the aid of a 5-inch length of Teflon spaghetti tubing. The end of the tubing is crimped shut and the sides are perforated with a large number of pinholes. When this tubing is immersed in the slurry and agitated slightly, a portion of the solution phase can be slowly removed without forming a mat of fibers on the tube. The solution sample is transferred out of the syringe through a Swinney adapter fitted with a small mesh stainless steel screen. This will remove any fibers which may have been picked up through the tubing. Approximately fifteen seconds were required to remove the tube from the agitator and withdraw the sample solution.

The 5-ml. aliquot was now ready for analysis of PEI content. The analysis was performed by means of the copper-complex test described earlier. In every case, a standard was prepared from the same stock polymer solution used to load the adsorption

tubes. The standard was diluted to approximately the same concentration as the initial polymer concentration of the adsorption tests. The dilution was performed with the same aqueous solvent used to prepare the fiber slurries.

Blank runs were performed by repeating the procedure without fibers. It was found that there was no loss of polymer due to handling or sorption on glassware. Similar tests were conducted with fibers but no polymer. The solution phase extracted from these slurries gave negligible absorbance at 269 nm. Evidently, there is no cellulosic material withdrawn from the slurry since carbohydrates give a slight color reaction with the cupric acetate.

The effect of pH on the equilibrium adsorption of various fractions was determined by making adsorption runs in various amounts of hydrochloric acid or sodium hydroxide. This same experiment was repeated using unfractionated PEI-63 and oxidized fibers. The oxidized fibers were prepared by treating forty grams of RD-101 fibers in two liters of 0.1N potassium dichromate and 0.2N sulfuric acid. The reaction was allowed to proceed for 18 hours at 25.0°C. Following this treatment the fibers were washed thoroughly with oxalic acid to remove any residual chromium. The fibers were then soaked in 0.001N sodium hydroxide and washed thoroughly with distilled water.

The effect of molecular weight was determined by measuring equilibrium isotherms for Fractions 63-4 through 63-8. These experiments were carried out up to initial polymer concentrations of about 500 mg./liter. Past this point the difference in solution concentration due to adsorption was too small to yield good results. These experiments were performed in 8.0×10^{-4}N sodium hydroxide. Contact times for equilibrium experiments were always in excess of 29 hours. The rate tests described later show that the system has achieved equilibrium after this period of time. The results of all equilibrium experiments are tabulated in Appendix IV.

The kinetics data were obtained by a batch method. A series of adsorption tubes were loaded at identical conditions of polymer, solvent, and fibers and placed on the agitation apparatus. At preselected times a tube was removed and sampled for polymer analysis. In this way, the entire rate curve could be constructed by varying the length of contact time between fibers and polymer. Rate data were obtained for Fractions 63-4 through 63-8 in 8.0×10^{-4} N sodium hydroxide to determine the effect of molecular weight on the rate. The importance of ionic strength was assessed by measuring the rate of adsorption of Fraction 63-8 in 8.0×10^{-4} N sodium hydroxide at sodium chloride concentrations of 0, 2, and 5 millimolar. The rate of adsorption of Fraction 63-7 was evaluated at five different initial concentrations between 27.4 and 191 mg./liter. Fraction 63-7 was also used to make a run in 8.0×10^{-5} N sodium hydroxide. To determine the effect of agitation, one run was made at a rotation rate of 45 r.p.m. and an angle of 30°. All other runs were made at 4.5 r.p.m. and 15°. The fiber content was held at 0.29% for all rate determinations. The results of the kinetics experiments are tabulated in Appendix V.

EXPERIMENTAL DATA AND DISCUSSION OF RESULTS

DIFFUSION EXPERIMENTS

EFFECT OF MOLECULAR WEIGHT

The concentration-diffusion coefficient curves for Fractions 63-4 through 63-8 are shown in Fig. 10 and 11. These data were taken in 8.0×10^{-4} N sodium hydroxide to match the conditions of the sorption tests. The diffusion coefficients were calculated according to the Creeth method and thus the concentration is expressed as the average concentration in the cell. A concentration of twenty fringes corresponds to approximately 500 mg./liter. It should be noted that the points for the lowest concentrations (less than five fringes) are highly uncertain due to the very few fringes available for analysis.

Two trends are readily apparent in Fig. 10 and 11. The diffusion coefficients of the higher molecular weight samples are much more sensitive to concentration changes than are those for the smaller molecules. The effect of polymer concentration on the diffusion coefficient may be due to either a thermodynamic or a hydrodynamic factor. The thermodynamic factor reflects deviations from solution ideality and, in general, causes the diffusion coefficient to increase with concentration. The hydrodynamic factor is a result of interactions between the motion of particles. This interaction has the effect of increasing the friction factor and thus decreasing the diffusion coefficient. Apparently, the thermodynamic factor predominates over the range of conditions studied.

The second trend is the decrease in the diffusion coefficient at infinite dilution, D_o, with increasing molecular weight. This is a result of the larger friction coefficient for the higher molecular weight species. The molecular weight-dependence is more clearly illustrated in Fig. 12 and Table I. In a study

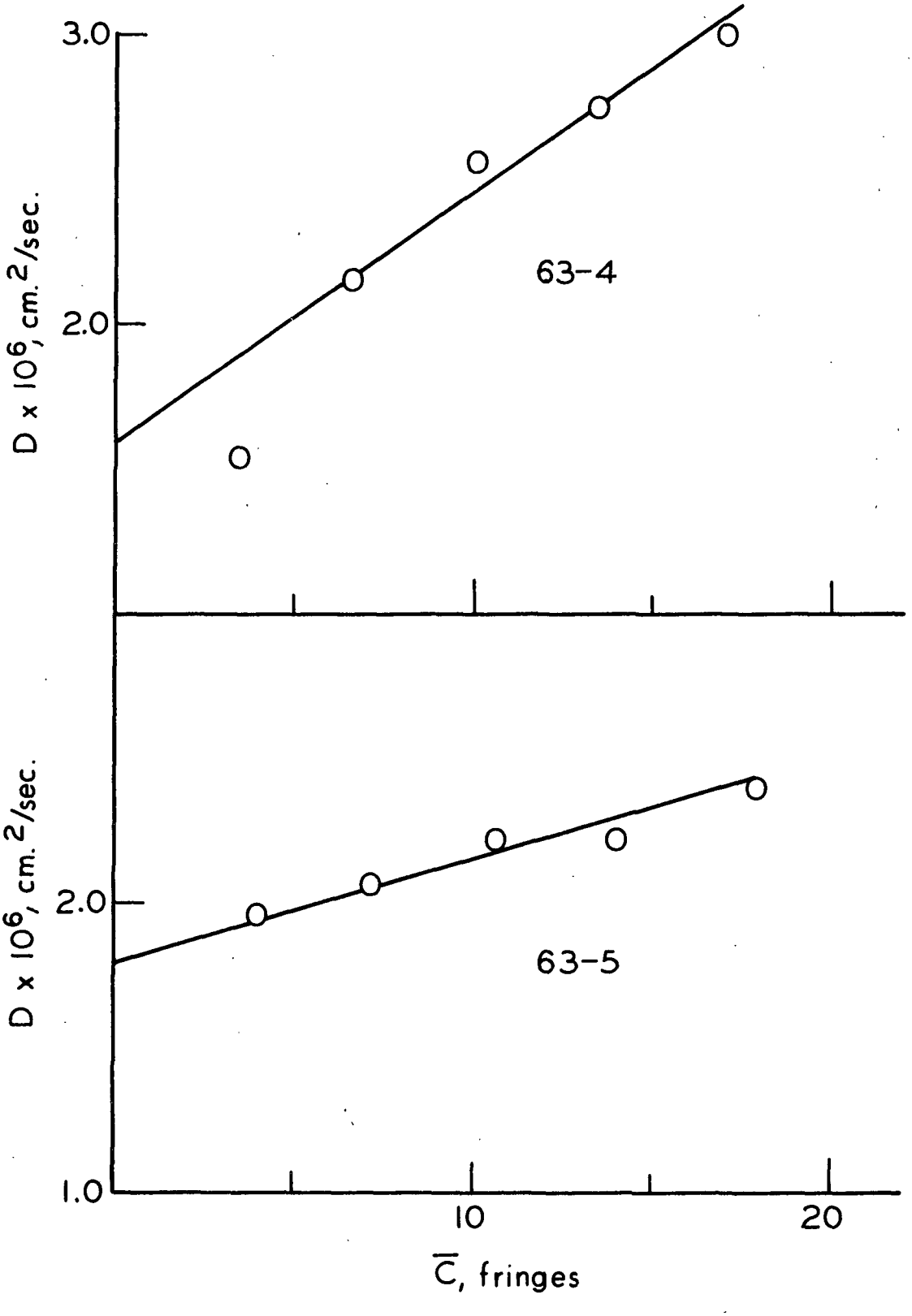

Figure 10. Effect of Concentration on Diffusion Coefficient

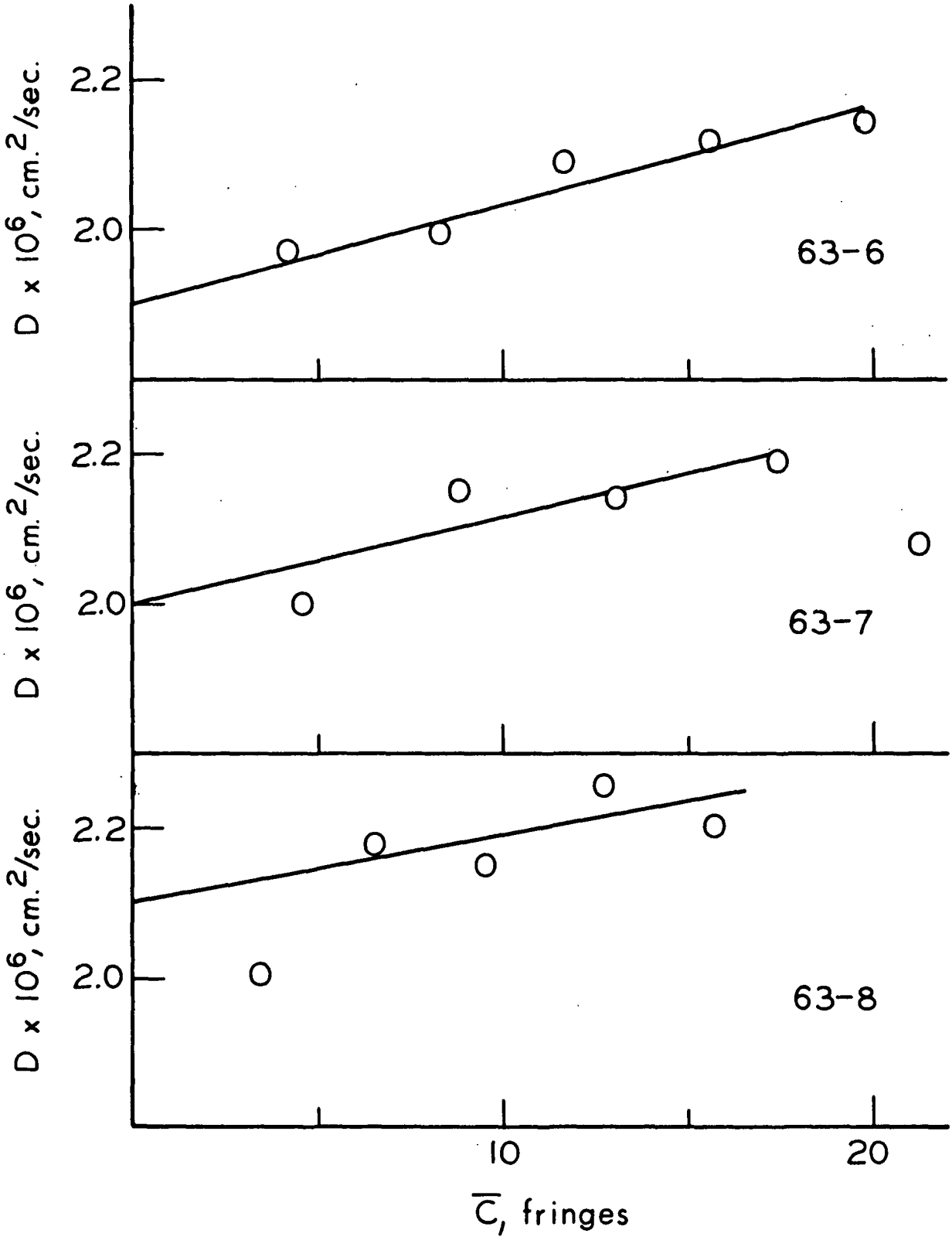

Figure 11. Effect of Concentration on Diffusion Coefficient

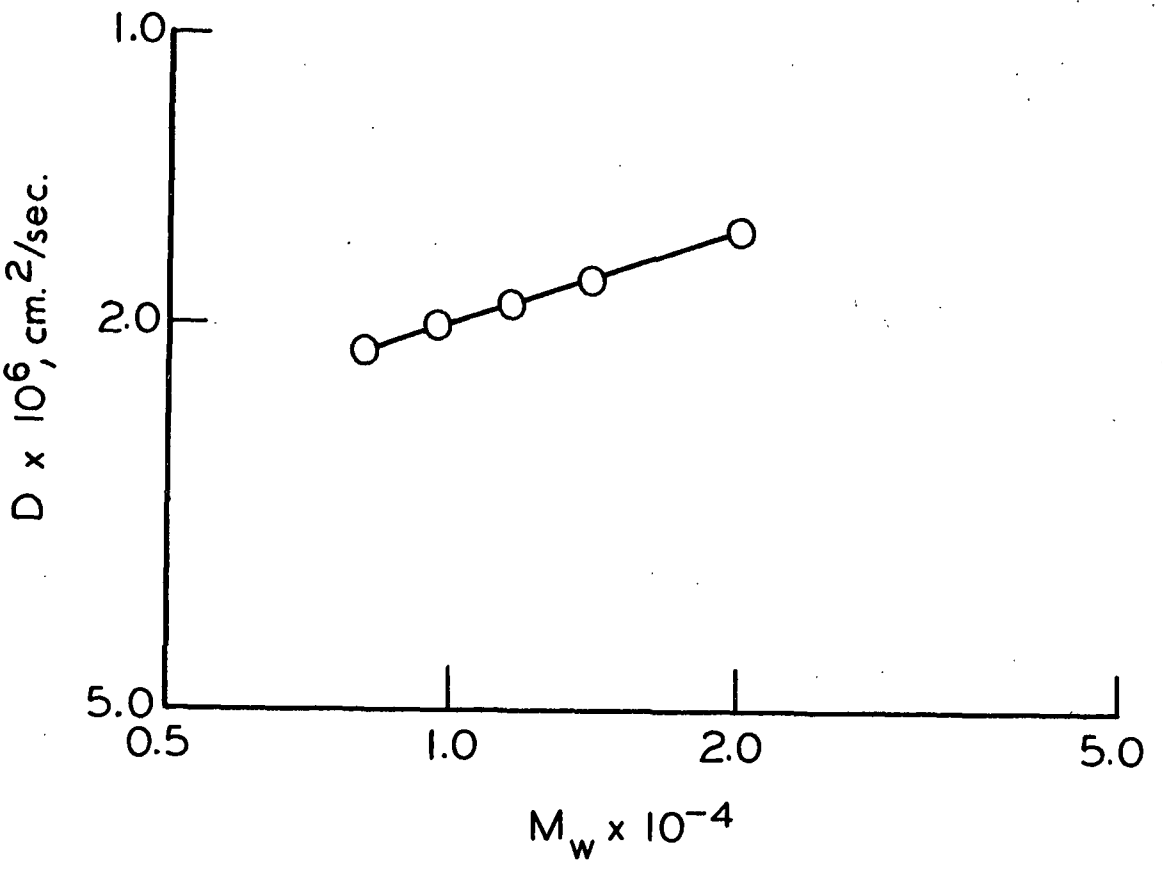

Figure 12. Effect of Molecular Weight on Diffusion Coefficient

TABLE I

DIFFUSION COEFFICIENTS AT INFINITE DILUTION

Fraction Number	Molecular Weight	Solution pH	NaCl Concn., mM	$\underline{D}_o \times 10^6$, cm.^{2}/sec.
63-8	8,00	10.9	0.0	2.1
63-8	8,000	10.9	2.0	1.69
63-8	8,000	10.9	5.0	1.25
63-7	9,500	10.9	0.0	2.0
63-7	9,500	9.5	0.0	2.6
63-6	11,500	10.9	0.0	1.90
63-5	14,000	10.9	0.0	1.80
63-4	20,000	10.9	0.0	1.60

of the diffusion behavior of poly-L-lysine, Daniel and Alexandrowicz (48) found a linear relationship between the logarithm of the degree of polymerization and the logarithm of the diffusion coefficient. According to Fig. 12 this linear relationship holds for the fractions of PEI studied.

For comparison with the data reported herein, Thompson, et al. (49) report a diffusion coefficient at infinite dilution of 1.6×10^{-6} cm.^{2}/sec. for an unfractionated sample of PEI (10,300 molecular weight) in pure water.

EFFECT OF IONIC STRENGTH

The diffusion coefficient of Fraction 63-8 was measured in 0, 2, and 3 millimolar sodium chloride plus 8.0×10^{-4}N sodium hydroxide in every case to match the conditions of the sorption tests. The concentration-diffusion coefficient curves for these experiments are shown in Fig. 13. The diffusion coefficients at infinite dilution are tabulated in Table I. Over the range of concentrations studied, there appears to be very little change in the slope due to the presence of sodium chloride. The diffusion coefficient at infinite dilution, however, decreases sharply on the addition of salt.

The effect of salt concentration on the diffusion coefficient is not well defined in the literature. Two references will be cited for comparison with the data obtained in this study. Daniel and Alexandrowicz (48) studied the diffusion of poly-L-lysine and found that by increasing the concentration of sodium chloride, the slope of the diffusion coefficient versus polymer concentration curve decreased. The range of sodium chloride concentration investigated was much higher than that studied in this work, from 0.01 to 1.0M. The authors found no significant change in the limiting diffusion coefficient with changing salt concentration. The limiting diffusion coefficient is defined as the coefficient at infinite dilution.

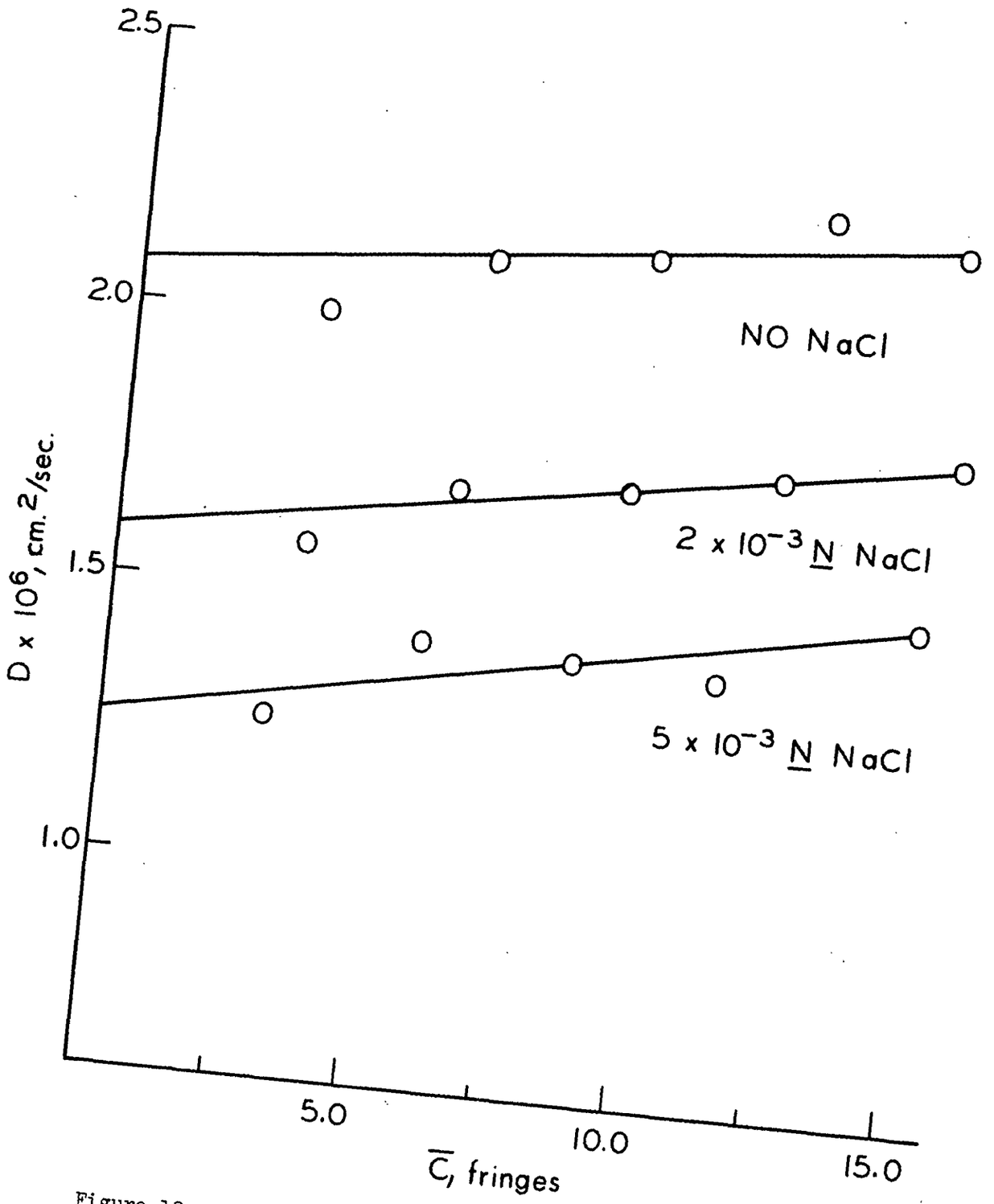

Figure 13. Effect of Sodium Chloride on Diffusion Coefficient

In an investigation of the diffusion coefficient of poly(sodium styrenesulfonate) in sodium chloride solutions, Suzuki, et al. (35) also found a marked decrease in the slope of the diffusion coefficient versus polymer concentration curve on increasing salt concentration. These authors, however, noted that the curves crossed at a polymer concentration of about 0.04 g./100 ml. This led to the observation that the limiting diffusion coefficient of poly(sodium styrenesulfonate) increases with increasing ionic strength. The range of sodium chloride concentrations studied was from 0.005 to 0.2M; again, much higher than that reported herein. Polymer concentrations studied varied from 0.04 to 0.4 g./100 ml. Over this range the authors found a significant positive deviation from linearity at higher concentrations when the diffusion coefficient was plotted as a function of polymer concentration. The data plotted in Fig. 13 (corresponding to a concentration range of from about 0.1 to 0.5 g./100 ml.) show no such upward curvature at the higher concentrations. The data of Daniel and Alexandrowicz also remain linear over the range studied (up to about 0.3 g./100 ml.).

It would appear that the differences in the three sets of data are due to differences in the degree of ionization of the three polymers, in the thermodynamic behavior of the systems, and possibly in the range of ionic strengths studied. Information on the degrees of ionization are not available. Another possible source of discrepancy is in the wide differences in the molecular weights of the polymers; 320,000 for the poly(sodium styrenesulfonate), 60,000 for the poly-L-lysine, and 8,000 for the PEI. It should be noted that all solutions were dialyzed against the solvent prior to the diffusion measurements.

EFFECT OF pH

The data shown in Fig. 14 illustrate the effect of sodium hydroxide concentration on the diffusional behavior of Fraction 63-7 in the absence of added salt.

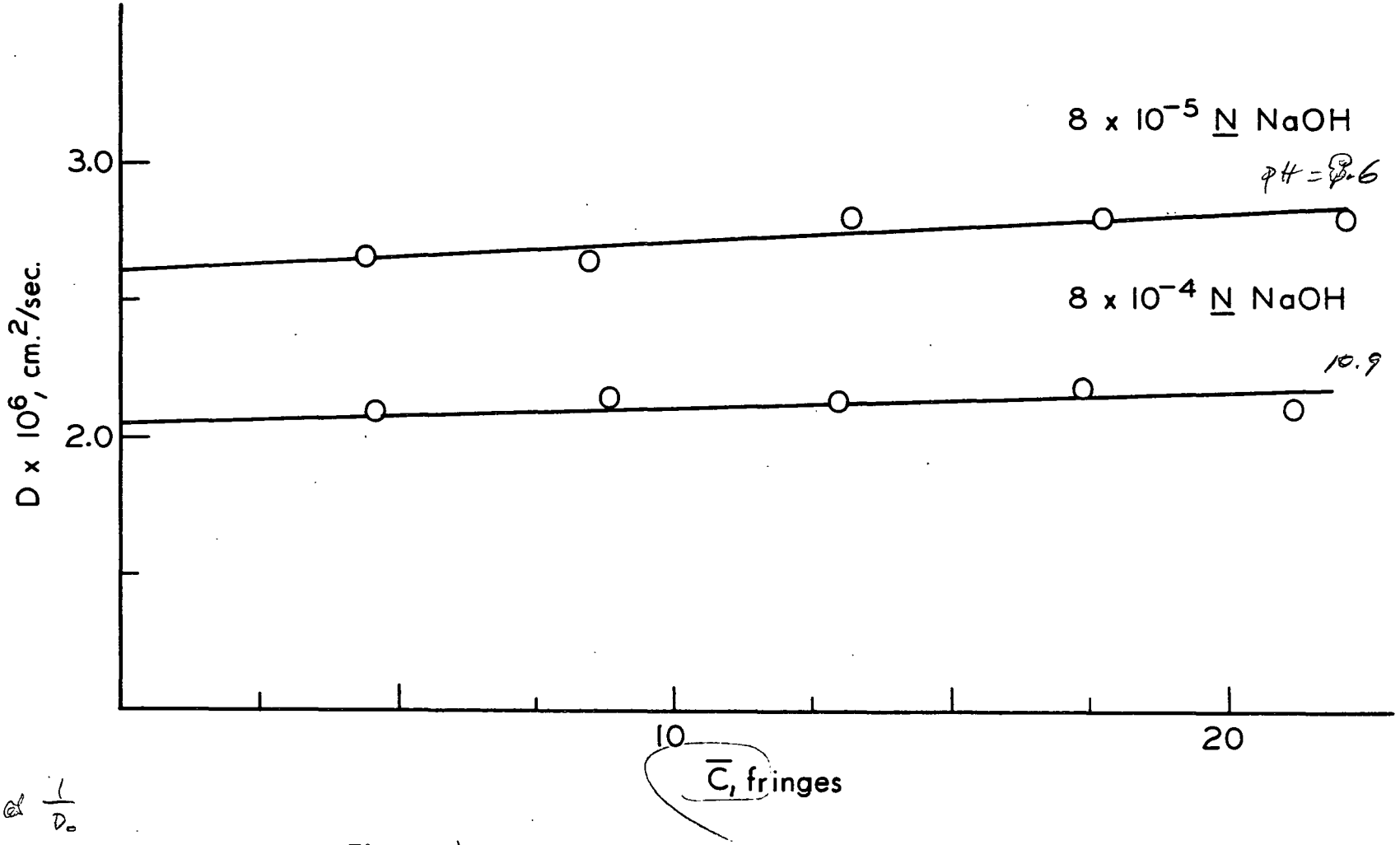

Real $\frac{1}{D_o}$

Figure 14. Effect of Sodium Hydroxide on Diffusion Coefficient

⇒ as pH ↑ (molecule getting smaller), diffusion coefficient ↓ ?

- doesn't agree ≈ Hoo's on p. 47.

The diffusion coefficients at infinite dilution are tabulated in Table I. The pH of the solutions in 8.0×10^{-5} N sodium hydroxide was about 9.6 while that in 8.0×10^{-4} N was about 10.9. Qualitatively, it may be said that an increase in the degree of ionization (decrease in hydroxide ion concentration) produces a more rapidly diffusing polymer. Kedem and Katchalsky (34) measured the diffusion coefficient of polymethacrylic acid over a range of polymer concentration and degree of ionization in the absence of added salt. These authors noted that the diffusion coefficient increased rapidly on going from a degree of ionization of zero to 0.15. It was found that the diffusion coefficient was only slightly affected by changes in polymer concentration.

DISCUSSION OF POLYELECTROLYTE DIFFUSION

A fundamental application of the diffusional theory of polyelectrolytes to the PEI system is outside the scope of this dissertation. It is informative, however, to consider the behavior of PEI in terms of theories proposed by others.

Nagasawa and Fujita (33) concluded on theoretical grounds that there are three factors which could affect the diffusion of a polyelectrolyte: (1) changes in molecular configuration due to intramolecular electrostatic repulsions; (2) electrophoretic interactions between polyion, counterions, and solvent; (3) changes in the osmotic or second virial coefficient. On the basis of data obtained with poly(styrenesulfonic acid) the authors concluded that only the first two effects operated on the diffusion coefficient.

Kedem and Katchalsky (34) studied the diffusion of polymethacrylic acid and found that, depending on experimental conditions, all three effects may apply. A comparison of the diffusion coefficient with the degree of ionization showed a very rapid increase in the diffusivity of the polymer up to about 15% ionization. The diffusion

coefficient was observed to decrease slightly between 15 and 25% ionization and then increase to another maximum at about 50% ionization. The authors reasoned that the extreme charge-dependence up to 15% ionization is due to the electrophoretic effect. That is, in this region there is a rapid increase in the number of counterions which exert a strong drag effect on the macromolecule. The more mobile counterions tend to diffuse ahead of the charged macroion and, in the process, create an unstable separation of charge. This charge separation causes the macromolecule to diffuse more rapidly than if it were uncharged. Between 15 and 25% ionization the polymer chain opens up and decreases the diffusion coefficient due to an increase in the friction factor. Above 50% ionization the large electrostatic field diminishes the osmotic coefficient which causes a decrease in the diffusion coefficient.

Alexandrowicz and Daniel (36) presented a theoretical analysis of the diffusion of a polyelectrolyte. They concluded that, unless the molecular configuration changes significantly with ionic strength, the limiting diffusion coefficient should be independent of salt concentration. Nagasawa and Eguchi (50), however, have shown that the electrophoretic effect does not fall out on extrapolation of sedimentation data to zero polymer concentration. Since the electrophoretic effect is similar in both sedimentation and diffusion, it may be expected to affect the limiting diffusion coefficient. Suzuki, et al. (35) provide evidence that the limiting diffusion coefficient is affected by both the electrophoretic effect and changes in the macromolecular configuration.

Since the degree of ionization is only a few percent or less for PEI under the conditions tested, intramolecular electrostatic repulsions are probably not sufficient to cause much macroion expansion. Therefore, the electrophoretic effect must be the important factor in causing the observed response of the diffusion coefficient to changes in the ionic strength and the solution pH. The electrophoretic effect would

cause an increase in the diffusion coefficient with the degree of ionization (decreasing pH) due to a larger number of the more mobile counterions per macroion. An increase in ionic strength would decrease the electrophoretic effect by decreasing the driving force for counterion diffusion. These predictions are compatible with experimental observations for the diffusion of PEI.

On the basis of the above findings it may be tentatively concluded that the electrophoretic effect is responsible for the observed diffusional behavior of PEI with respect to changes in ionic strength and polymer charge density. Due to the paucity of diffusional data and the lack of auxiliary data, it is not possible to completely rule out the other effects.

EQUILIBRIUM ADSORPTION EXPERIMENTS

EFFECT OF pH

It was necessary to ascertain the pH-dependence of adsorption in order to determine the optimum pH for the kinetic experiments. The effect of pH on the equilibrium adsorption of Fraction 63-6 is shown in Fig. 15. The pH was adjusted with sodium hydroxide and hydrochloric acid. The initial polymer concentration was 96.0 mg./liter and the fiber consistency was 0.29%. The sensitivity to pH above pH 9.0 is similar to that observed for the sorption of PEI onto unbleached kraft pulp as reported by Sarkanen, et al. (37). In order to determine if the pH-dependence is affected by polymer molecular weight, the experiment was repeated with Fractions 63-8 and 63-2 as well as unfractionated PEI-63. The results of these experiments are presented in Fig. 16. It is apparent that the magnitude of adsorption is strongly dependent on molecular weight. The pH, however, appears to affect the adsorption of each of the fractions in a similar manner. In every case, the maximum adsorption occurs at around pH 10.8-11.0.

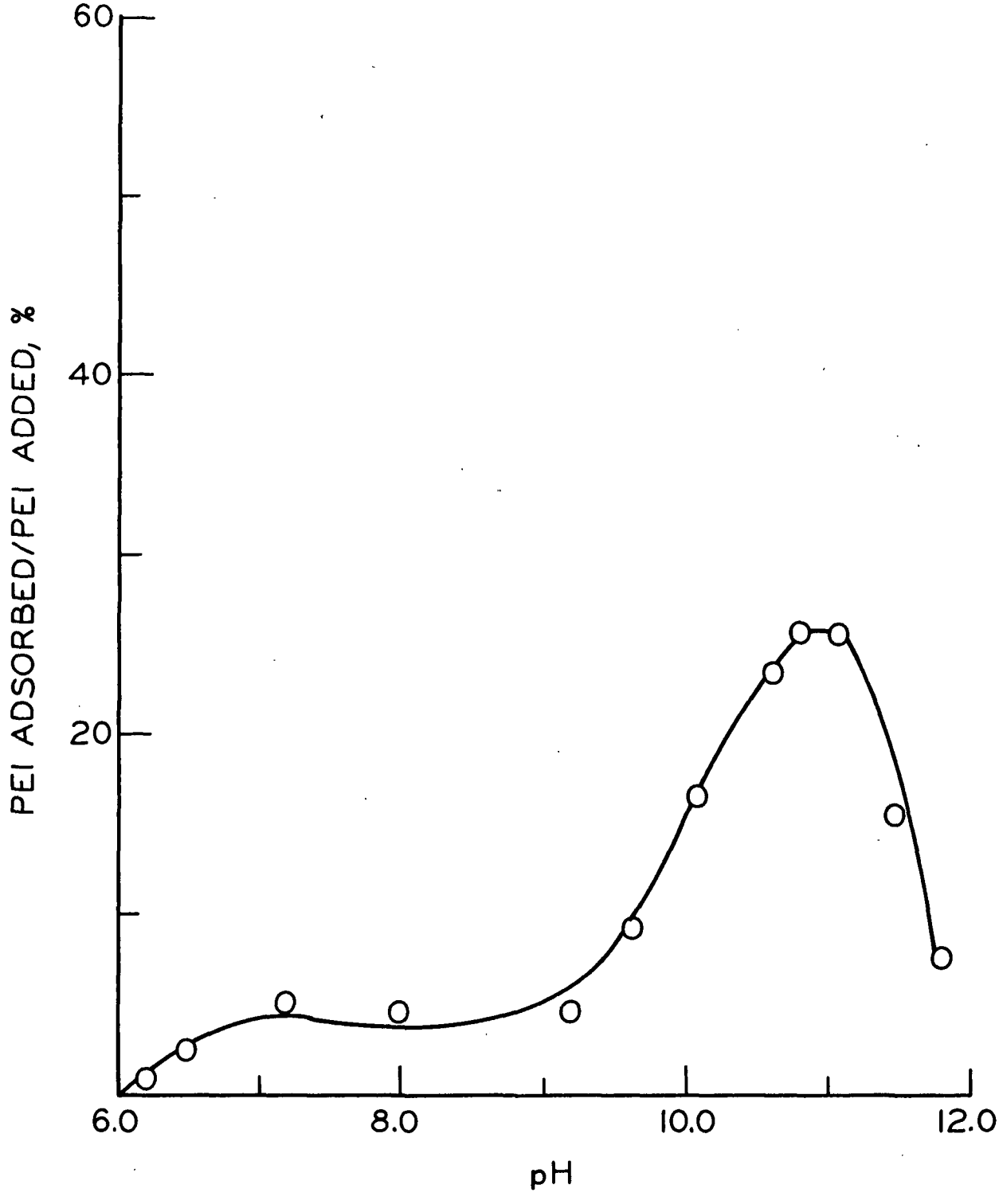

Figure 15. Effect of pH on Retention

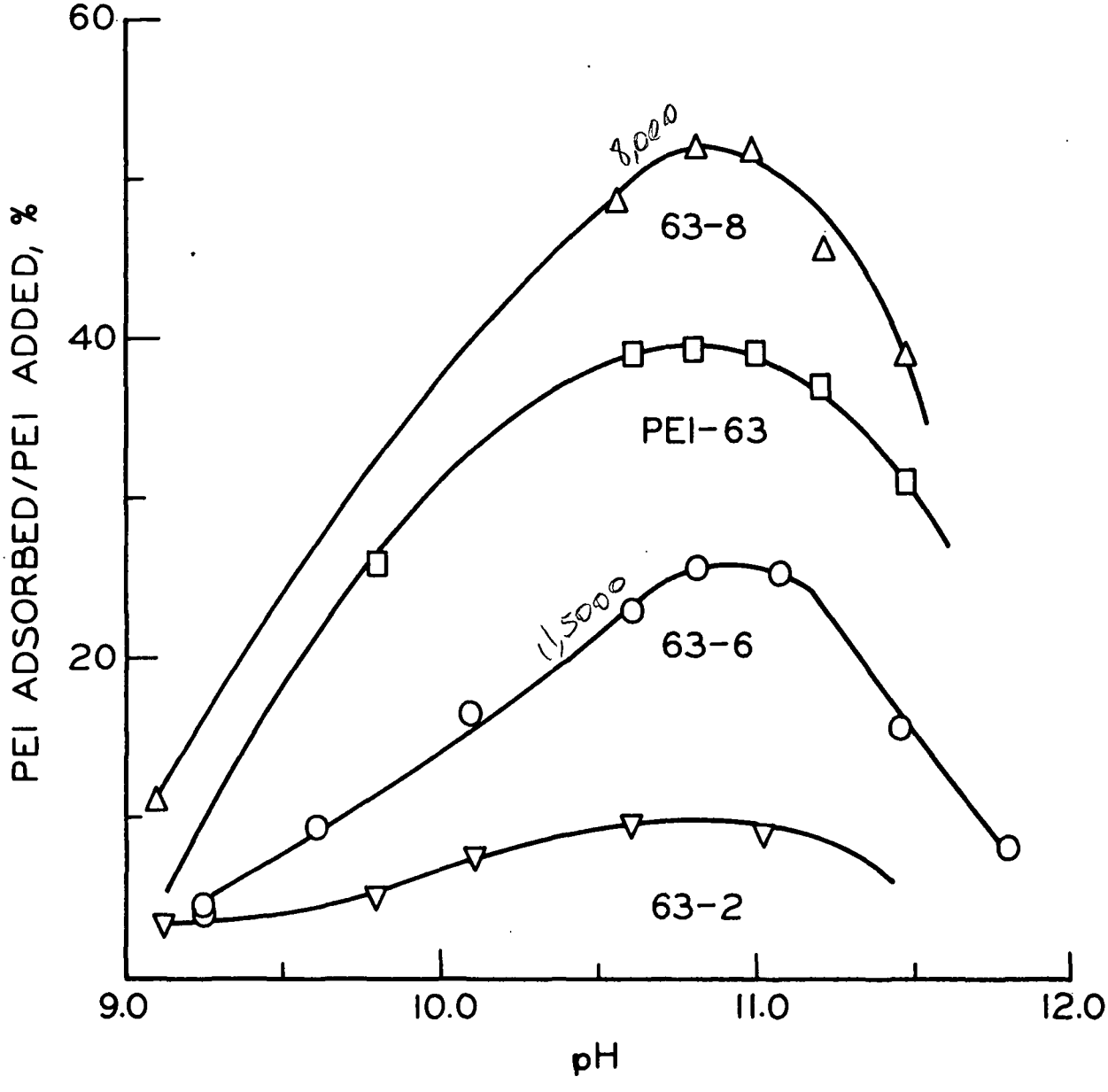

Figure 16. Effect of pH on Retention

Kindler's Thesis

Rate of polymer adsorption was ~~floated by~~ increased by

1) ~~Co~~ = increasing Co
2) ~~decrease~~ ~~decreasing~~ increasing pH
3) decreasing ionic strength
4) decreasing MW
5) agitation

PEI → control # SA 1117 - 633974

Fraction #	Mw
63-8	8,000
63-7	9,500
63-6	11,500
63-5	14,000
63-~~4~~	20,000

The role of the fiber carboxyl content was briefly investigated. The adsorption of unfractionated PEI-63 onto oxidized RD-101 fibers was measured as a function of pH. These fibers were oxidized by a chromic acid treatment which caused significant degradation of the cellulose. A large amount of colloidal-sized material was generated which could not be removed entirely by washing. This material passed through the sampling tube and thus interfered somewhat with the analysis. For this reason, the magnitudes shown in Fig. 17 must not be interpreted quantitatively. It can be stated, however, that an increase in the carboxyl content of the fibers has the effect of broadening the maximum and shifting it downward on the pH scale.

EFFECT OF MOLECULAR WEIGHT AND POLYMER CONCENTRATION

Equilibrium adsorption isotherms were constructed for each of Fractions 63-4 through 63-8. These measurements were required in order to determine the Langmuir constants which are essential to the theoretical rate curve calculations. In addition, the equilibrium data provide auxiliary information useful to the interpretation of the rate data.

The Langmuir equation was derived under a set of assumptions which certainly do not apply to polymer adsorption. Silberberg (2, 51), however, has shown theoretically that the Langmuir form should be followed for most polymer adsorption systems.

The Langmuir equation is given as follows:

$$\Gamma = K \Gamma_m C_e/(1 + KC_e), \qquad (7)$$

where Γ is the specific adsorption at equilibrium concentration C_e, Γ_m is the specific adsorption at saturation, and K is the Langmuir constant. The Langmuir constant is often referred to as the "affinity" for adsorption. By expressing adsorbed polymer in terms of concentration and rearranging, the Langmuir equation can be written as follows:

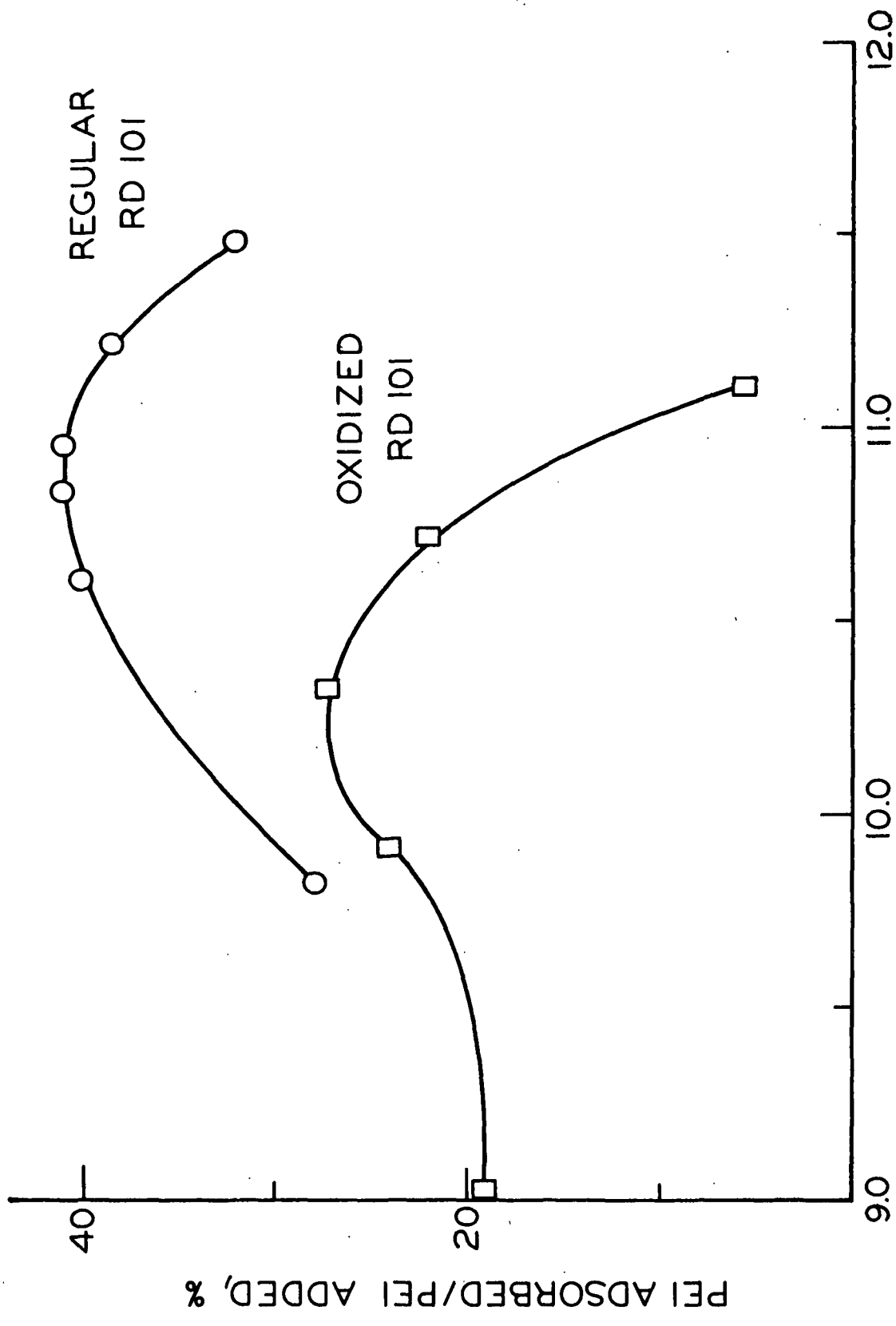

Figure 17. Effect of Oxidation on Retention

$$\frac{C_e}{C_e^*} = \frac{1}{C_m K} + \frac{C_e}{C_m} \qquad (8)$$

where C_e^* is the loss in solution concentration due to sorption at C_e, and C_m is the loss in solution concentration when the substrate is saturated with adsorbate. According to Equation (8), Langmuir behavior implies a linear relationship between C_e and C_e/C_e^*. The slope should equal C_m^{-1} and the intercept is equivalent to $(C_m K)^{-1}$.

The results of the equilibrium experiments are shown in Fig. 18 through 22 for the five fractions studied in 8.0×10^{-4} N sodium hydroxide. In each case the polymer solution was agitated in a slurry of 0.29% fiber solids for 29 hours. The results are presented according to Equation (8) along with the standard isotherm presentation of Γ vs. C_e. The Langmuir constants were determined from these plots and are tabulated in Table II for each of the fractions studied.

TABLE II

LANGMUIR CONSTANTS AND SATURATION ADSORPTION VALUES FOR FRACTIONS OF PEI

Fraction	M_w	K, liter/mg.	C_m, mg./liter
63-4	20,000	0.015	17.0
63-5	14,000	0.0091	34.0
63-6	11,500	0.0081	57.0
63-7	9,500	0.020	65.0
63-8	8,000	0.082	78.0

The amount of polymer adsorbed at saturation is clearly greater for the smaller molecules. This is interpreted as a direct reflection of the differences in accessibility due to the porous nature of the adsorbent. The larger molecules are

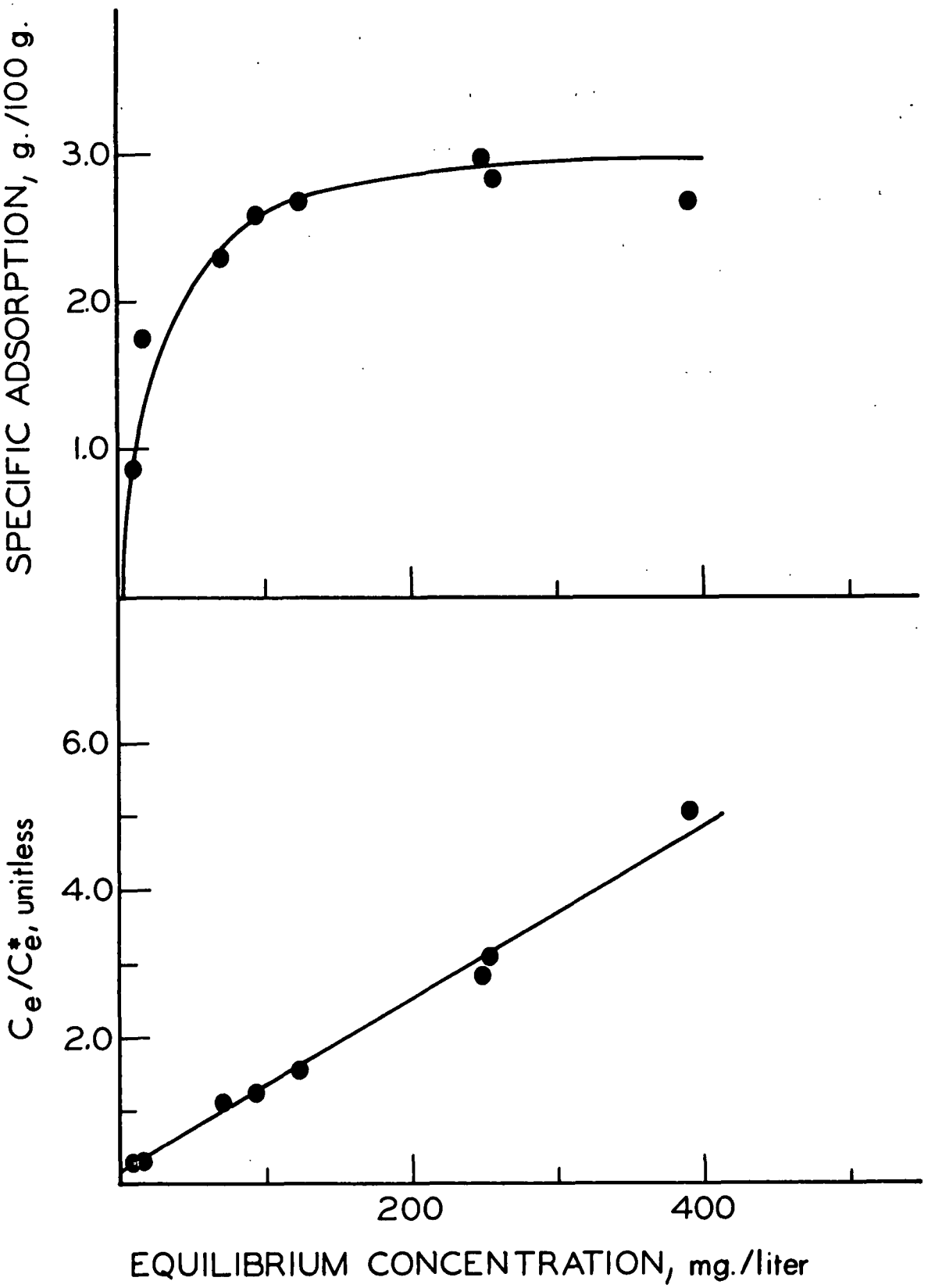

Figure 18. Equilibrium Isotherms for 63-8 ($\underline{M}_w$ = 8000) in 8.0 x 10^{-4} $\underline{N}$ NaOH

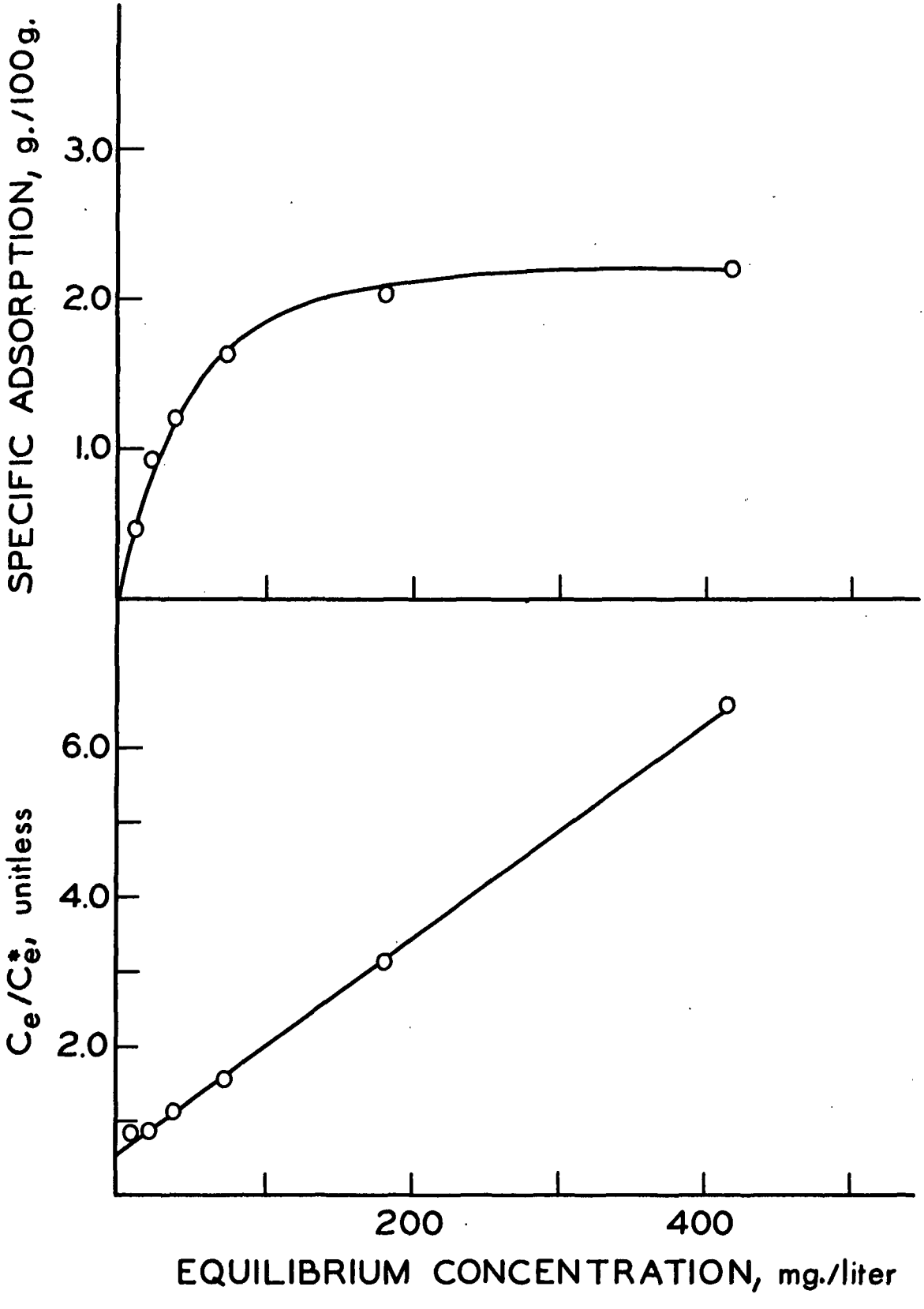

Figure 19. Equilibrium Isotherms for 63-7 ($\underline{M}_{\underline{w}}$ = 9500) in 8.0 x 10^{-4} $\underline{N}$ NaOH

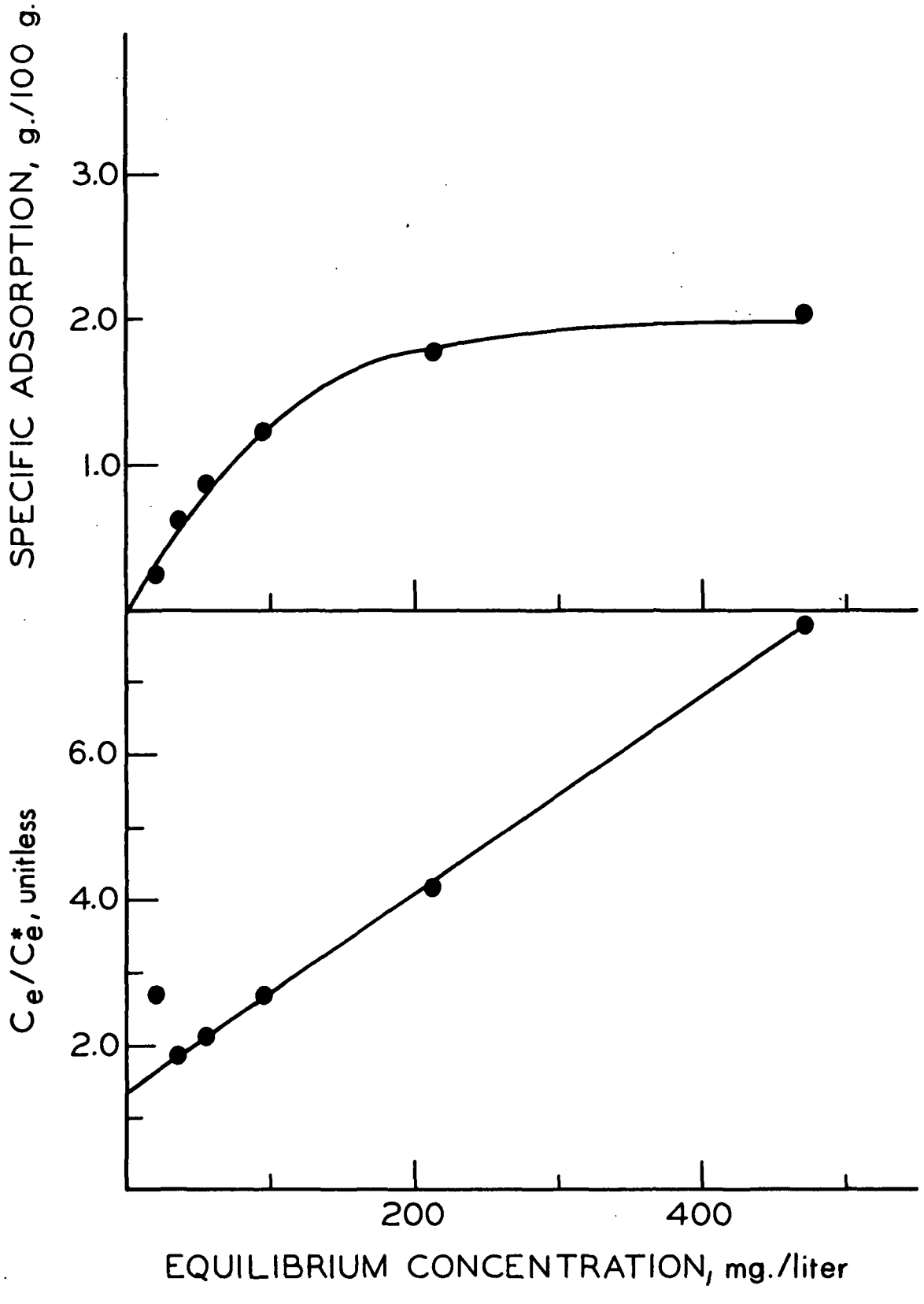

Figure 20. Equilibrium Isotherms for 63-6 ($\underline{M}_w$ = 11,500) in 8.0 x 10^{-4} $\underline{N}$ NaOH

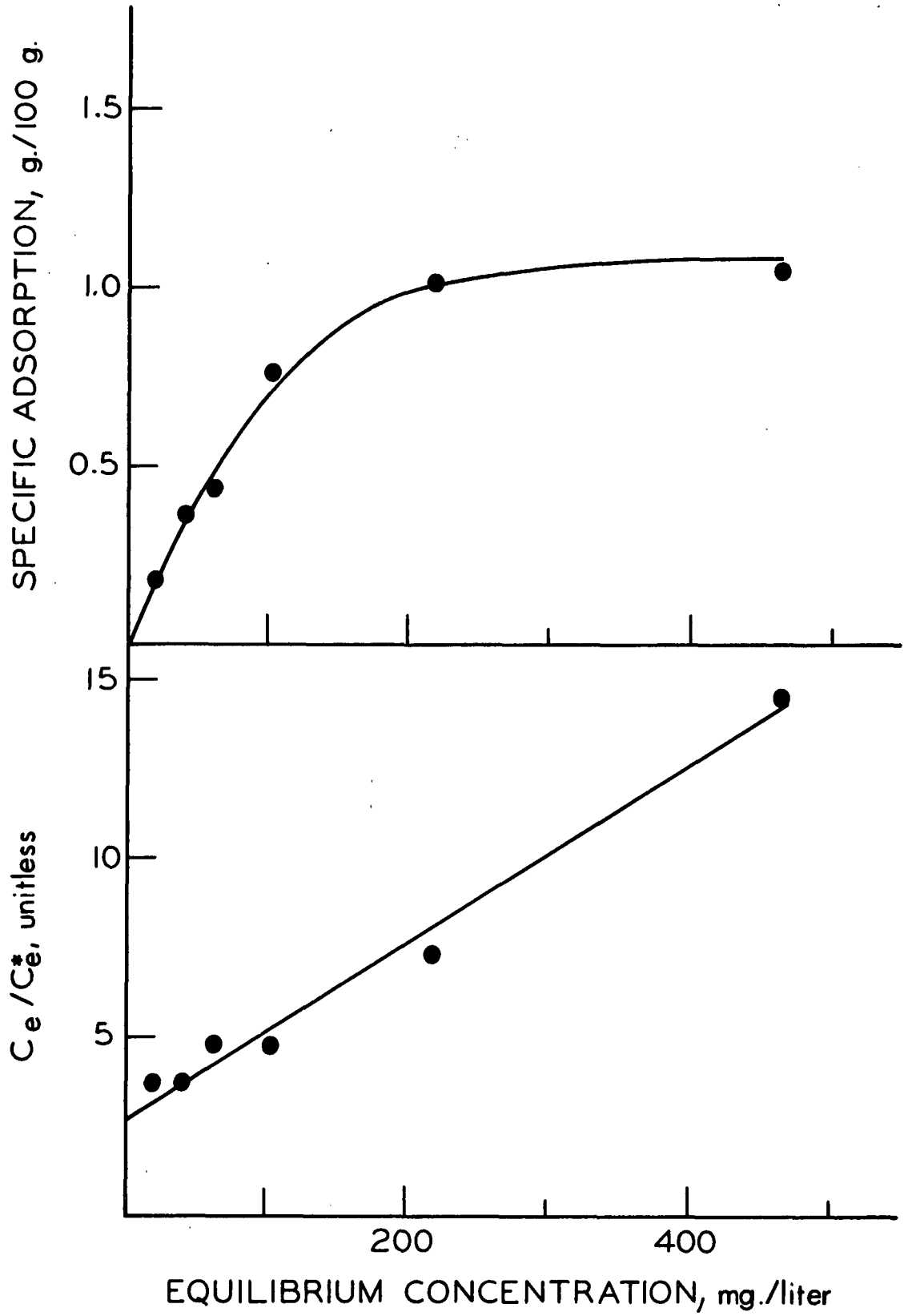

Figure 21. Equilibrium Isotherms for 63-5 ($\underline{M}_{\underline{w}}$ = 14,000) in 8.0 x 10^{-4} $\underline{N}$ NaOH

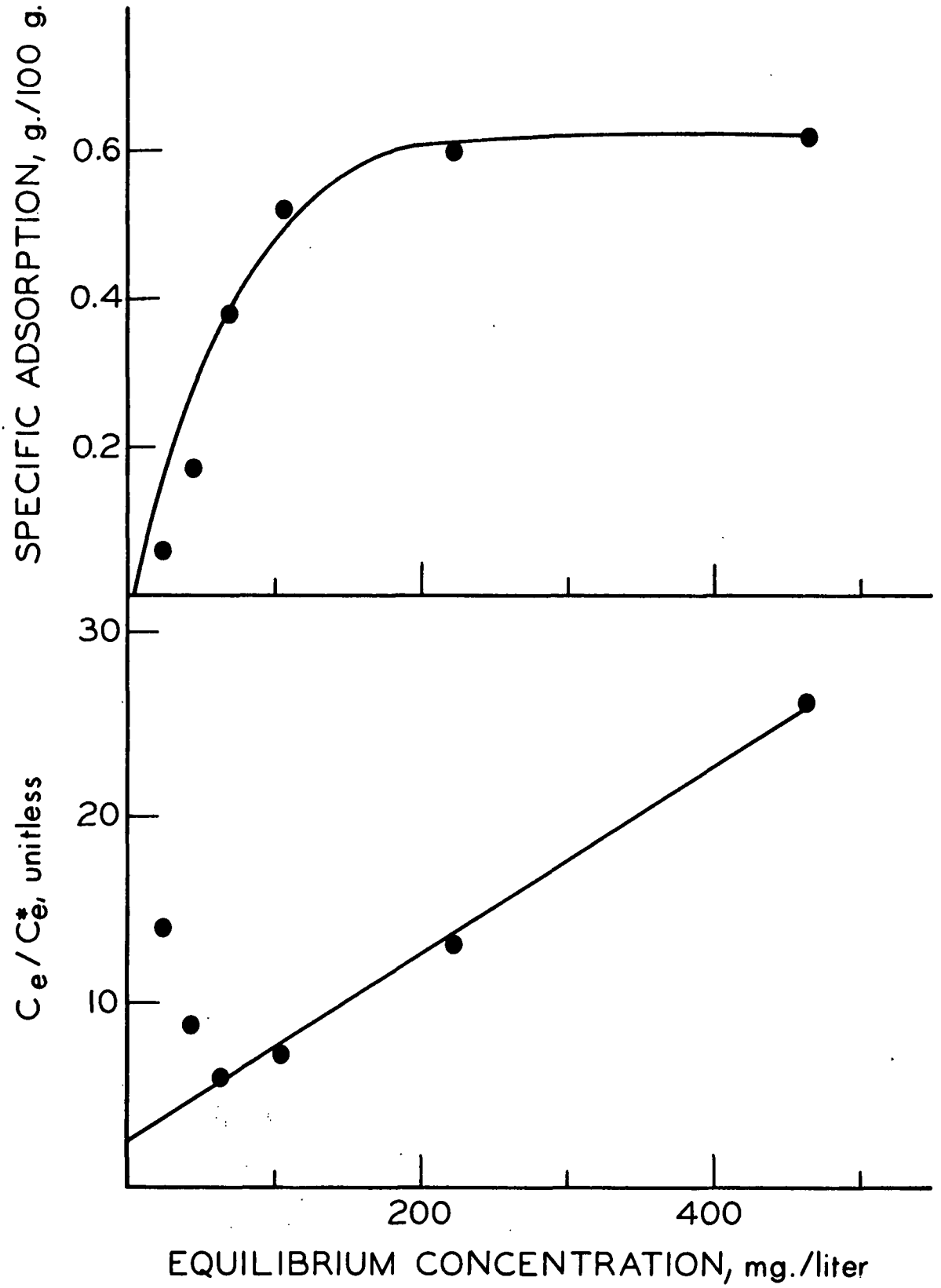

Figure 22. Equilibrium Isotherms for 63-4 ($\underline{M}_w$ = 20,000) in 8.0 x 10^{-4} $\underline{N}$ NaOH

apparently excluded from a significant portion of the fiber which is accessible to the lower molecular weight fractions.

The Langmuir constant does not exhibit a uniform trend with respect to molecular weight. This is caused, at least in part, by the large error in determining these values and the low magnitudes involved. The Langmuir constant may be dependent upon two opposing molecular weight effects. The accessibility factor would lead to a decrease in the Langmuir constant with increasing molecular weight. On the other hand, the thermodynamic factor would produce an increase in $\underline{K}$ with increasing molecular weight. The data may reflect the relative effects of these two mechanisms.

An equilibrium isotherm was also determined for Fraction 63-7 in $8.0 \times 10^{-5}\underline{N}$ sodium hydroxide. The pH of this solution was 9.6 ± 0.2 as compared with 10.9 ± 0.2 for the previous runs in $8.0 \times 10^{-4}\underline{N}$ sodium hydroxide. The constants as determined from the Langmuir equation are 19.6 mg./liter for $\underline{C_m}$ and 0.019 for $\underline{K}$. The Langmuir constant is virtually unchanged on going from pH 10.9 to 9.6 but the amount adsorbed at saturation decreases by more than a factor of three. The results of this experiment are shown in Fig. 23.

Langmuir isotherms were not measured as a function of sodium chloride concentration. For the rate curve calculations, the saturation adsorption was assumed to be independent of ionic strength. The Langmuir constant was calculated from the known $\underline{C_e^*}$ and $\underline{C_e}$ values.

DISCUSSION OF ADSORPTION MECHANISM

The mechanism of retention of cationic polyelectrolytes by cellulose fibers has received considerable attention in the past. Trout (38) has shown that the adsorption of PEI is enhanced by a high carboxyl content on the fibers and proposes

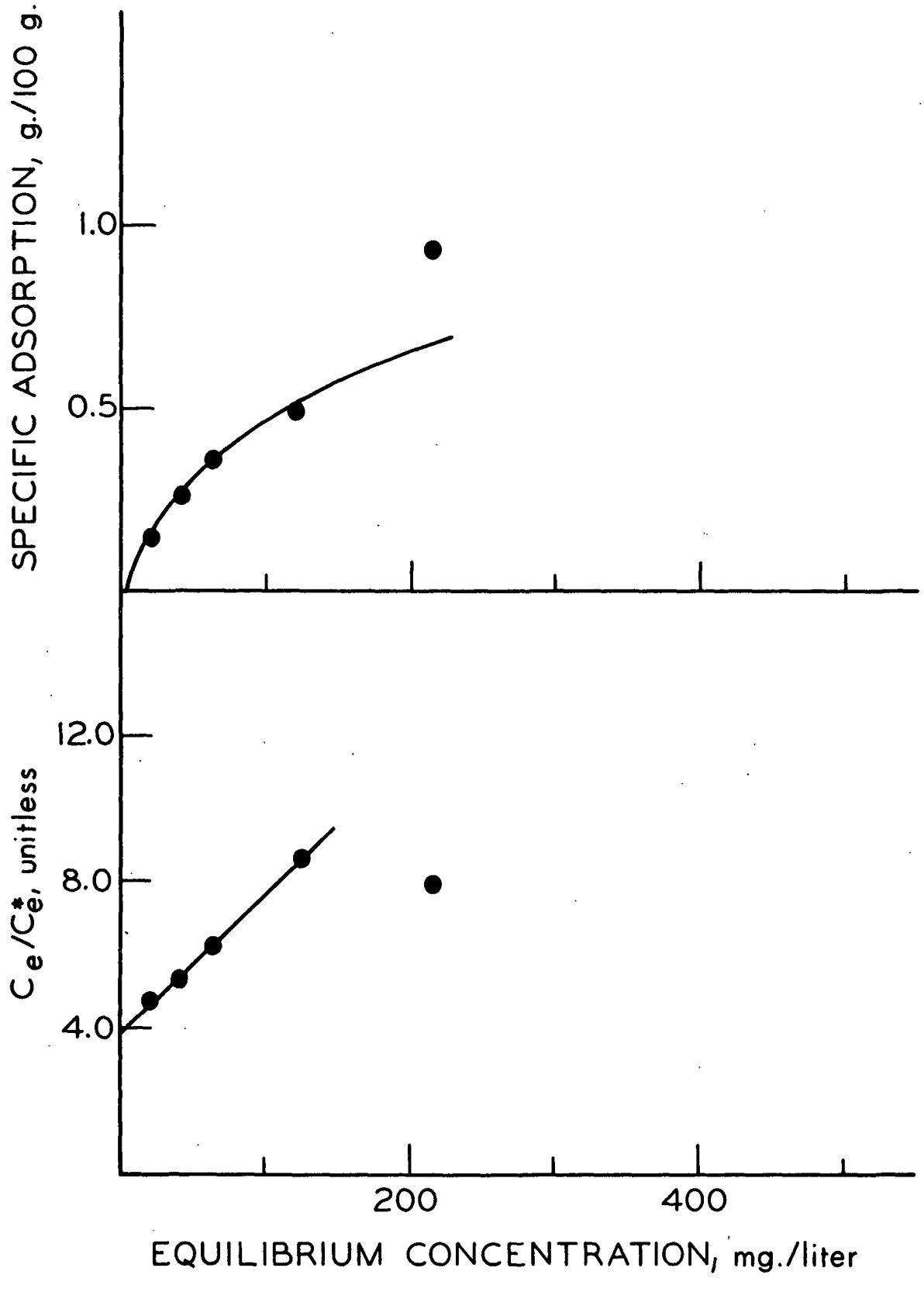

Figure 23. Equilibrium Isotherms for 63-7 ($\underline{M}_w$ = 9500) in 8.0 x 10^{-5} $\underline{N}$ NaOH

an ion-exchange mechanism. The ion-exchange reaction is thought to occur between ionized carboxyl groups on the fiber and cationic groups on the polymer. Bates (23) has recently provided evidence that polyamide-epichlorohydrin resins are adsorbed on pulp by the same mechanism. Studies of the interactions between PEI and carboxymethylcellulose have led Philipp and Lang (52) to conclude that both ion-exchange reactions and hydrogen bonding function to bind the polymer to the carbohydrate. Attempts to provide evidence substantiating covalent bond formation have been unsuccessful (53, 54).

At a sufficiently high pH, the ionization of hydroxyl groups on the cellulose chain may provide additional sites for adsorption by ion exchange. The pH at which this mechanism would become important can be estimated by examining the ionization curves of the individual components in the system.

The concentration of ionized hydroxyl groups on cellulose is plotted as a function of pH in Fig. 24. This curve is calculated on the basis of a dissociation constant (K_a) of 2×10^{-14} (55) and a fiber content of 0.29%. It is assumed that only the C-2 hydroxyl contributes to the ionization. A similar curve representing the ionization of a secondary amine is also presented in Fig. 24. The dissociation constant for ethylenediamine ($K_b = 10^{-4}$) was assumed for the polyamine. A polymer concentration of 100 mg./liter was used to prepare this curve. The concentrations of fiber and polymer were chosen to match experimental conditions. The maximum adsorption would occur at the pH at which the two curves intersect. According to Fig. 24, the optimum pH would be at about 11.4. The actual ionization constant for PEI would probably be somewhat less than that for a monomeric secondary amine due to polyelectrolyte effects. This would have the result of shifting the PEI ionization curve downward on the pH scale. The presence of carboxyl groups on the cellulose would shift the fiber ionization curve upward on the concentration scale.

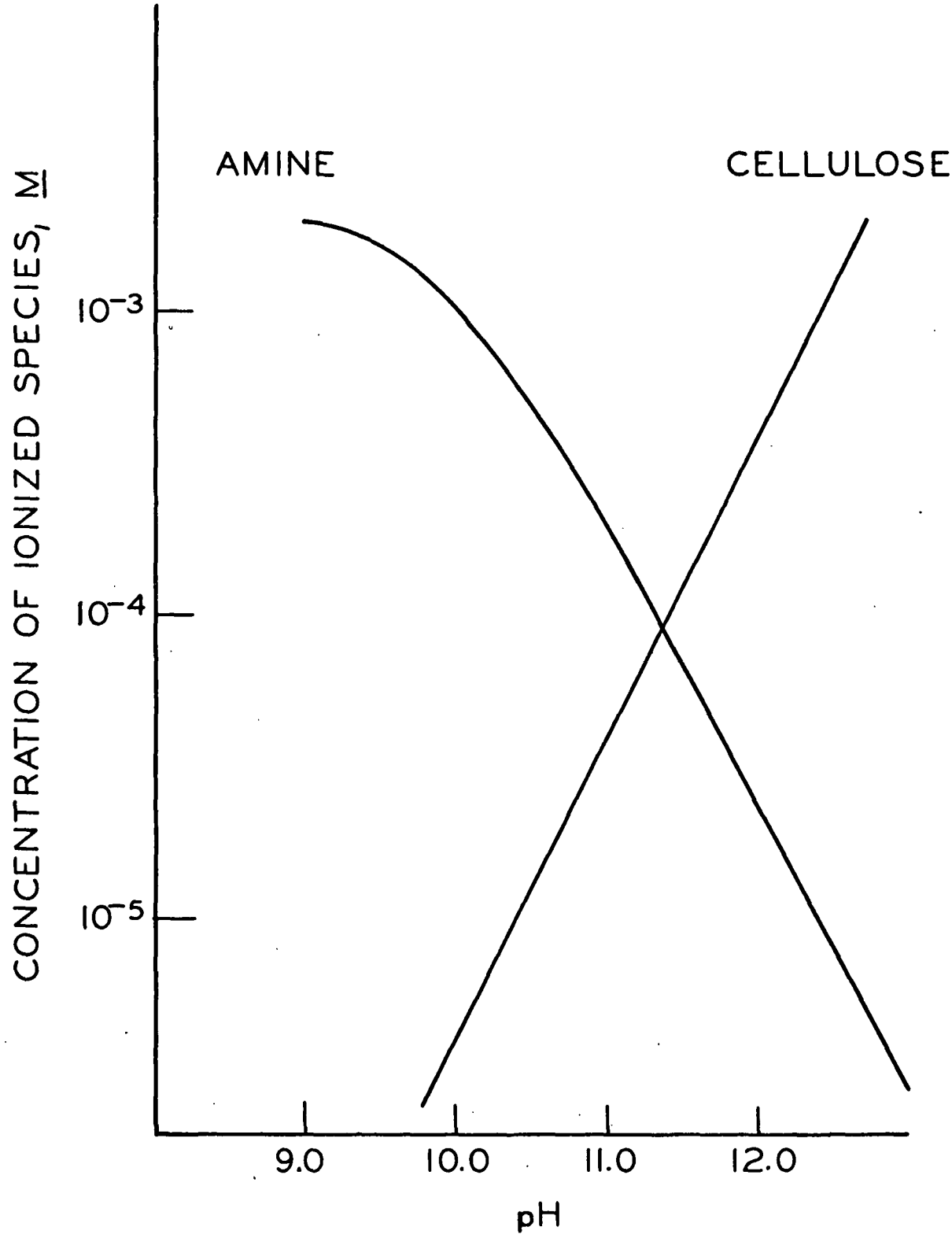

Figure 24. Ionization Curves for Secondary Amine and Cellulose

Either of these effects would cause the maximum to occur at a lower pH than the predicted 11.4. The experiments with oxidized fibers (see Fig. 17) verify that an increase in carboxyl content shifts the maximum to a lower pH. In view of these observations, the predicted maximum at 11.4 is held to be in good agreement with the observed maxima at pH 10.8. It is concluded that the predominant adsorption mechanism at high pH is an ion-exchange reaction between ionized cellulosic hydroxyls and cationic groups on the polymer. Carboxyl groups on the fiber and fiber-polymer hydrogen bonding may also contribute to the adsorption process.

RATE OF ADSORPTION EXPERIMENTS

EFFECT OF MOLECULAR WEIGHT

The adsorption rate was measured for each of Fractions 63-4 through 63-8 to cover a range of molecular weights between 8000 and 20,000. All runs were made with the RD-101 fibers at 0.29% consistency. Sorption occurred out of 8.0×10^{-4} N sodium hydroxide to give a pH of 10.9 ± 0.2. The agitation rate was constant at 4.5 r.p.m. with the tubes at a 15° angle. Initial polymer concentrations varied between 96 and 133 mg./liter. The temperature of adsorption was controlled at 25.0 ± 0.2°C.

The results of these experiments are shown in Fig. 25. Some data points at long times are left off to facilitate the construction of the plot. These data are listed in Appendix V. The initial slopes of the rate curves are estimated from Fig. 25 and tabulated in Table III. The strong dependence of the initial rate on molecular weight is evident. The initial rates must be corrected for concentration differences before quantitative interpretation is attempted. This will be done in a later section.

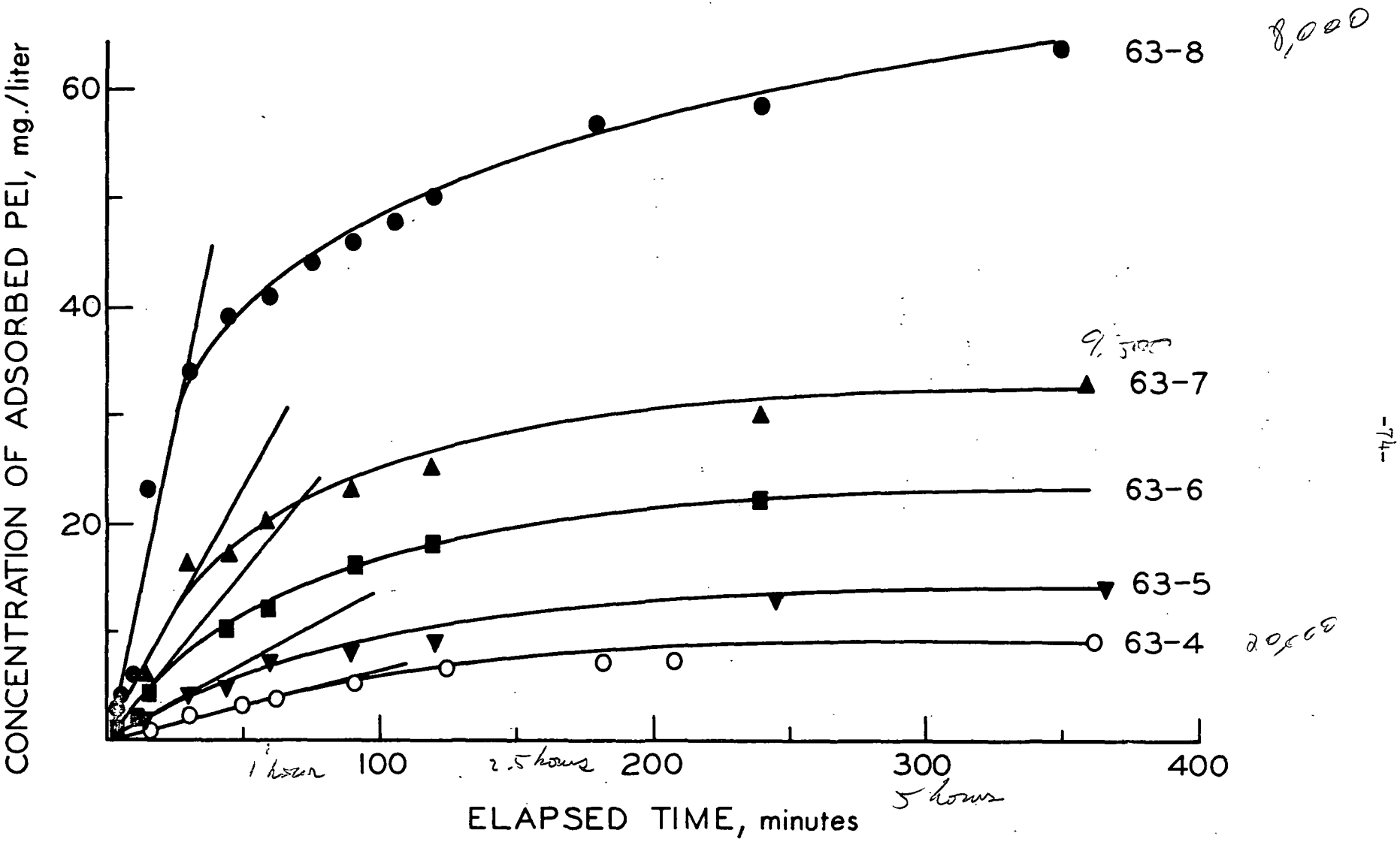

Figure 25. Effect of Molecular Weight on Sorption Rate

TABLE III

EFFECT OF MOLECULAR WEIGHT ON INITIAL RATE

Fraction Number	Molecular Weight	Initial Concn., mg./liter	Initial Rate x 10^2, mg./liter-sec.
63-8	8,000	133.0	1.87
63-7	9,500	96.0	0.74
63-6	11,500	106.0	0.50
63-5	14,000	99.0	0.23
63-4	20,000	96.2	0.11

EFFECT OF INITIAL CONCENTRATION

The adsorption rate of Fraction 63-7 was measured at a series of initial polymer concentrations ranging from 27.4 to 191 mg./liter. All other conditions were the same as those described for the molecular weight experiments. The rate curves are displayed in Fig. 26. The initial rates were estimated from the rate curves and are listed in Table IV.

TABLE IV

EFFECT OF POLYMER CONCENTRATION ON INITIAL RATE

Fraction Number	Initial Concn., mg./liter	Initial Rate x 10^2, mg./liter-sec.
63-7	191.0	1.56
63-7	137.0	1.10
63-7	96.0	0.74
63-7	54.7	0.46
63-7	27.4	0.23

The initial rate is plotted as a function of the initial concentration in Fig. 27. The linear relationship predicted by mass-transfer theory is verified.

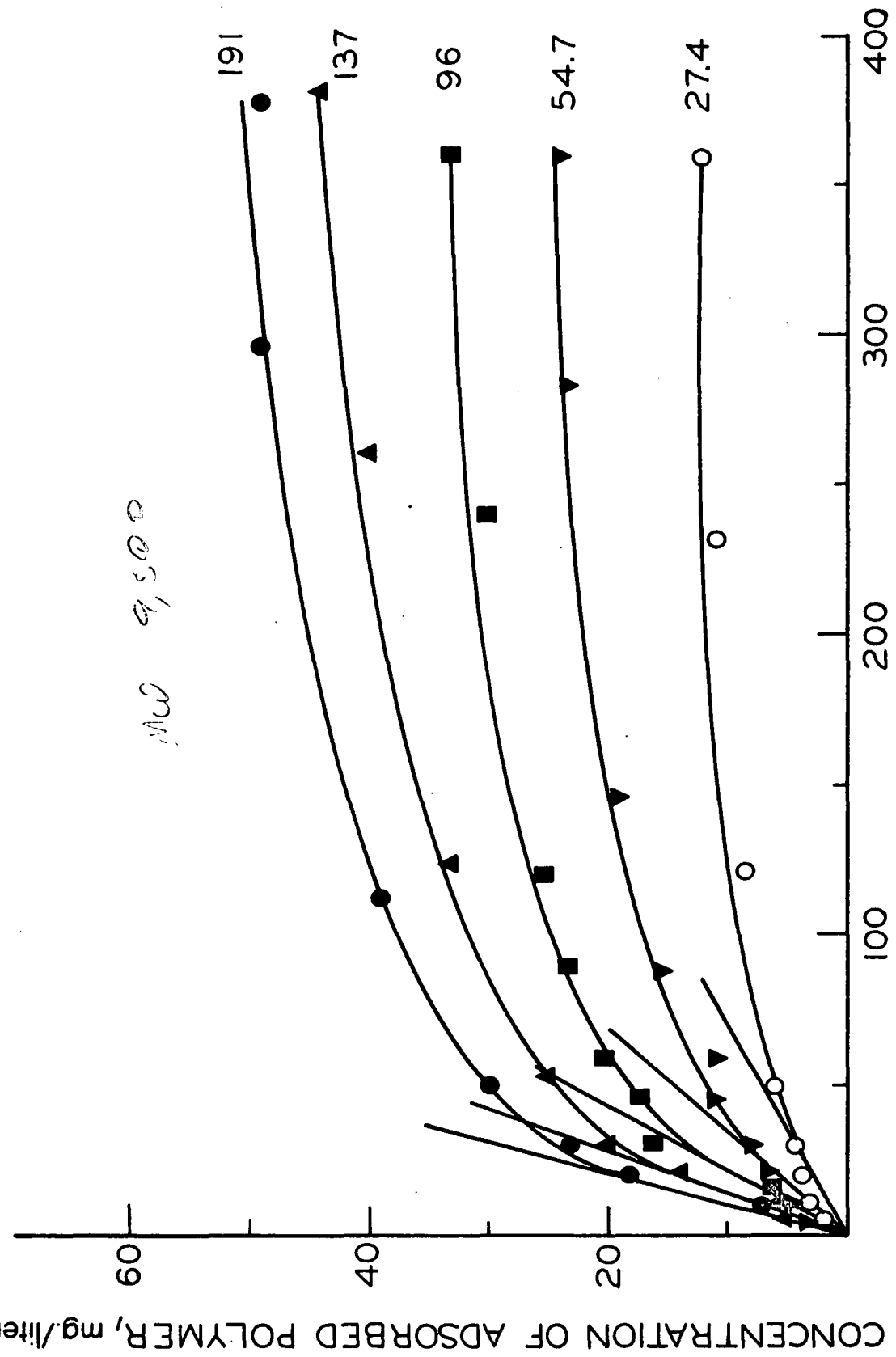

Figure 26. Effect of Polymer Concentration on Sorption Rate, Numbers on Curves Refer to Polymer Concentration in Mg./Liter

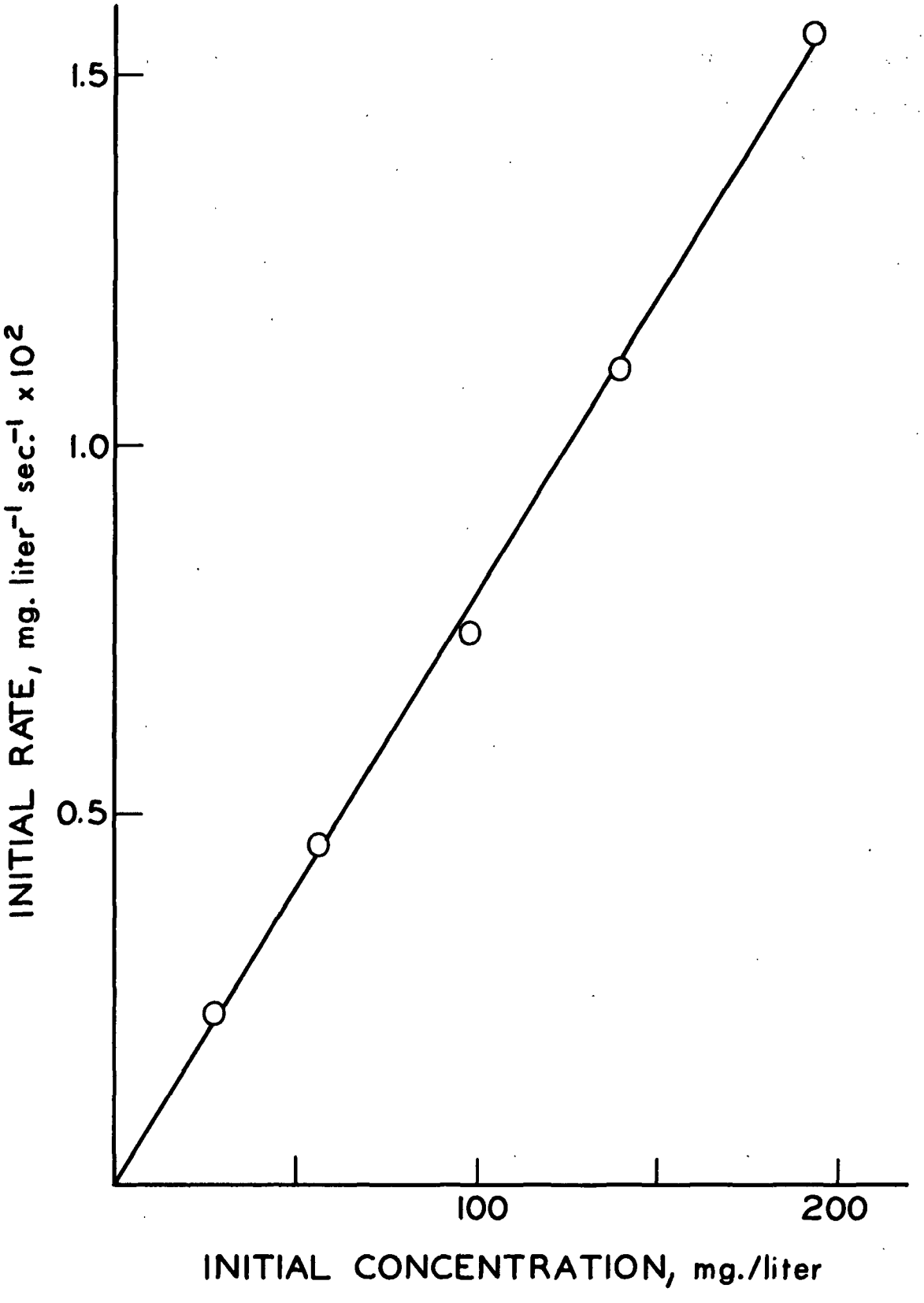

Figure 27. Effect of Polymer Concentration on Initial Rate

EFFECT OF IONIC STRENGTH

Adsorption rate measurements were performed using Fraction 63-8 in an aqueous solvent consisting of 8.0×10^{-4} N sodium hydroxide plus a series of various amounts of sodium chloride. The initial polymer concentration was 133 mg./liter. All other conditions were the same as described for the molecular weight experiments. The experimental rate curves are shown in Fig. 28 and the initial rates are tabulated in Table V.

TABLE V

EFFECT OF IONIC STRENGTH ON INITIAL RATE

Fraction Number	NaCl Concn., mM	Initial Rate x 10^2, mg./liter-sec.
63-8	0	1.87
63-8	2.0	1.30
63-8	5.0	1.10

The decrease in rate with the increase in ionic strength is in accord with the effect of salt concentration on the diffusion coefficient described earlier. The quantitative relationship will be developed in a later section.

EFFECT OF pH

The effect of pH on adsorption rate was investigated briefly. The adsorption rate of Fraction 63-7 was measured at pH 9.5 and compared with the rate at pH 10.9. The initial polymer concentration was the same in each experiment at 96.0 mg./liter. All other conditions were identical to those described earlier. The results can be seen in Fig. 29. At very small times, the initial rate does not appear to depend very strongly on pH. After a short period of time, however, the slope of the curve at pH 9.5 begins to decrease rather nonuniformly. This curve approaches equilibrium much more slowly than does the curve at pH 10.9.

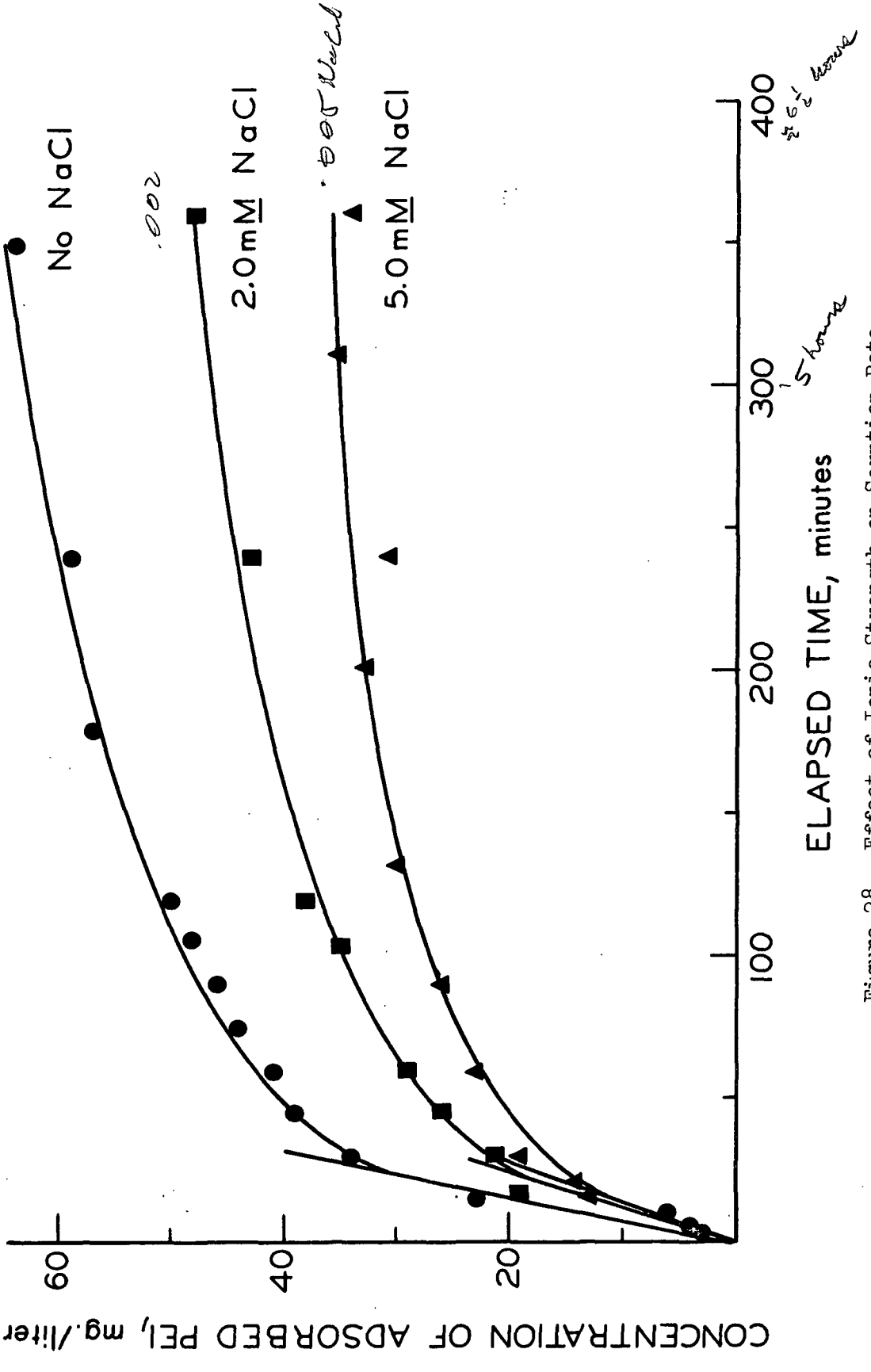

Figure 28. Effect of Ionic Strength on Sorption Rate

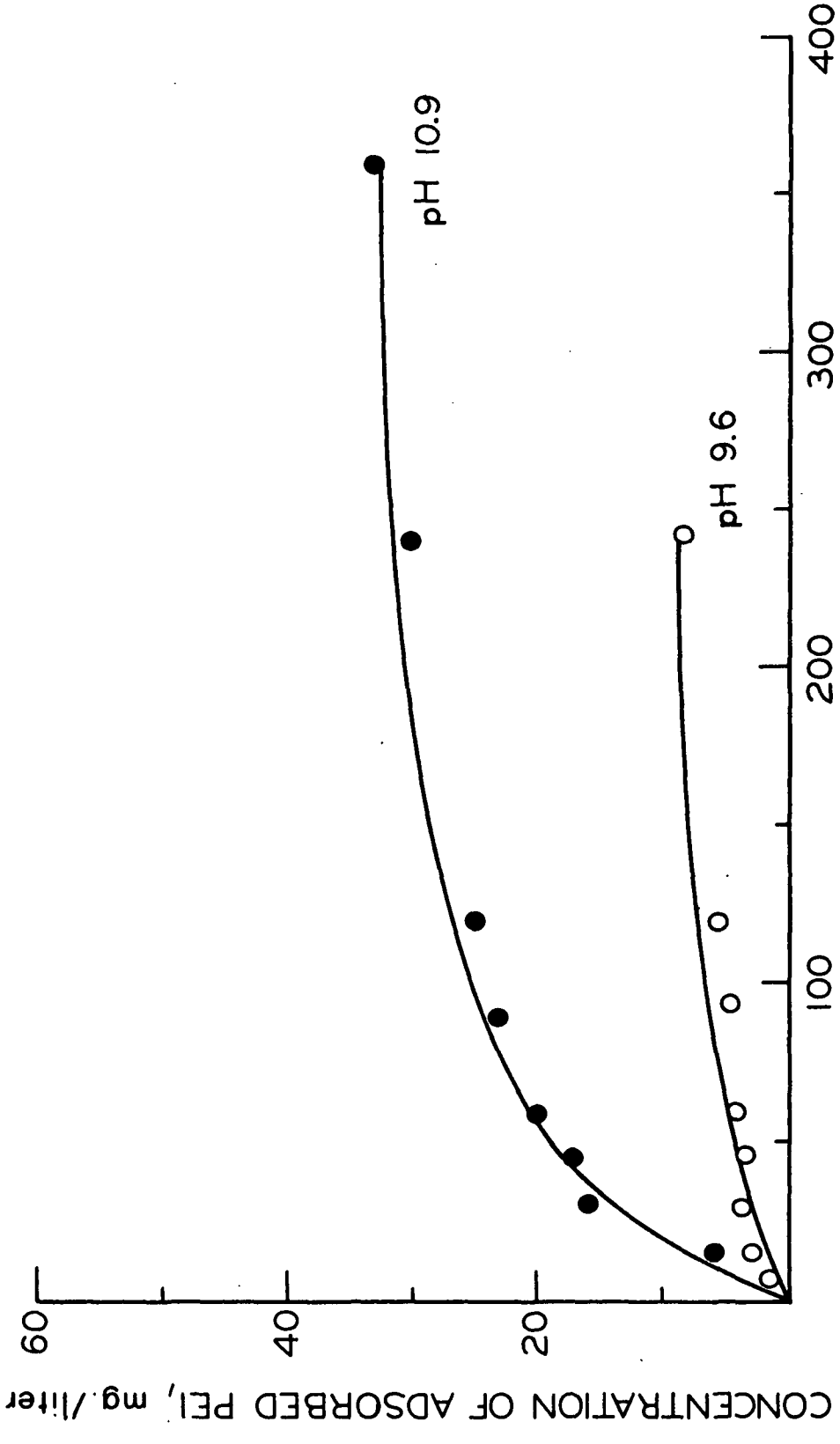

Figure 29. Effect of pH on Sorption Rate

EFFECT OF AGITATION

An attempt was made to determine the effect of agitation on sorption rate utilizing the agitation apparatus described previously. Two kinetic runs were made with Fraction 63-8 at an initial concentration of 133 mg./liter and in an aqueous solvent of 8.0×10^{-4} N sodium chloride (pH 10.9). In the second run the rotation rate was increased from 4.5 to 45 r.p.m. and the tube angle was increased from 15 to 30°. All other conditions were the same as described earlier. Since the fibers are very nearly of the same density as the solvent, it appeared as though the shear conditions were little changed in the two experiments. The two rate curves are compared in Fig. 30 and seem to be virtually identical.

The type of agitation provided by the apparatus used in these experiments is so slight with cellulose fiber slurries that increasing the rotation rate produces no significant changes in the degree of agitation inside the tube. Conclusive agitation-dependence experiments would require a different form of agitation.

REPRESENTATION OF DATA ACCORDING TO MASS-TRANSFER THEORY

DERIVATION OF THEORETICAL RATE CURVE

Fick's first law can be used to describe the material flux at the surface of the adsorbent,

$$(dN/dt)_{x=0} = -DA(\partial C/\partial x)_{x=0} \qquad (9)$$

where $(\partial C/\partial x)_{x=0}$ is the concentration gradient.

Assuming a linear concentration gradient, Equation (9) can be rewritten in terms of the concentration at the interface, C_f, the concentration at the imaginary shear

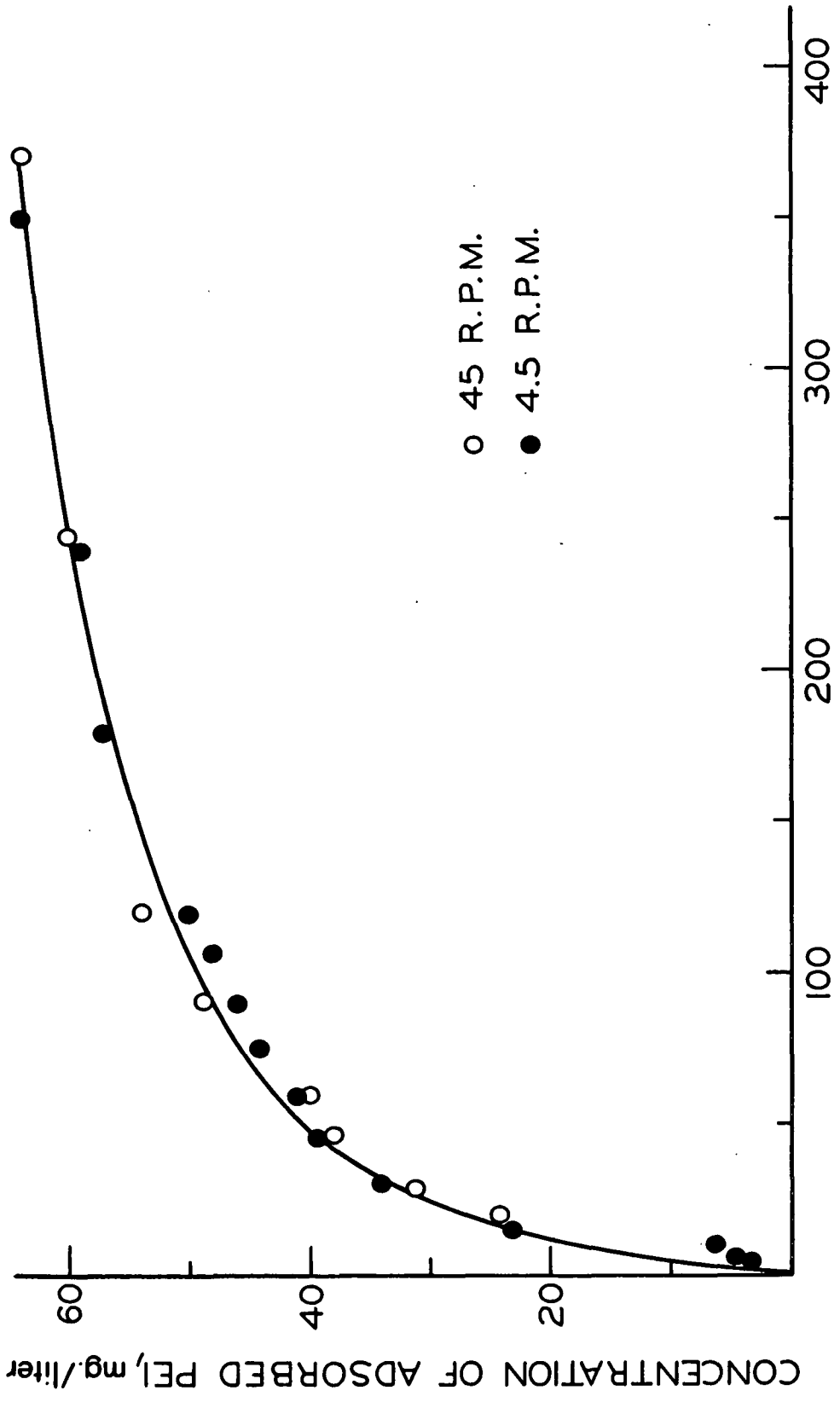

Figure 30. Effect of Agitation on Sorption Rate

plane, C_s, and the effective diffusional film thickness, δ,

$$dN/dt = -(DA/\delta)(C_s - C_f). \tag{10}$$

If the rate of reaction is very fast compared to the rate of mass-transfer, then the rate of polymer crossing the solid-liquid interface will be equal to the rate of adsorption. Thus, if N^* is the weight of adsorbed polymer, the rate can be expressed as,

$$dN^*/dt = -(DA/\delta)(C_s - C_f). \tag{11}$$

The concentration of polymer in solution at the interface may be assumed to be in equilibrium with adsorbed polymer at any instant in time. It has been shown experimentally that this equilibrium condition is given by the Langmuir equation,

$$C_f = N^*/[K(N_m - N^*)] \tag{12}$$

where N^* is the weight of adsorbed polymer, K is the Langmuir constant, and N_m is the weight of polymer adsorbed at saturation.

The concentration of polymer in the bulk phase at any time t, is given as the difference between the initial concentration, N_o/V, and the concentration adsorbed at time t, which is N^*/V, where V is the solution volume:

$$C_s = (N_o - N^*)/V. \tag{13}$$

Substituting Equations (12) and (13) into Equation (11) gives the differential rate equation in terms of the sorbed polymer weight,

$$\frac{dN^*}{dt} = \frac{DA}{\delta}\left[\frac{N_o - N^*}{V} - \frac{N^*}{K(N_m - N^*)}\right]. \tag{14}$$

The area term in Equation (14) must be written to account for the consumption of effective surface area as adsorption progresses. If A_o is the initial surface area, the time-dependent area can be expressed in terms of the amount of polymer sorbed at time t, as follows:

$$A = A_o(1 - N^*/N_m). \tag{15}$$

Putting Equation (15) into Equation (14) and expressing polymer content in terms of concentration yields

$$\frac{dC^*}{dt} = \frac{DA_o}{V\delta}\left[\left(\frac{1}{C_m}\right)C^{*2} - \left(\frac{C_o}{C_m} + \frac{1}{KC_m} + 1\right)C^* + C_o\right] \tag{16}$$

where C^* is the concentration of polymer adsorbed at time t, C_o is the initial solution concentration, and C_m is the concentration of polymer adsorbed at saturation.

The analytical solution to Equation (16) is given by,

$$C^* = \frac{C_m(b + \sqrt{-q})\ [1 - \exp(yt)]}{[2\ \exp(yt) - B]}, \tag{17}$$

where

$$b = -\left(\frac{C_o}{C_m} + \frac{1}{KC_m} + 1\right) \tag{18}$$

$$q = \frac{4C_o}{C_m} - b^2 \tag{19}$$

$$B = \frac{b + \sqrt{-q}}{b - \sqrt{-q}} \tag{20}$$

and

$$y = \left(\frac{\sqrt{-q}D}{V}\right)\left(\frac{A_o}{\delta}\right). \tag{21}$$

For small times when $\underline{C}^* << \underline{C}_o$, Equation (16) reduces to

$$\left(\frac{dC^*}{dt}\right)_{t\to o} = \frac{D^{0.66} A_o C_o}{V g_{-1}} \qquad (22)$$

where $\underline{g}_{-1}$ is a constant depending only on the hydrodynamic conditions of the system and comes from the substitution $\delta = \underline{g}_{-1} \underline{D}^{0.34}$.

All of the variables in Equations (17) and (22) have been determined experimentally except for the accessible surface area and the hydrodynamic constant. The method for evaluating these factors will be outlined in the following sections.

THE ACCESSIBLE SURFACE AREA

The effective surface area of a porous surface such as a cellulose fiber should be a function of the molecular weight of the adsorbing polymer. A small molecule would see a greater accessible area than would a larger molecule. That this factor is important to the cellulose fiber-PEI system is verified by the greater equilibrium saturation adsorption for the lower molecular weight fractions. The influence of this effect can be estimated from existing data even though the absolute magnitude of the accessible area cannot be measured directly.

The relative sizes of the molecules in the various fractions are related to the limiting diffusion coefficients through the friction coefficient, $\underline{f}$,

$$D_o = kT/f \qquad (23)$$

where $\underline{k}$ is the Boltzmann constant and $\underline{T}$ is the absolute temperature. Stoke's equation gives the friction factor in terms of an equivalent hydrodynamic radius, $\underline{R}_e$, (56),

$$f = 6\pi\eta R_e \qquad (24)$$

where η is the viscosity of the solvent. The equivalent hydrodynamic radius can be calculated from Equations (23) and (24) as follows:

$$R_e = \frac{kT}{6\pi\eta D_o} \qquad (25)$$

The equivalent hydrodynamic radius cannot be used to calculate the actual area covered by the polymer molecule on the fiber surface. In order to make this calculation, it would be necessary to know the configuration of the adsorbed polymer and the extent of the lateral polymer-polymer interactions on the fiber surface. This information is presently unavailable. As a first approximation it will be assumed that the projected area of the polymer sphere is proportional to the area of fiber surface covered by the adsorbed polymer molecule. An effective accessible surface area, $\underline{S}_e$, can then be calculated for each fraction from the equivalent hydrodynamic radius of the polymer and the amount of polymer adsorbed at saturation ($\underline{S}_e = 6.02 \times 10^3 \pi \Gamma \underline{R}_e^2 / \underline{M}_w$). The results of these calculations are summarized in Table VI. For comparison, the geometrical surface area of these fibers is about 0.2×10^4 cm.^{2}/g.

2000 cm^2/gm

TABLE VI

EFFECTIVE ACCESSIBLE SURFACE AREA AS A FUNCTION OF MOLECULAR WEIGHT

Fraction Number	Molecular Weight	$\underline{R}_e$, A.	$\underline{S}_e$, cm.^{2}/g.
63-8	8,000	11.5	9.5×10^4
63-7	9,500	12.0	6.5×10^4
63-6	11,500	12.5	4.9×10^4
63-5	14,000	13.1	2.3×10^4
63-4	20,000	14.9	1.3×10^4

The assumptions inherent in this calculation are as follows. The polymer adsorbs in the same configuration as it had in solution. There is no lateral

interaction between polymer molecules on the fiber surface. The adsorption does not exceed monolayer coverage. The equivalent hydrodynamic radius is a true reflection of the solution configuration of the polymer. And finally, the polymer molecules are packed perfectly on the surface. Since the validity of some of these assumptions seems doubtful, it is necessary to emphasize that the area so calculated is only proportional to the true accessible area. Therefore,

$$A_o = g_2 W_f S_e \tag{26}$$

where S_e is the effective accessible surface area calculated according to the above assumptions, g_2 is a proportionality constant, and W_f is the weight of fiber in the adsorption system. The fiber weight factor must be included since S_e is a specific surface area and A_o is the total amount of surface area in the system. The proportionality factor goes to unity as the assumptions given above are realized.

INITIAL RATE

Combining Equations (22) and (26) yields the following differential equation for the initial adsorption rate:

$$(dC^*/dt)_{t\to o} = (g_2/g_1)(D^{0.66} S_e W_f C_o/V). \tag{27}$$

With the exception of the two constants g_1 and g_2, all of the quantities in Equation (27) have either been measured experimentally or can be calculated from experimental data. The equation predicts that a plot of the initial rate as a function of $(D^{0.66} S_e W_f C_o/V)$ will yield a straight line passing through the origin and having a slope of (g_2/g_1). Such a plot for the data presented previously is shown in Fig. 31. The limiting diffusion coefficients were used for these calculations. The data points represent only those runs made in 8.0×10^{-4} N sodium hydroxide. The slope and intercept along with the 95% confidence limits for each were determined by least-squares analysis. The slope was found to be $2.86 \times 10^{-3} \pm 0.28 \times 10^{-3}$ cm.$^{-0.32}$sec.$^{0.66}$.

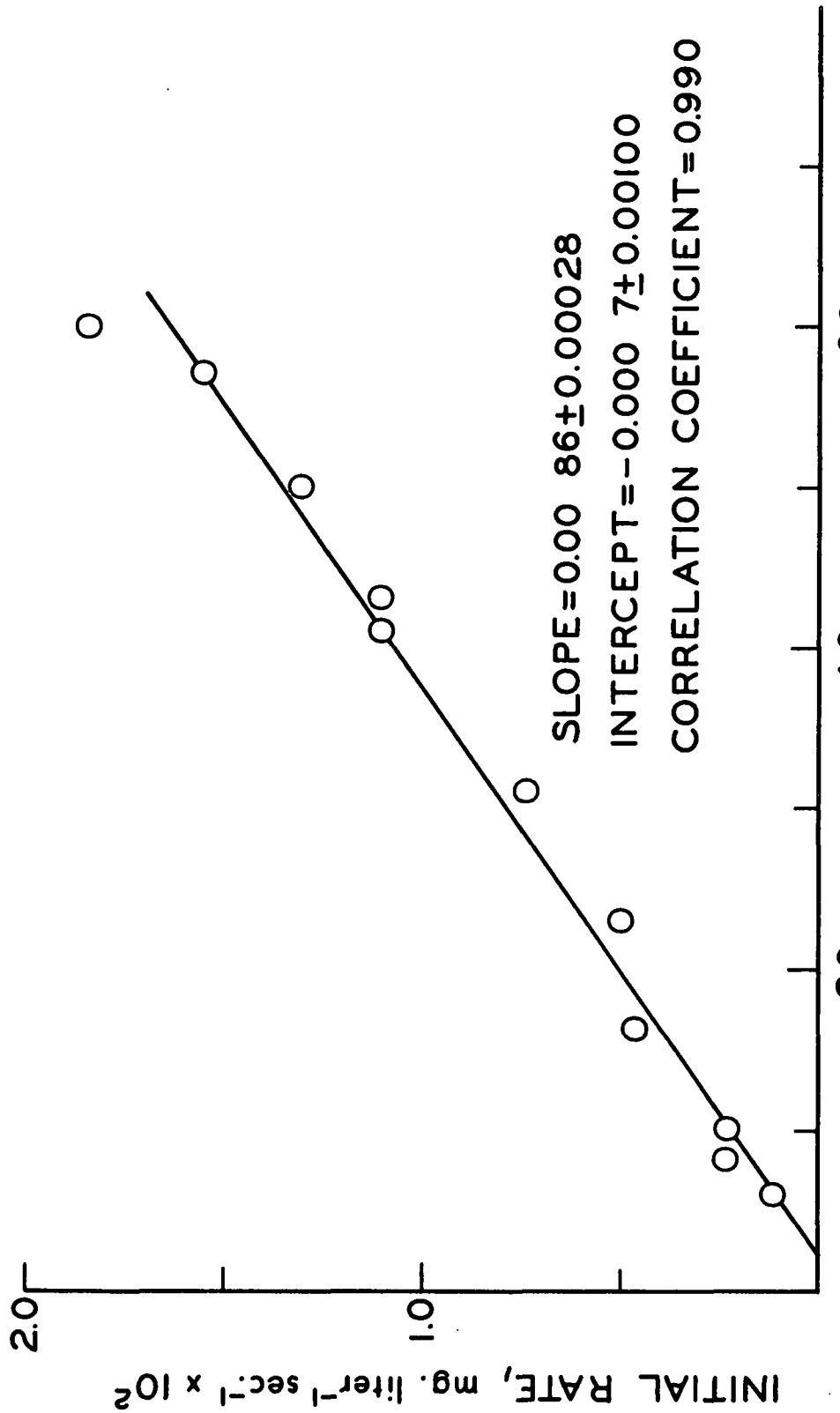

Figure 31. Plot of Initial Rate as a Function of Experimental Parameters According to Theoretical Equation

The intercept is $-0.57 \times 10^{-3} \pm 1.00 \times 10^{-3}$ mg./liter sec. which includes the origin as predicted. The correlation coefficient for the linear representation is 0.990 indicating a good straight-line fit. Accordingly, this test provides substantiating evidence for the ability of the elementary mass-transfer theory to predict initial adsorption rates. It also affords the determination of the ratio of the experimentally undetermined constants, $(\underline{g}_2/\underline{g}_1)$.

OVERALL RATE CURVE

Utilizing the same substitutions for $\underline{A}_o$ and δ as was done for the initial rate treatment yields,

$$C^* = \frac{C_m(b + \sqrt{-q})\ [1 - \exp(yt)]}{[2\ \exp(yt) - B]} \qquad (17)$$

where

$$y = \left(\frac{D^{0.66} S_e W_f}{V}\right)\left(\sqrt{-q}\right)\left(\frac{g_2}{g_1}\right) \qquad (28)$$

and $\underline{B}$, $\underline{b}$, and $\underline{q}$ are constants related to the equilibrium adsorption properties as previously defined. According to Fig. 31, the ratio $(\underline{g}_2/\underline{g}_1)$ is constant for all runs and is known from the slope of that line. On making this substitution into Equation (28) all parameters on the right side of Equation (17) are known experimentally or can be calculated from experimental data using some previously described assumptions. At this point it is possible to calculate $\underline{C}^*$ for selected values of $\underline{t}$ and generate the entire rate curve for comparison with the experimental curves. This comparison is shown in Fig. 32 through 43 for each of the adsorption runs. In these figures the circles represent the experimental rate data and the solid curves are the theoretical rates.

In general, it may be said that the theory provides for an excellent prediction of the rate curves. There are, however, significant deviations of theory from

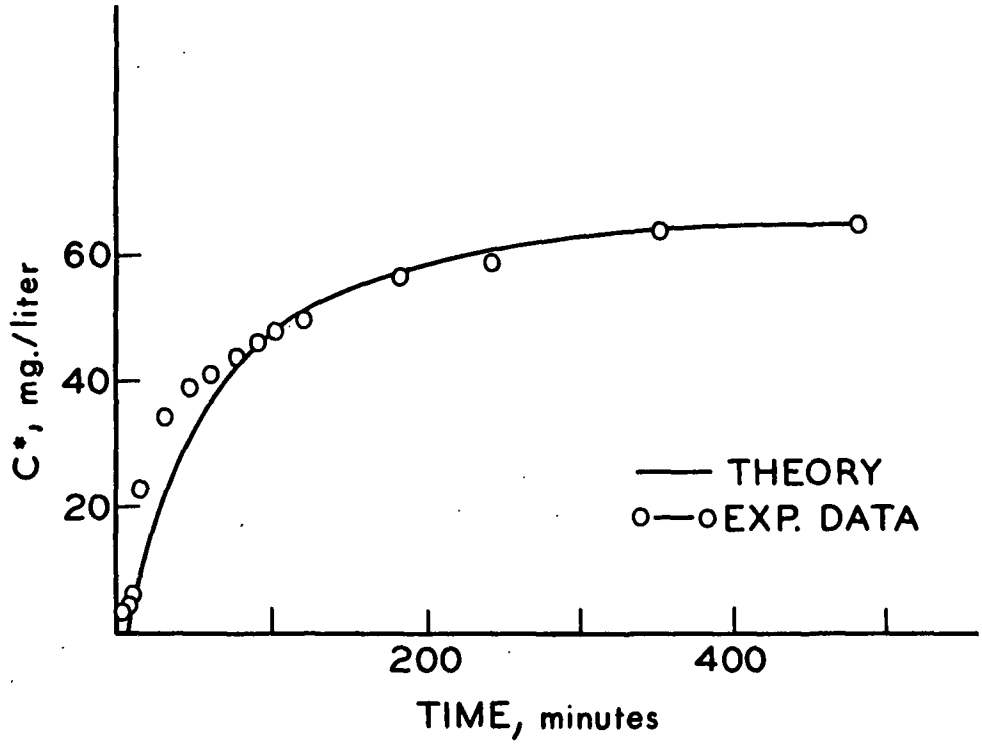

Figure 32. Rate Curve for 63-8 at pH 10.9, $\underline{C}_o$ = 133 Mg./Liter

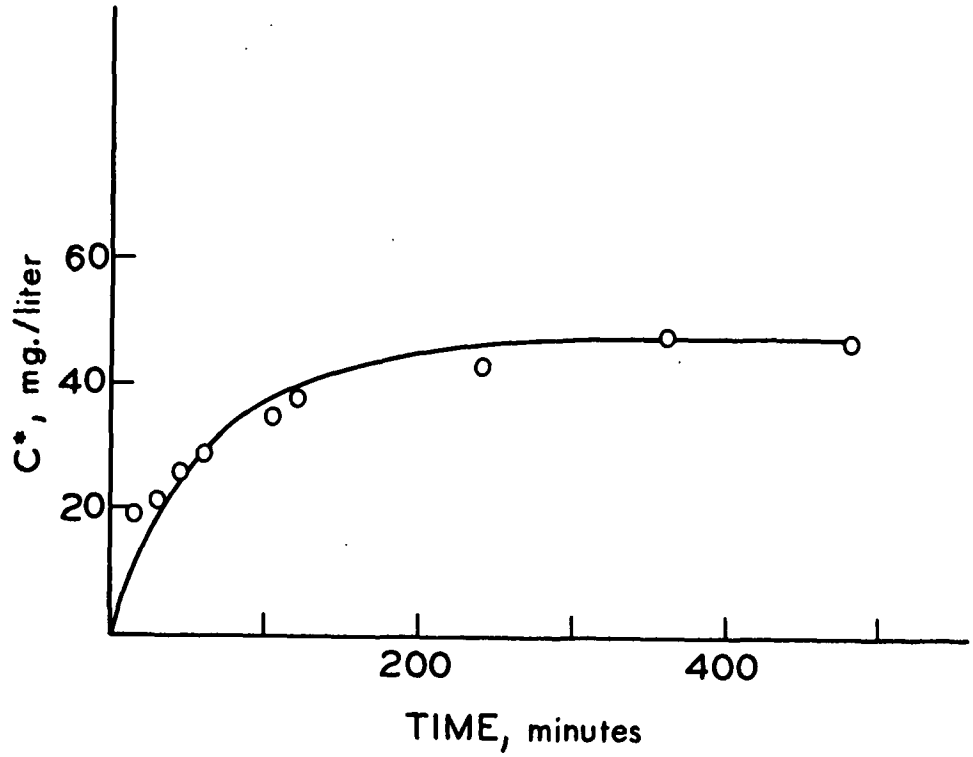

Figure 33. Rate Curve for 63-8 at pH 10.9 in 2.0 m$\underline{M}$ NaCl, $\underline{C}_o$ = 133 Mg./Liter

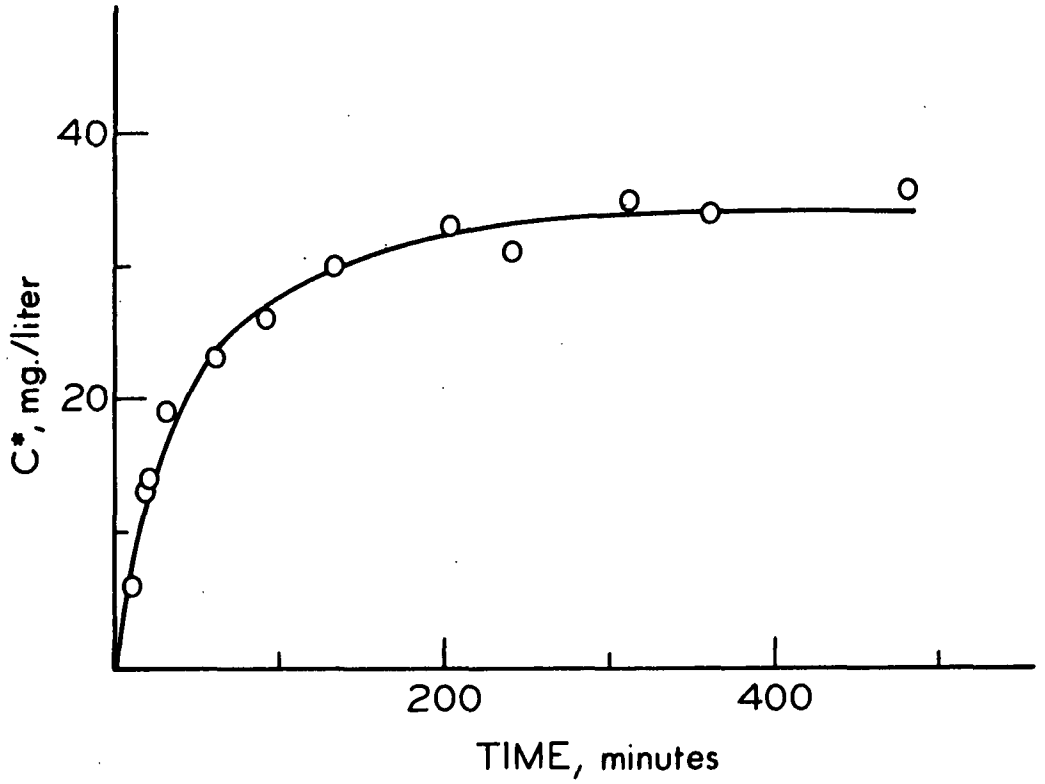

Figure 34. Rate Curve for 63-8 at pH 10.9 in 5.0 mM NaCl, C_o = 133 Mg./Liter

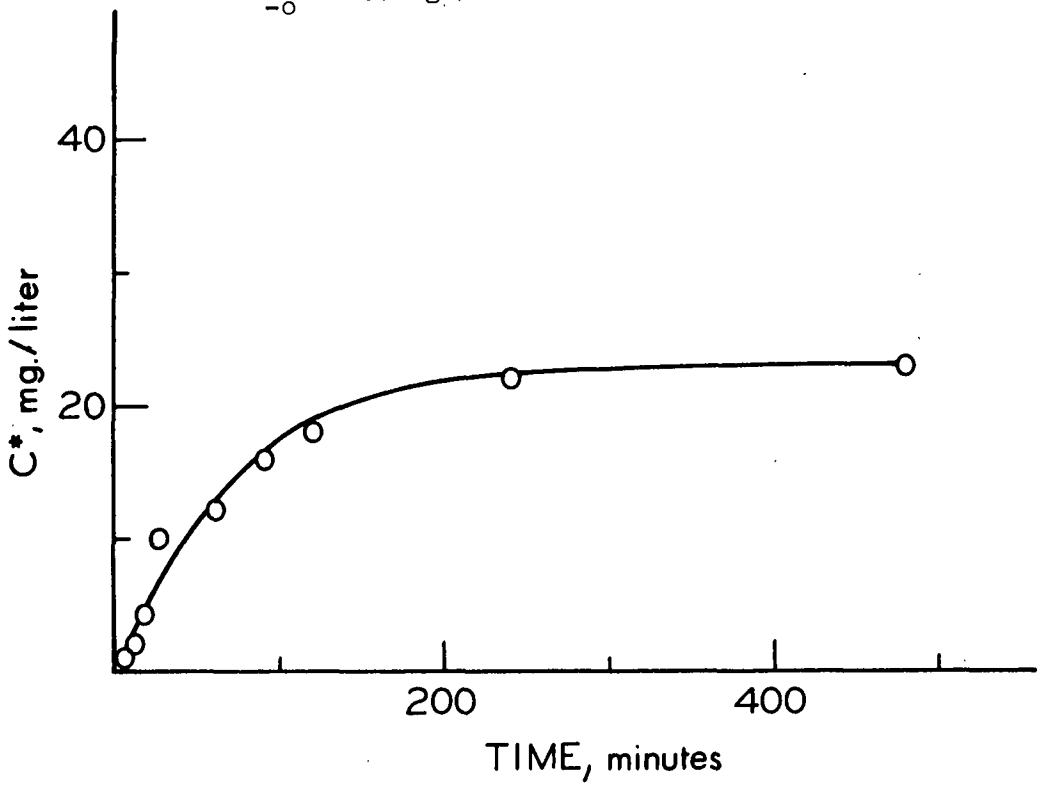

Figure 35. Rate Curve for 63-6 at pH 10.9, C_o = 106 Mg./Liter

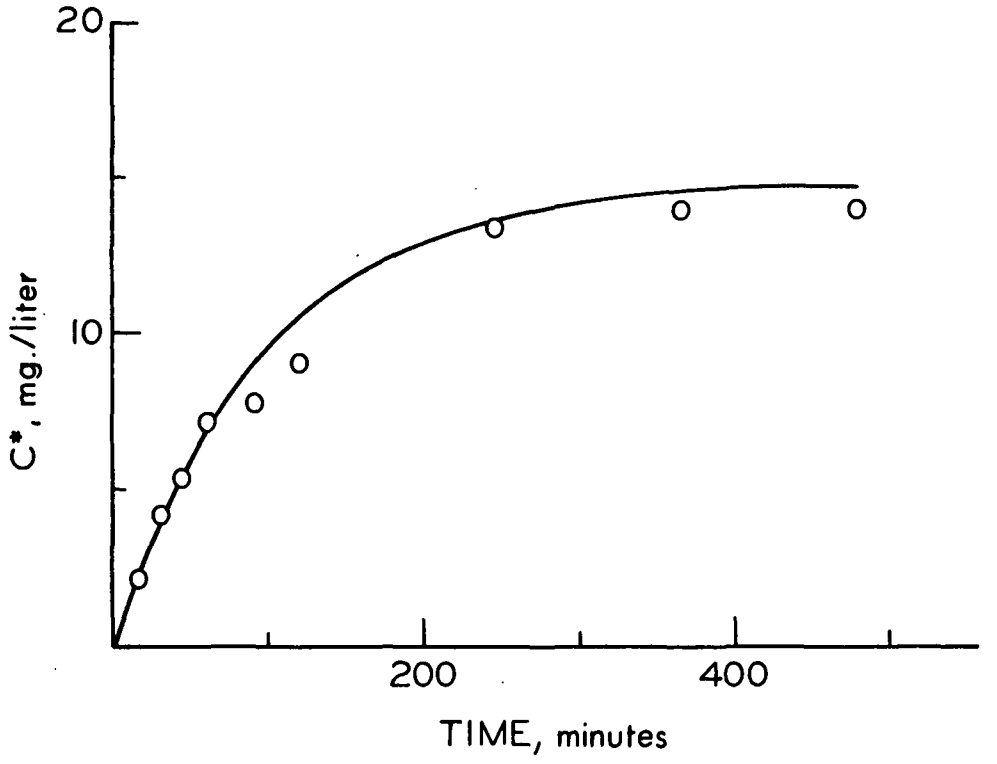

Figure 36. Rate Curve for 63-5 at pH 10.9, $\underline{C}_o$ = 99 Mg./Liter

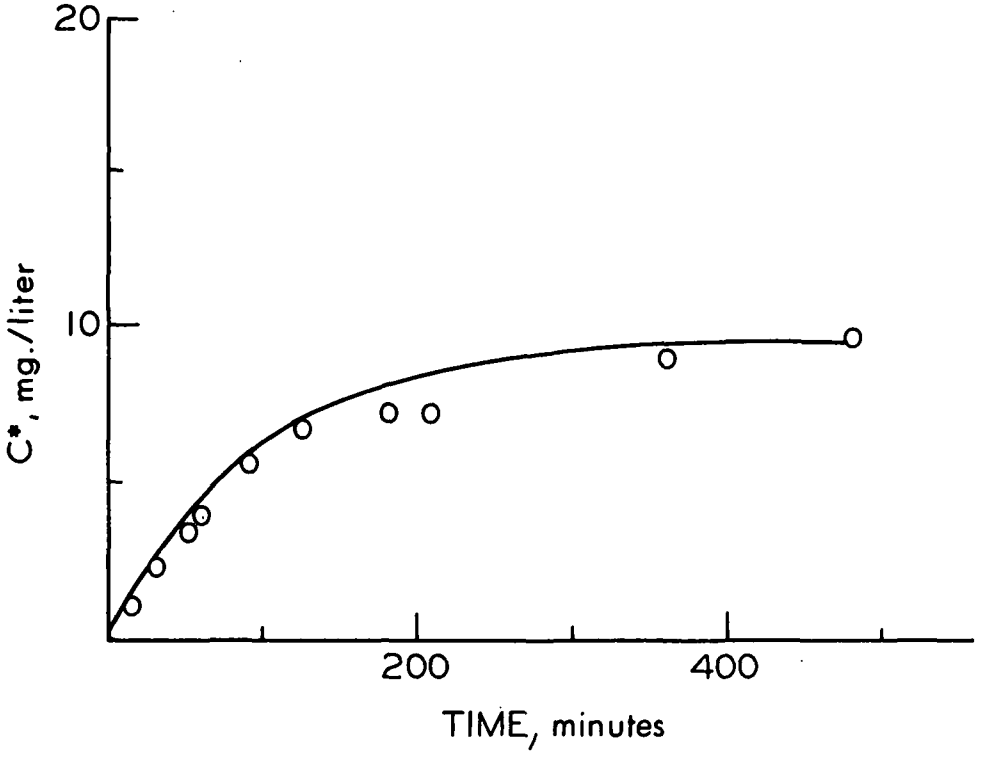

Figure 37. Rate Curve for 63-4 at pH 10.9, $\underline{C}_o$ = 96 Mg./Liter

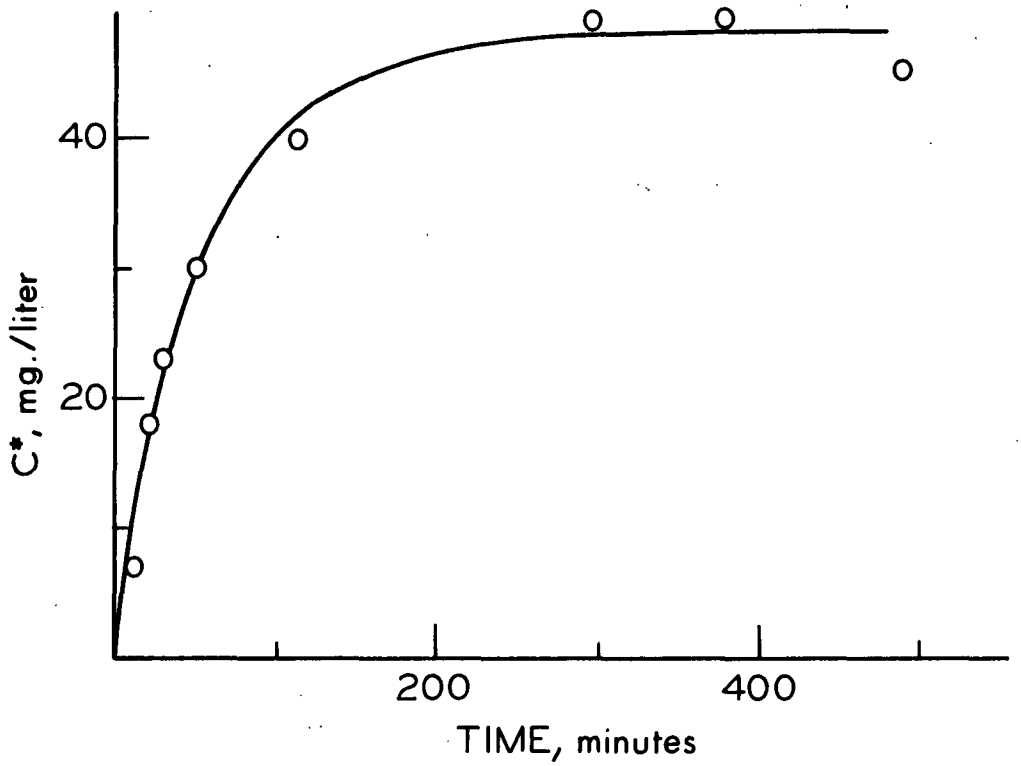

Figure 38. Rate Curve for 63-7 at pH 10.9, $\underline{C}_o$ = 191 Mg./Liter

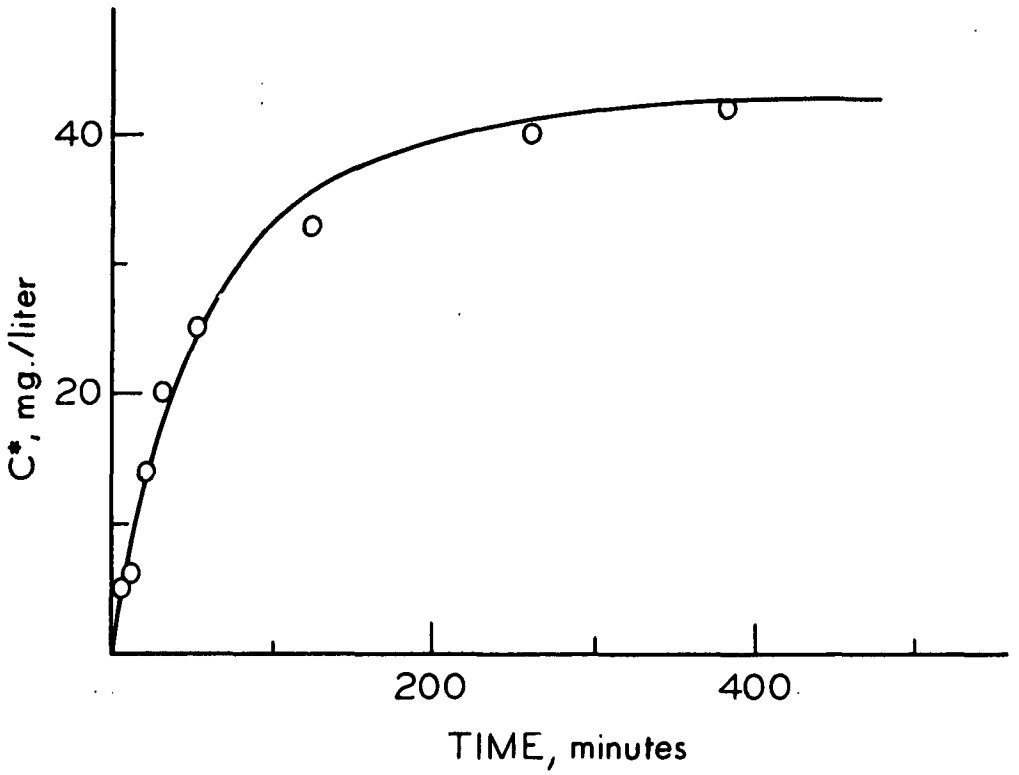

Figure 39. Rate Curve for 63-7 at pH 10.9, $\underline{C}_o$ = 137 Mg./Liter

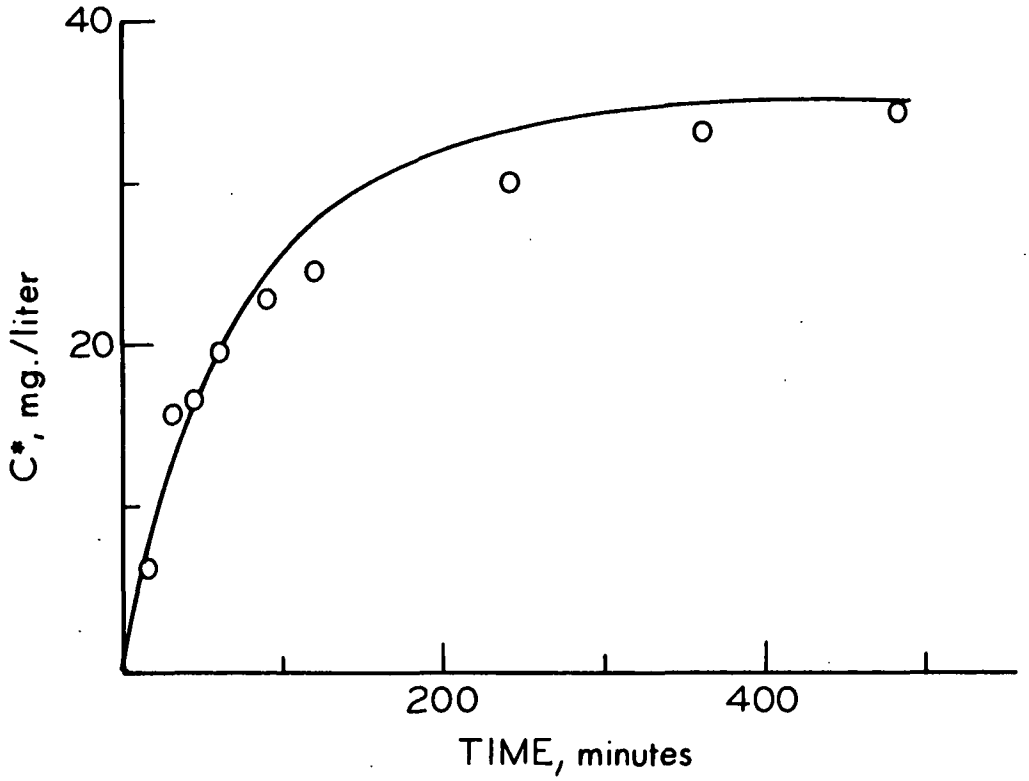

Figure 40. Rate Curve for 63-7 at pH 10.9, $\underline{C}_o$ = 96 Mg./Liter

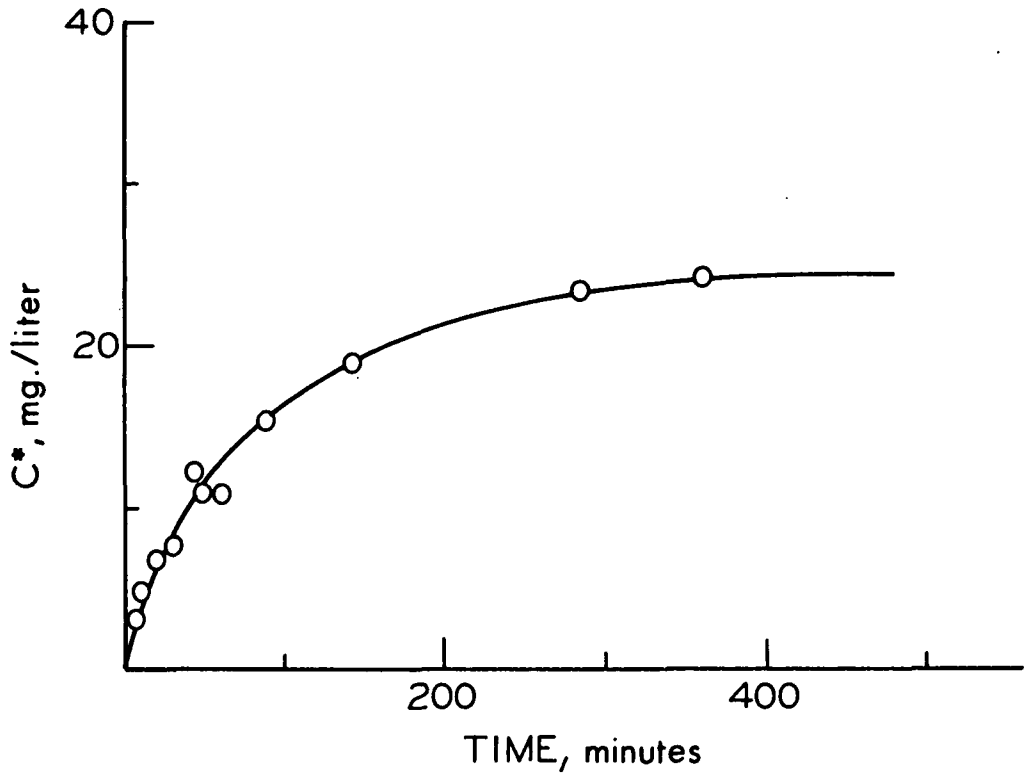

Figure 41. Rate Curve for 63-7 at pH 10.9, $\underline{C}_o$ = 54.7 Mg./Liter

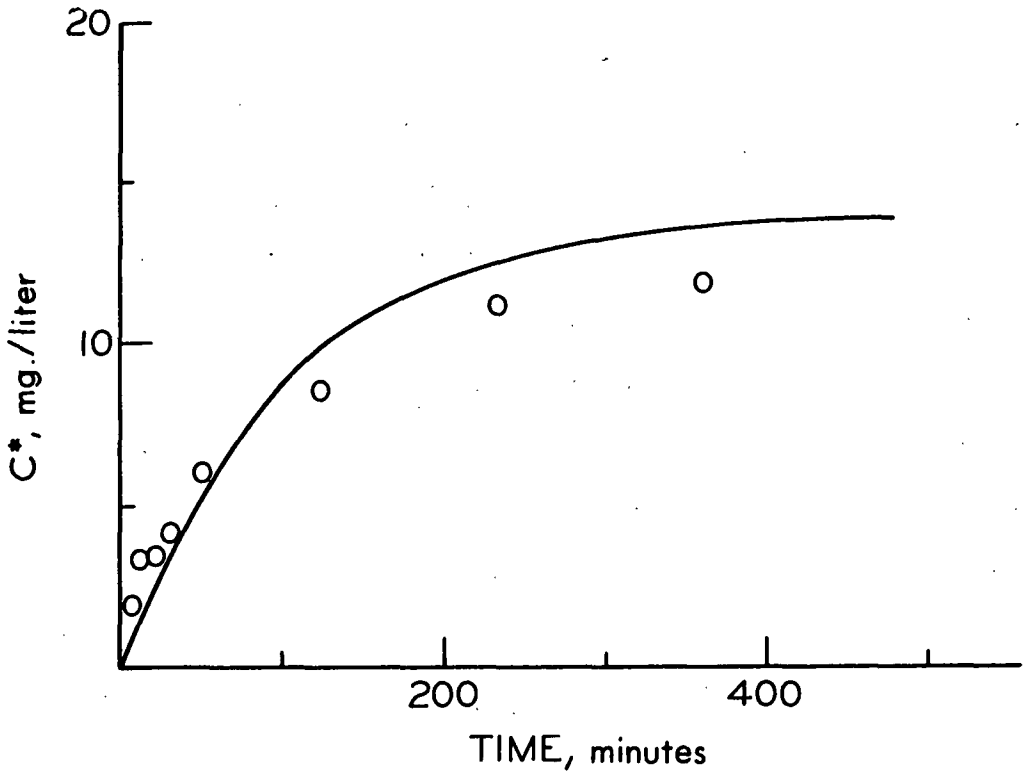

Figure 42. Rate Curve for 63-7 at pH 10.9, $\underline{C}_o$ = 27.4 Mg./Liter

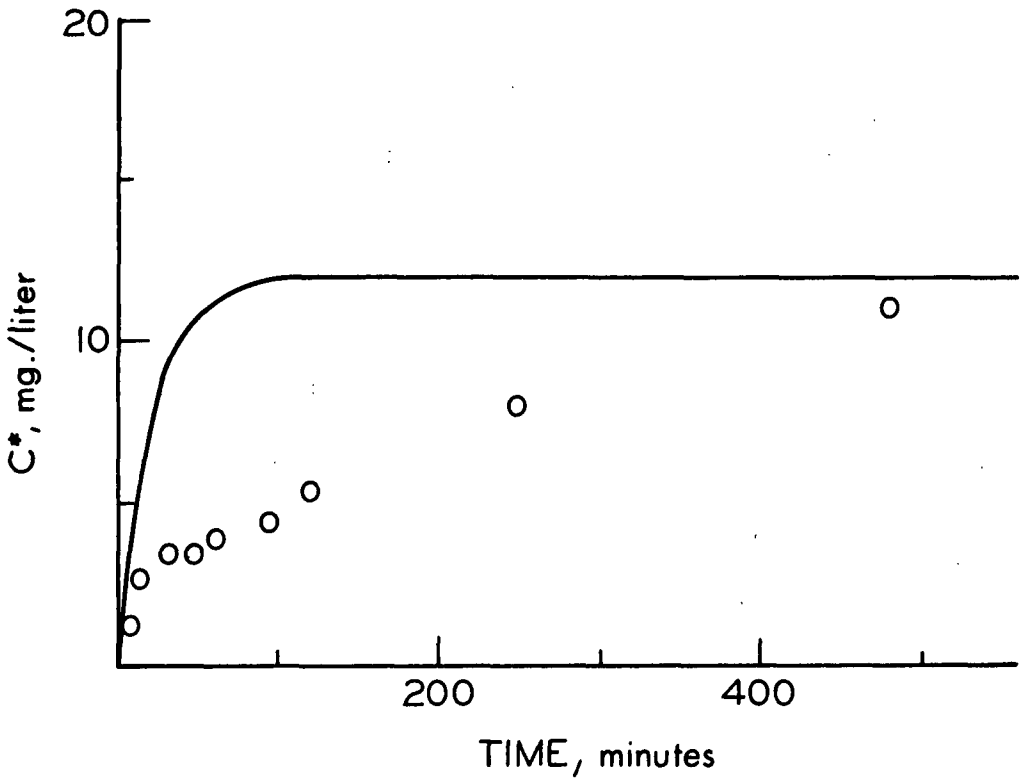

Figure 43. Rate Curve for 63-7 at pH 9.6, $\underline{C}_o$ = 96 Mg./Liter

experiment at low molecular weight (Fig. 32), low concentration (Fig. 42), and low hydroxyl concentration (Fig. 43). Each of these cases will be discussed individually.

Considering the curve in Fig. 32 first, it may be noted that Fraction 63-8 has a slightly higher charge density than do the other fractions. This is reflected by a higher pH of aqueous solutions at comparable concentrations and by a lower absorbance at comparable pH. As discussed previously, charge interactions between negative fibers and positive polymer would accelerate the initial rate. The rate at later times would be retarded if the fiber attains a net positive charge due to adsorbed polymer. These effects are not predicted by theory and, thus, would be identified by deviations from the theoretical curves. The initial deviation of Fig. 32 is in accord with this reasoning. The reduction in the rate at later times is probably not apparent due to the relatively low charge density of the polymer under the conditions of adsorption.

The effect of added neutral salt on the rate would be twofold. Increased ionic strength would alter the diffusion coefficient of the polymer. Since the diffusion coefficient has been measured at the salt concentrations employed in the adsorption runs, this effect can be predicted by theory. The second effect of ionic strength operates directly on the electrostatic interaction between fiber and polymer. The increased simple ion concentration will function to shield the fiber charge from the polymer charge. In this way, the effect of electrostatic interactions on the rate will be decreased. If the initial deviation observed in Fig. 32 is due to electrostatic attractions, then an increase in neutral salt concentration should decrease the magnitude of deviation. This is confirmed experimentally by comparing Fig. 32, 33, and 34.

The deviation at low concentration (Fig. 42) may be explained by similar reasoning. It has been established that the degree of ionization of a polyelectrolyte

increases with decreasing concentration. Thus, Polymer 63-7 would be expected to show a greater deviation from theory in dilute solution (Fig. 42) than at the higher concentrations (Fig. 38 through 41).

The failure of simple mass-transfer theory observed at lower pH (see Fig. 43) is also in accord with the charge interaction concept. At pH 9.6 the degree of ionization of cellulosic hydroxyls is very low (see Fig. 24). Due to the low negative charge density of the fiber, the initial rate is similar to that predicted by theory. As adsorption proceeds, however, the fiber begins to assume a significant positive charge due to sorbed polymer units and the rate is significantly retarded.

It may be concluded at this point that the simple mass-transfer theory successfully accounts for the effect of a number of variables on the adsorption rate. Exceptions are encountered when the charge density on the fiber and the polymer are sufficiently high to produce significant electrostatic interactions between the polymer and the fiber. It has been shown that the effect of polymer molecular weight on the rate operates only through the diffusion coefficient and the equilibrium adsorption properties. The initial polymer concentration influences the rate according to a first-order expression as predicted by simple mass-transfer theory. It has been demonstrated that salt concentration and pH affect the rate by changing the diffusion coefficient of the polymer and also by altering the magnitude of electrostatic interactions. The first mechanism predominates at low charge densities while the effect of the latter increases with charge density.

THICKNESS OF EFFECTIVE DIFFUSIONAL FILM

Additional information about the nature of the adsorption process can be derived from a consideration of the magnitude of the effective diffusional film thickness. This thickness can be calculated from a knowledge of the hydrodynamic film

constant, g_1, and the diffusion coefficient. If the assumptions introduced in the calculation of A_o are valid, then g_2 is equal to unity and g_1 is equal to the inverse of the slope of Fig. 31. Using this value and a diffusion coefficient of 2.0×10^{-6} cm.^{2}/sec., the effective film thickness is calculated ($\delta = g_1 D^{0.34}$) to be approximately four centimeters. This is about one thousand times greater than the film thickness calculated for the dissolution processes described previously. A four centimeter film thickness is clearly a physical impossibility. The remainder of this section will discuss possible reasons for this abnormally high magnitude. First, the assumptions inherent in the mathematical approximation will be discussed. This will be followed by a reexamination of the system description.

Examination of Assumptions

The choice of g_2 equal to unity contributes directly to the calculation of the magnitude of δ and needs to be discussed. If the assumptions of no lateral repulsions between polymer molecules on the surface and of perfect packing were invalid, the true surface area, A_o, would be greater than $W_f S_e$. The assumption that the polymer maintains its solution configuration on sorption might also lead to an erroneously low calculated area. It is believed that the polymer flattens out on sorption and so occupies more area than the projected area of the hydrodynamic sphere. Finally, the calculation of the effective hydrodynamic radius assumes that the accelerated diffusion due to the presence of the counterions is negligible. The diffusion data indicate that this is not rigorously true. Thus, the true radius of the sphere must be greater than that calculated. All of these effects indicate that g_2 is probably greater than unity. Therefore, the above assumptions tend to make δ smaller and not larger than the true value.

No provision was made in the derivation for the fact that diffusion is to a cylinder and not a plane surface. In a mathematical study of the uptake of solute by a hollow cylinder, Crank (57) has shown that the difference in uptake rates

between a solid cylinder and a plane sheet is less than 10%. At short times, the difference is very much less. A hollow cylinder would behave even more like a plane sheet than would a solid cylinder. Therefore, the assumption of a plane surface cannot contribute to the extraordinarily large diffusional film.

It is feasible that the assumption of a linear concentration gradient could lead to a highly erroneous result. Attempts at solving the differential rate equation in stirred solution without imposing the requirement of a linear gradient have proved difficult. If the system is not stirred, however, the mathematics can be handled. A solution for this condition is given by Reinmuth (58). If it is assumed that no forced convection exists in the system, the predicted rate should be slower than that actually observed in a stirred solution. The solution given by Reinmuth and the experimental parameters for the cellulose-PEI system predict that the sorption process should approach equilibrium in a matter of a few minutes instead of a few hours which was observed experimentally. This observation does not verify the validity of the linear gradient but it does show that this assumption is not responsible for the large diffusional film.

At present, it must be concluded that the unreasonable film thickness is due to an incomplete description of the system and not to the mathematical analysis. It appears as though the adsorption process can be well described on the basis of a diffusion-controlled reaction but that mass transfer across a physical plane does not represent the only barrier to flow. In other words, it is necessary to acknowledge the presence of an additional barrier to mass transport. The nature of this barrier will be discussed in the following section.

Physical Meaning of Large Diffusional Film Thickness

There are several physical processes which could potentially contribute to an abnormally large diffusional film thickness. This section will discuss the relative importance of each process as it might apply to the system described herein.

Diffusion into Porous Structure

The development of the mass-transfer equations assumed that the adsorption was controlled by diffusion across a film of solvent to a discrete interface. We know, however, that in an aqueous suspension, a cellulose fiber does not present a discrete interface to the solvent. The surface is a highly hydrated and porous structure. Much of the adsorption of polyethylenimine may take place within this gel-type structure. The diffusion step in this medium would be very much slower than in pure solvent and will become the rate-controlling step. In this case, the rate would be expected to exhibit the same dependence on the diffusion coefficient as was predicted by the case of diffusion across a film of solvent. The effective diffusional film thickness would be much larger than in the case of diffusion across a solvent film. This is due, at least in part, to the large resistance through which the polymer must pass in order to penetrate the fiber structure.

Many experimental observations of this and similar systems are consistent with the concept of diffusion into pores and subsequent adsorption. According to the equilibrium data, the lower molecular weight fractions show a greater specific adsorption at saturation than do the larger molecular weights. In other words, the smaller molecules are capable of diffusing into narrow pores which are inaccessible to the higher molecular weight species. Stone, et al. (22) have given evidence that pores in regenerated cellulose are sufficiently large to permit inclusion of dextran molecules as large as 100 A. in diameter. The range of molecular sizes investigated in this study is well below this limit.

A previous study (12) of the adsorption of very high molecular weight polyethylenimine onto fines-free bleached sulfite pulp provides important substantiating evidence for the importance of this phenomenon. Two PEI samples of molecular weights of approximately 50,000 and 100,000 were utilized. Both polymers were highly

cross-linked and unfractionated. The 100,000 molecular weight sample gave a higher specific adsorption at saturation than did the lower molecular weight material. Under conditions of agitation and concentration similar to those described for this study, the high molecular weight material approached equilibrium in about thirty minutes. The importance of these results to the current discussion are as follows. These polymer samples are probably largely excluded from the porous internal structure of the fiber. This being the case, the dominant molecular weight effect is not one of accessibility but rather one of thermodynamics. Thermodynamically, adsorption of the larger molecules is favored, as was observed experimentally. Since most of the adsorption occurs on the fiber surface, the rate should be fairly rapid. For the 100,000 molecular weight polymer, the rate is an order of magnitude faster than for the low molecular weight samples described in this study.

There are some experimental observations which are difficult to explain on the basis of a rate controlled only by diffusion into pores. The agitation-dependence observed by other workers is not readily explained by this theory alone. However, the agitation effect will become increasingly important as the polymer size, and thus inaccessibility, increases. Nearly all of the polymer adsorption rates published in the literature are too slow to be explained on the basis of diffusion across a solvent film alone. This includes much of the available data on nonporous solids. It is likely, however, that many of these "nonporous" solids, such as some carbon blacks, exhibit significant pore structure at a level comparable to the polymer size.

On the basis of the above observations, it is concluded that diffusion into the porous structure of cellulose is a major contributor to the large apparent diffusional film, at least for polymers under 20,000 molecular weight. It is possible that other mechanisms might also contribute to the slow adsorption rate. These will be discussed briefly on the following page.

Entropy Barrier

It is feasible that the system is affected by the presence of an entropy barrier generated between either sorbed PEI or partially soluble cellulose chains and completely solvated PEI near the surface. This phenomenon would be analogous to that used to explain the polymeric stabilization of colloidal dispersions in nonpolar solvents. Heller and Pugh (59, 60) have provided experimental evidence for the existence of entropy barriers. Theoretical analyses have been given by Clayfield and Lumb (61) and by Meier (62).

The entropy barrier concept is used to explain some concepts of the polymeric stabilization of colloidal dispersions. When two polymer chains are brought sufficiently close together such that the thermal motion of groups of segments is restricted, the entropy of the system is decreased and the condition is thermodynamically unstable. Thus, the system will revert to a situation in which the thermal motions of segments do not occupy the same volume element in order that the entropy can be maximized. This type of action would retard the rate of approach to the surface if the PEI molecule encountered partially dissolved cellulose segments free of active sites. This phenomenon would not be expected to affect the rate of adsorption at a completely hydrophobic surface. However, a polymer molecule approaching a hydrophobic surface partially covered with adsorbed polymer might encounter an entropy barrier due to loops of sorbed polymer extending into the bulk phase. In this latter case, the initial rate would not be affected by such a barrier since, at early times, the amount of sorbed polymer is insignificant.

Solvent Interactions

In terms of recent water structure theory, cellulose is thought to be a structure breaker (63) which, if anything, would produce an increase in the diffusion of the polymer in the vicinity of the fiber. The polar groups on the cellulose

chain, however, are immediately surrounded by adsorbed water which must be displaced in order for the polymer to interact directly with the fiber surface. This displacement process may represent a barrier to the diffusion of polymer to the fiber surface.

Reorientation of Polymer

Two pieces of evidence for the importance of the reorientation of sorbed polymer chains are cited in the Literature Review (24, 25). This reorientation could conceivably contribute to a slow approach to equilibrium but it does not appear to account for the slow initial rate.

On the other hand, if it is necessary for the approaching polymer to be oriented in such a way as to expose its active groups to the surface, an overall decrease in the rate would be predicted. For the low degree of ionization at which measurements were made, this is a possibility. However, the dynamic situation of the charged groups on the polymer would seem to decrease the importance of this concept.

SUMMARY OF CONCLUSIONS

The rate of adsorption of polyethylenimine onto regenerated cellulose fibers is controlled by a mass-transfer process. This process is not, however, adequately described by diffusion across a stagnant layer surrounding the fiber as was previously supposed. Stagnant layer theory predicts an adsorption rate which is at least an order of magnitude more rapid than that observed experimentally in this study. This observation is not unique to the results reported herein, but is general for nearly all of the available rate data in the literature for other systems. It is necessary to acknowledge the presence of additional barriers to mass flow. For the system described in this dissertation, the diffusion into and the subsequent adsorption onto the internal porous structure represents the predominant barrier to rapid adsorption. Other potential retarding effects of lesser importance include the presence of entropy barriers, solvent interactions, and polymer reorientation. Although these phenomena are not expected to play a major role in the adsorption of PEI by cellulose fibers, they may become very significant to the adsorption of polymers onto nonporous substrates.

A brief theoretical analysis of a diffusion-controlled process indicates that the initial adsorption rate should be directly proportional to the initial polymer concentration and to the total surface area of fiber present in the system. The first-order behavior with respect to polymer concentration was verified experimentally.

As a mass-transfer process, the adsorption rate is strongly influenced by the diffusion coefficient of the adsorbate. According to elementary mass-transfer theory, the initial rate should be proportional to $\underline{D}^{0.66}$. The dependence of sorption rate on adsorbate molecular weight over a range of from 8,000 to 20,000 is due in part to this relationship. The accessible surface area of the substrate is also dependent on the molecular weight.

The effect of polymer charge density on the adsorption rate is twofold: (1) the diffusion coefficient of a polyelectrolyte is sensitive to changes in solution pH and ionic strength, and (2) electrostatic interactions between polymer and fiber will be superimposed on the diffusion process. At a low degree of polymer ionization (less than a few percent ionized groups) the diffusion mechanism predominates. As the polymer charge density increases, however, the electrostatic interactions become important. The electrostatic interaction effect for a cationic polymer is manifested by an accelerated initial rate followed by a retarded approach to equilibrium. At early times the electrostatic attraction between the negative fiber and the cationic polymer enhances the mass-transfer process. As adsorption proceeds, however, the net electrostatic charge on the fiber becomes positive due to sorbed polymer. Thus, the electrostatic interaction might be one of repulsion and the rate process may be retarded. The relative magnitudes of the extent of attraction and repulsion depend on the charge density of the fiber and the polymer as well as the amount of polymer adsorbed. At low degrees of polymer ionization and when only small amounts of polymer are available for adsorption the retardation effect may not be noticeable. The acceleration effect becomes negligible when the fiber charge density is reduced to relatively small values. The effect of the electrostatic attraction and repulsion decreases with increasing salt concentration due to ionic shielding.

Independent diffusion measurements indicate that the diffusion coefficient of PEI is influenced by an electrophoretic effect at the pH conditions studied (9.6 and 10.9). The highly mobile counterions tend to diffuse ahead of the polyion and, in the process, create an unstable separation of charge. Thus, the macroion is pulled along more rapidly than if the only driving force for diffusion was the gradient of polymer concentration. The electrophoretic effect is enhanced by a high polymer charge density and is decreased by the presence of salt in the system. This diffusional behavior is reflected in the adsorption rate studies.

At the conditions studied (above pH 9.0) the predominant retention mechanism appears to be an ion-exchange reaction. The cationic amine groups on the polymer chain interact with ionized cellulosic hydroxyls on the fiber. There is probably also some retention due to ion exchange with carboxyl groups on the fiber and polymer-fiber hydrogen bonding.

SUGGESTIONS FOR FUTURE RESEARCH

The diffusion of polymers into porous structures is certainly deserving of further research. A rigorous study would require a substrate for which the porosity could be better characterized and controlled than is currently possible for cellulose. Some of the substrates which are used for gel permeation experiments offer excellent possibilities for this application. Quantitative information concerning the rate of polymeric diffusion into cellulose might be generated from experiments designed to measure the rate of transport through cellophane films.

The molecular weight partitioning which occurs during adsorption (10-12) should be investigated in more detail for polyelectrolyte-cellulose systems. Further elucidation of this phenomenon would provide information concerning reversibility and the importance of the accessibility of adsorption sites to polymers of various molecular weights. The fractionation procedure developed in this thesis affords the possibility of performing exchange experiments. These experiments would involve the sorption of low molecular weight polymer followed by treatment with a higher molecular weight fraction. The extent of exchange could be determined by following the change in molecular weight of polymer in the solution phase.

Several years ago, Thode (64) suggested that the application of Donnan potential theory to cellulose fibers might provide a better understanding of the polymer retention process. This is particularly true if the polymer penetrates into the fibrous structure. Neale (65, 66) applied Donnan theory to the distribution of simple ions in a cellulose-fiber slurry with good success. The same author was also able to describe dye retention in terms of the Donnan potential (67). In view of recent developments concerning the retention of polyelectrolytes by cellulose fibers, Thode's recommendation is even more pertinent.

NOMENCLATURE

A = accessible surface area of substrate at time t, cm.^{2}

A_o = accessible surface area of substrate at time t = o, cm.^{2}

B = $(b + \sqrt{-q})/(b - \sqrt{-q})$, dimensionless variable in adsorption rate equation

b = $-(C_o/C_m + 1/KC_m + 1)$, dimensionless variable in adsorption rate equation

C = solute concentration, mg./liter

C^* = concentration of adsorbed solute at time t, mg./liter

C_e = equilibrium solute concentration in solution, mg./liter

C^*_e = concentration of adsorbed solute in equilibrium with a bulk phase concentration of C_e, mg./liter

C_f = concentration of solute in solution at the solid-liquid interface at time t, mg./liter

C_j = solute concentration corresponding to fringe pair j and $(J/2) + j$, fringes

C_m = concentration of adsorbed solute at saturation, mg./liter

C_o = concentration of solute in solution at t = o, mg./liter

C_s = concentration of solute in solution in well-mixed region at time t, mg./liter

C_{sa} = saturation concentration of solute in dissolution processes, mg./liter

D = diffusion coefficient of solute, cm.^{2}/sec.

D_o = diffusion coefficient of solute at infinite dilution, cm.^{2}/sec.

D' = diffusion coefficient of solute before time correction, cm.^{2}/sec.

f = friction coefficient, g./sec.

g_1 = hydrodynamic film constant defined by $\delta = g_1 D^{0.34}$, cm.$^{0.32}$ sec.$^{0.34}$

g_2 = proportionality constant defined by $A_o = g_2 W_f S_e$, dimensionless

J = total number of Rayleigh fringes

j = Rayleigh fringe number

K = Langmuir constant, liter/mg.

k = first order rate constant, sec.$^{-1}$

M_w = weight average molecular weight as determined by sedimentation equilibrium, g./mole

$\underline{N}$ = weight of solute crossing the solid-liquid interface in time $\underline{t}$, mg.

$\underline{N}^*$ = weight of adsorbed solute at time $\underline{t}$, mg.

$\underline{N}_m$ = weight of the maximum amount of solute adsorbed by the adsorbent at equilibrium, mg.

$\underline{N}_o$ = weight of solute initially present in the system, mg.

$\underline{q}$ = $4 \frac{\underline{C}_o}{\underline{C}_m} - \underline{b}^2$, dimensionless variable in adsorption rate equation

$\underline{R}$ = universal gas constant, 8.314×10^7 erg(g. mole °K)$^{-1}$

$\underline{R}_e$ = equivalent hydrodynamic radius, cm.

$\underline{r}$ = distance from axis of rotation, cm.

$\underline{S}_e$ = specific surface area calculated from adsorption and diffusion data, cm.^{2}/g.

$\underline{T}$ = absolute temperature, °K

$\underline{t}$ = time, sec.

$\underline{t}'$ = uncorrected time factor in diffusion experiments, sec.

$\underline{V}$ = total volume of the system, liter

$\underline{\bar{v}}$ = partial specific volume of polymer, cm.^{3}/g.

$\underline{W}_f$ = total weight of fibers in system, g.

$\underline{x}$ = distance, cm.

$\underline{y}$ = $(\sqrt{q}\ \underline{D}/\underline{V})(\underline{A}_o/\delta)$, sec.$^{-1}$

$\underline{Z}$ = upper integration limit of error function

β = integration variable of error function

Γ = specific adsorption, g./100 g.

Γ_m = specific adsorption at saturation, g./100 g.

δ = effective thickness of diffusional film, cm.

η = solvent viscosity, g. sec.$^{-1}$ cm.$^{-1}$

ρ = solvent density, g./cm.^{3}

ω = angular velocity, sec.$^{-1}$

$\Delta\underline{C}$ = total concentration difference in diffusion cell, fringes

$\Delta\underline{t}$ = time correction factor in diffusion experiments, sec.

ACKNOWLEDGMENTS

Many people have contributed directly or indirectly to the successful completion of this thesis. The author is indebted to each one for his or her assistance.

Several people stand out as being particularly helpful and are worthy of special mention: J. W. Swanson served as chairman of the thesis advisory committee and was a constant source of encouragement and constructive criticism; D. G. Williams and H. A. Swenson also served on the advisory committee and unselfishly lent much of their time and knowledge to the execution of the thesis; many stimulating discussions with R. H. Atalla provided a source of encouragement and enthusiasm; J. A. Carlson provided invaluable assistance to the molecular weight and diffusion coefficient measurements; Miss O. A. Smith took the electron micrographs; and M. C. Filz, Jr. aided in the design and construction of the apparatus.

Finally, the author's wife, Mrs. Trudy A. Kindler deserves special recognition for displaying outstanding patience and encouragement throughout the thesis and for typing the original manuscript.

LITERATURE CITED

1. Hughes, R. E., and von Frankenburg, C. A. High polymers. In Annual reviews of physical chemistry. Vol. 14. p. 291. Palo Alto, Calif., Annual Reviews, Inc., 1963.

2. Silberberg, A., J. Phys. Chem. 66:1884-907(1962).

3. Patat, F., Killman, E., and Schliebener, C., Rubber Chem. Technol. 39:36-87 (1966).

4. Wet strength in paper and paperboard. TAPPI Monograph Series no. 29. New York, Technical Association of the Pulp and Paper Industry, 1965.

5. Swanson, J. W. In Trans. of the Symposium on Consolidation of the Paper Web. Vol. 2. p. 741-76. London, Tech. Sect., Brit. Paper and Board Makers' Assoc., 1966.

6. Claesson, I., and Claesson, S., Phys. Rev. 73:1221(1948).

7. Hobden, J. F., and Jellinek, H. H. G., J. Polymer Sci. 11:365-78(1953).

8. Binford, J. S., and Gessler, A. M., J. Phys. Chem. 63:1376-8(1959).

9. Jankovics, L., J. Appl. Polymer Sci. 9:545-52(1965).

10. Emery, P. H. Polymer adsorption and fractionation in the polystyrene-dichloroethane-carbon black system. Doctor's Dissertation. Appleton, Wis., The Institute of Paper Chemistry, 1965. 186 p.

11. Farrar, N. O. Partitioning and reversibility of polymer adsorption in the polystyrene, 1,2-dichloroethane, carbon black system. Doctor's Dissertation. Appleton, Wis., The Institute of Paper Chemistry, 1967. 100 p.

12. Kindler, W. A., and Swanson, J. W. Some aspects of the adsorption of polyethylenimine by pulp fibers. Unpublished report, 1967.

13. Russo, V. A., and Thode, E. F., Tappi 43:209-18(1960).

14. Becher, J. J., Hoffman, G. R., and Swanson, J. W., Tappi 44:296-9(1961).

15. Thode, E. F., Swanson, J. W., Kurath, S. F., and Hoffman, G. R., Tappi 42:170-4 (1959).

16. Kurath, S. F., Chu, C. Y., and Swanson, J. W., Tappi 42:175-9(1959).

17. Forsman, W. C., and Hughes, R. E., J. Chem. Phys. 38:2130-5(1963).

18. Gilliland, E. R., and Gutoff, E. B., J. Phys. Chem. 64:407-10(1960).

19. Frisch, H. L., and Simha, R., J. Phys. Chem. 58:507-12(1954).

20. Howard, G. J., and McConnell, P., J. Phys. Chem. 71:2974-95(1967).

21. Allen, G. G., Akagane, K., Neogi, A. N., Reif, W. M., and Mattila, T., Nature 225:175-6(1970).

22. Stone, J. E., Treiber, E., and Abrahamson, B., Tappi 52:108-10(1969).

23. Bates, N. A., Tappi 52:1157-61(1969).

24. Peterson, C., and Kwei, T. K., J. Phys. Chem. 65:1330-3(1961).

25. Steinberg, G., J. Phys. Chem. 71:292-301(1967).

26. Bircumshaw, L. L., and Riddiford, A. C., Quart. Revs. (London) 6:157-85(1952).

27. Nernst, --., Z. Physikal. Chem, 47:52(1904); as cited in (26).

28. Moelwyn-Hughes, E. A. The kinetics of reaction in solution. 2nd. ed. Oxford, Clarendon Press, 1947. 424 p.

29. Frank-Kamenetskii, D. A. Diffusion and heat exchange in chemical kinetics. Princeton, New Jersey, Princeton University Press, 1955. 370 p.

30. King, C. V., and Cathcart, W. H., J. Am. Chem. Soc. 59:63-7(1937).

31. Chilton, T. H., and Colburn, A. D., Ind. Eng. Chem. 26:1183-7(1934).

32. Kenaga, D. L., Kindler, W. A., and Meyer, F. J., Tappi 50:381-7(1967).

33. Nagasawa, M., and Fujita, H., J. Am. Chem. Soc. 86:3005-12(1964).

34. Kedem, O., and Katchalsky, A., J. Polymer Sci. 15:321-34(1955).

35. Suzuki, Y., Noda, I., and Nagasawa, M., J. Phys. Chem. 73:797-803(1969).

36. Alexandrowicz, Z., and Daniel, E., Biopolymers 1:447-71(1963).

37. Sarkanen, K. V., Dinkler, F., and Stannett, V., Tappi 49:4-9(1966).

38. Trout, P. E. The mechanism of the improvement of the wet strength of paper by polyethylenimine. Doctor's Dissertation. Appleton, Wis., The Institute of Paper Chemistry, 1951. 96 p.

39. Perrine, T. D., and Landis, W. R., J. Polymer Sci., Pt. A-1 5, no. 8:1993-2005 (1967).

40. Handbook of chemistry and physics. 42nd. ed. Cleveland, Ohio, Chemical Rubber Publishing Co., 1961.

41. Private communication. Dr. R. D. Conlon, Director of Research, Nester/Faust Corporation.

42. Gosting, L. J. Measurement and interpretation of diffusion coefficients of proteins. In Advances in protein chemistry. Vol. XI. p. 429. New York, Academic Press, 1956.

43. Instruction manual, Beckman Model E ultracentrifuge. Palo Alto, Calif., Beckman Instruments, Inc., 1964.

44. Tables of probability functions. Vol. 1. Federal Works Agency, Works Projects Administration (Sponsored by National Bureau of Standards, 1941).

45. Longsworth, L. G., J. Am. Chem. Soc. 74:4155-62(1952).

46. Creeth, J. M., J. Am. Chem. Soc. 77:6428-40(1955).

47. Tostevin, J. E. The hydrodynamic properties of the alditol oligosaccharides. Doctor's Dissertation. Appleton, Wis., The Institute of Paper Chemistry, 1966. 96 p.

48. Daniel, E., and Alexandrowicz, Z., Biopolymers 1:473-95(1963).

49. Thompson, G., Rice, S. A., and Nagasawa, M., J. Am. Chem. Soc. 85:2537-44(1963).

50. Nagasawa, M., and Eguchi, Y., J. Phys. Chem. 71:880-90(1967).

51. Silberberg, A., J. Phys. Chem. 66:1872-83(1962).

52. Philipp, B., and Lang, H., Tappi 52:1179-83(1969).

53. Jurecic, A., Lindh, T., Church, S. E., and Stannett, V., Tappi 41:465-8(1958).

54. Jurecic, A., How, C. M., Sarkanen, K., Donofric, C. P., and Stannett, V., Tappi 43:861-5(1960).

55. Stamm, A. J. Wood and cellulose science. New York, The Ronald Press Company, 1964.

56. Tanford, C. Physical chemistry of macromolecules. 2nd. ed. New York, John Wiley and Sons, 1963.

57. Crank, J. The mathematics of diffusion. Oxford, Clarendon Press, 1956. 347 p.

58. Reinmuth, W. H., J. Phys. Chem. 65:473-6(1961).

59. Heller, W., and Pugh, T. L., J. Polymer Sci. 47:203-17(1960).

60. Pugh, T. L., and Heller, W., J. Polymer Sci. 47:219-27(1960).

61. Clayfield, E. J., and Lumb, E. C., J. Colloid Interface Sci. 22:269-84(1966).

62. Meier, D. J., J. Phys. Chem. 71:1861-8(1967).

63. Goring, D. A. I., Pulp Paper Mag. Can. 67:T519-24(1966).

64. Thode, E. F., Tappi 42:983-5(1959).

65. Neale, S. M., and Standring, P. T., Proc. Royal Soc. A213:530-45(1952).

66. Farrar, J., and Neale, S. M., J. Colloid Sci. 7:186-95(1952).

67. Neale, S. M., Trans. Faraday Soc. 43:325-31(1947).

68. Operating directions for the Coleman Model 29 Nitrogen Analyzer. Maywood, Illinois, Coleman Instruments, Inc., 1960.

69. Teller, D. C. Sedimentation equilibrium of macromolecules. Doctor's Dissertation. Berkeley, Calif., University of California, 1965.

APPENDIX I

DETERMINATION OF NITROGEN CONTENT OF PEI SOLUTIONS BY MICRO-DUMAS METHOD

The nitrogen content of Fractions 63-5 through 63-8 was determined by means of a micro-Dumas method using a Coleman Model 29 Nitrogen Analyzer. The operating cycle of this instrument is divided into three automatic steps. The first step consists of purging the entire combustion train with purified carbon dioxide to drive out entrapped air. In the second step, the sample is broken down into its elemental constituents by combustion. Finally, the combustion products are swept over oxidizing and reducing materials, leaving only nitrogen and the carbon dioxide sweeping gas. This gaseous mixture is scrubbed thoroughly in a caustic solution to effect removal of the carbon dioxide. The nitrogen, which is the only gas remaining, is collected and measured in a 5.000 $cm.^3$ stainless steel syringe linked to a digital counter by a precision micrometer screw.

A 0.100-ml. aliquot of the polymer solution was pipetted into the sample chamber. The oven temperature was set at 800°C. and the post temperature at 600°C. From this point the manufacturers directions were followed without modification (68).

The quantity of nitrogen in the sample, $\underline{N}$ (g./100 ml.), was calculated from,

$$N = \frac{P_c V_c}{T V_s} \times 4.49 \times 10^{-2} \qquad (29)$$

where $\underline{P_c}$ is the corrected barometric pressure, $\underline{V_c}$ is the corrected nitrogen volume, $\underline{T}$ is the absolute temperature of the syringe, and $\underline{V_s}$ is the sample volume. The PEI concentration is calculated from the theoretical nitrogen content of 32.53%.

The results are summarized in Table VII; all data were calculated at a corrected barometric pressure of 746.3 mm. Hg and a blank of 9 microliters.

TABLE VII

DATA FROM DUMAS NITROGEN ANALYSIS

Sample	$\underline{V}_c$, ml.	$\underline{T}$, °K	PEI Concn. (Av.), g./liter
63-5	0.317	304.0	1.06
	0.314	303.9	
	0.308	303.9	
63-6	0.351	304.0	1.19
	0.354	304.0	
63-7	0.365	304.5	1.23
	0.363	304.1	
63-8	0.369	303.9	1.25
	0.370	303.9	

APPENDIX II

DETERMINATION OF MOLECULAR WEIGHT BY SEDIMENTATION EQUILIBRIUM ANALYSIS

There are essentially two different approaches to sedimentation equilibrium experiments. The conventional slow-speed method yields the most reliable weight-average molecular weight but requires two to three days of centrifuge time. This technique requires one run to determine the equilibrium distribution of the sample in the centrifugal field and a second synthetic boundary run to calibrate the Rayleigh optical system. The second, and newer approach, is referred to as the high speed or Yphantis method and has the advantages of requiring only a single run and less machine time. Unfortunately, however, the Yphantis technique is applicable only to samples having a very narrow molecular-weight distribution and an average molecular weight in excess of about 40,000. An attempt was made to use the Yphantis method for the analysis of the PEI-63 fractions but the molecular weights were too low to yield reliable results. The remainder of this discussion will be limited to the use of the slow-speed method.

The weight-average molecular weight can be derived from the concentration distribution of the polymer in a centrifugal field by means of the following classical equation:

$$M_w = \frac{2RT}{\omega^2(1 - \bar{v}\rho)} \frac{2.303d \log C}{d(r^2)} \qquad (30)$$

where R is the universal gas constant, T is the absolute temperature, ω is the angular velocity of the rotor, $\bar{v}$ is the partial specific volume of the polymer, ρ is the solvent density, and C is the polymer concentration at a distance r from the axis of rotation.

According to Equation (30) a plot of log C versus r^2 will exhibit a slope which is proportional to the molecular weight. For a monodisperse, ideal system the plot

will be linear over the entire cell. If deviations from ideality can be assumed to be negligible, any nonlinearity can be attributed to polydispersity. By calculating the molecular weight at the top and the bottom of the cell, as well as a whole cell average, the degree of polydispersity of the sample can be estimated. These computations can be facilitated by the use of a computer program given by Teller (69) and modified by the Institute computer staff.

The concentration distribution in a centrifugal field was measured in a Beckman Spinco Model E ultracentrifuge utilizing the Rayleigh optical system. The operation and description of this instrument are given elsewhere (43). The solution-concentration measurements were made with a double-sector synthetic boundary cell. For all sedimentation runs, the triple-sector rotor cell was used in order that three solutions could be run at the same time.

All runs were made at 25.0°C. in an aqueous solvent of 0.10N NaCl to suppress charge effects. The polymer solutions were dialyzed against the solvent to eliminate Donnan effects. Each fraction was measured at four dilutions to account for concentration effects. Rotor speeds varied between 20,410 and 33,450 r.p.m., depending on molecular weight.

The Rayleigh interference patterns produced by the polymer solutions and the pure solvent were photographed at intervals of time and tested against one another to assure that equilibrium conditions were met. Fringe numbers and positions were determined from these photographs with the aid of an x-y microcomparator fitted with digital and punched-card read-out devices. The photographic plates for these experiments as well as the operating conditions are filed in the Calder Biochemistry Laboratory at The Institute of Paper Chemistry.

The partial specific volumes and solvent densities were measured pycrometrically at the same temperature and solvent conditions used in the sedimentation experiments. The partial specific volumes for Fractions 63-6 and 63-4 at infinite dilution is 0.708 $cm.^3/g$. The density of 0.10N NaCl at 25.0°C. was determined to be 1.0011 $g./cm.^3$.

The calculated molecular weights are given as a function of polymer concentration in Table VIII. It can be observed that the fractions are quite narrow in molecular weight distribution. The molecular weight at infinite dilution is taken as the characteristic value for each fraction.

TABLE VIII

RESULTS OF SEDIMENTATION EQUILIBRIUM EXPERIMENTS

Fraction Number	Concn., fringes	$\underline{M}_w$ (Meniscus)	$\underline{M}_w$ (Bottom)	$\underline{M}_w$ (Average)	$\underline{M}_w$ (at Infinite Dilution)
63-4	25.4	8,900	9,280	8,930	20,000
	12.7	13,100	13,650	12,810	
	6.4	15,470	16,480	15,860	
	3.2	19,360	21,970	19,150	
63-5	15.4	10,660	15,010	11,290	14,000
	7.7	9,430	11,410	10,710	
	3.8	10,840	14,150	12,550	
63-6	26.4	4,940[a]	6,220[a]	5,440	11,500
	13.2	N.D.[a]	N.D.[a]	7,000	
	6.6	N.D.[a]	N.D.[a]	8,500	
	3.3	N.D.[a]	N.D.[a]	10,500	
63-7	27.8	4,090	4,810	4,320	9,500
	13.2	8,090	8,730	7,820	
	6.9	8,320	8,960	8,380	
	3.5	8,960	9,440	8,830	
62-8	20.1	3,310	3,930	3,680	8,000
	10.0	6,040	6,190	6,090	
	5.0	9,000	6,810	7,100	
	2.5	5,840	7,370	6,750	

[a] N.D. = not determined.

APPENDIX III

PROGRAM FOR CALCULATION OF DIFFUSION COEFFICIENT

This program calculates apparent diffusion coefficients from Rayleigh diffraction fringe data by the method of Longsworth and Creeth. The name of the program is DIFCO. The following constants are used in the numerical inverse solution to the error function.

```
C     DOUBLE PRECISION CM,CO,C1,C2,B1,B2,B3,SP,F,T,BLC,RECT,X1,Y11,Y12,P
      DOUBLE PRECISION H(99),X2,Y21,Y22,Y23,Y31,Y32,Y33,DX,DY,Y1,Y2,Y3,Y
      DOUBLE PRECISION FS,FSJ,FJ(99),S,S2,Z(99),  R(99),U,DELH(99),Q(99)
      DOUBLE PRECISION DAQY,DEV(99),DA,DELZ(99),DR(99),Y13,YF,PF,DAQ(99)
      CO=1.7787391
      C1=0.802853
      C2=0.014605998
      B1=2.0262682
      B2=0.3785538
      B3=0.0036995827
      SP=2./SQRT(3.14159)
      NP=0
C     F IS THE MAGNIFICATION FACTOR.
      F=2.1463
C     NPRS=NUMBER OF DIFFERENT PAIRINGS OF DATA.
C     NPTNS=TOTAL NUMBER OF FRINGE PATTERNS.
C     FS=TOTAL NUMBER OF FRINGES.
C     J=NUMBER OF WHOLE FRINGES INCLUDED IN DATA.
C     NUPLT=PLATE NUMBER.
C     NUSAM=SAMPLE NUMBER.
C     BLC=BASELINE CORRECTION, DY/DX.
C     C=CONVERSION FACTOR FROM 1/12000 INCH TO CM.
      CM=0.00021167
      IORDR=5
      IOPRT=6
11    READ(IORDR,500)NUPLT,NUSAM,J,T,BLC,NPRS,NPTNS
500   FORMAT(I8,2X,I8,2X,I2,2X,F15.8,2X,F15.8,2X,I2,2X,I2)
C     RECT=RECIPROCAL TIME
      RECT=1./T
      WRITE(IOPRT,5000)NUPLT,NUSAM
5000  FORMAT(1H1,' PLATE NUMBER',2X,I8,',    SAMPLE NUMBER',2X,I8)
      WRITE(IOPRT,5001)J,RECT
5001  FORMAT(1H ,' WHOLE FRINGES',2X,I2,',    RECT=',2X,F15.8)
      READ(IORDR,501)X1,Y11,Y12,Y13
501   FORMAT(F5.0,F5.0,5X,F5.0,5X,F5.0)
C     H(I)=FRINGE POSITION
      READ(IORDR,502)(H(I),I=1,J)
502   FORMAT(8(F5.0,5X))
      DO 4 I=1,J
      H(I)=H(I)*CM
4     CONTINUE
      READ(IORDR,503)X2,Y21,Y22,Y23
```

```
503  FORMAT(F5.0,F5.0,5X,F5.0,5X,F5.0)
     READ(IORDR,504)Y31,Y32,Y33
504  FORMAT(5X,F5.0,5X,F5.0,5X,F5.0)
C    CALC. OF FRACTIONAL FRINGE
     DX=X1-X2
     DY=BLC*DX
     Y1=(Y11+Y12+Y13)/3.
     Y2=(Y21+Y22+Y23)/3.
     Y3=(Y31+Y32+Y33)/3.
     Y=Y1-Y2-DY
     YF=Y3-Y2
     PF=Y/YF
     FSJ=J
     FS=FSJ+PF
     IF(PF)22,23,23
22   J=J-1
23   WRITE(IOPRT,4000)FS
4000 FORMAT(1H ,'TOTAL NUMBER OF FRINGES',3X,F15.8)
     NP=NP+1
     M=J/2
     N=1
C    CALC. OF ERF,UPPER LIMIT,AND CONC. COEFF.
     DO 5 I=1,J
     AI=I
     FJ(I)=(2.*AI-FS)/FS
     IF(FJ(I))2,3,3
2    FJ(I)=-FJ(I)
3    S=ALOG(2./(1.-FJ(I)))
     S=SQRT(S)
     S2=4.4466*((S-.8326)**.4814)
     S2=SIN(S2)
     S2=0.0031*S2
     Z(I)=S-((S**2.*C2+S*C1+C0)/(S**3.*B3+S**2.*B2+S*B1+1.))+S2
     S=SP/EXP(Z(I)**2.)
     P=-(FJ(I)**2.+Z(I)*FJ(I)*S+S**2./2.-1.)/2.
     R(I)=P/S
5    CONTINUE
     WRITE(IOPRT,5002)
5002 FORMAT(1HO,2X,'I',5X,'FRINGE POSITION',8X,'ERF Z',15X,"Z",15X,
    1'R(I)')
     DO 51 I=1,J
     WRITE(IOPRT,5003)I,H(I),FJ(I),Z(I),R(I)
5003 FORMAT(1H ,I4,3X,F15.8,3X,F15.8,3X,F15.8,3X,F15.8)
51   CONTINUE
6    S=0.
     U=0.
     DO 9 I=1,M
     L=J+1-I
     DELH(I)=H(I)-H(L)
     IF (DELH(I))14,15,15
14   DELH(I)=-DELH(I)
15   DELZ(I)=Z(I)+Z(L)
     DR(I)=R(L)-R(I)
     Q(I)=DELH(I)/DELZ(I)
```

```
C     DAQ(I)=DIFFUSION COEFFICIENT OF THE FRINGE PAIR CONSIDERED.
      DAQ(I)=(Q(I)**2.)/(4.*T*F**2.)
      S=S+Q(I)
      U=U+DAQ(I)
9     CONTINUE
C     PRINT NORMALIZED FRINGE DEVIATIONS AND THE CORRESPONDING DIFFUSION COEFF.
      WRITE(IOPRT,5004)
5004  FORMAT(1HO,2X,'NORM FR DEV',5X,'DISSUFION COEFF.')
      DO 91 I=1,M
      WRITE(IOPRT,5005)Q(I),DAQ(I)
5005  FORMAT(1H ,F15.8,3X,E15.8)
91    CONTINUE
      P=M
      YF=AVERAGE VALUE OF NORMALIZED FRINGE SEPARATIONS
35    YF=S/P
C     DAQY=AVERAGE VALUE OF DAQ
      DAQY=U/P
      DO 26 I=1,M
      S=DELH(I)/YF
      DEV(I)=S-DELZ(I)
26    CONTINUE
      WRITE(IOPRT,5009)
5009  FORMAT(1HO,2X,'FRINGE DEV.',7X,'DELTA R(Z*)')
      DO 27 I=1,M
      WRITE(IOPRT,5006)DEV(I),DR(I)
5006  FORMAT(1H ,F15.8,3X,F15.8)
27    CONTINUE
C     DA=DIFFUSION COEFFICIENT.  AVE. EXCLUD. FIRST AND LAST.
      S=0.
      U=0.
      M=M-1
      DO 19 I=2,M
      L=J-I+1
      DELH(I)=H(I)-H(L)
      IF(DELH(I))141,151,151
141   DELH(I)=-DELH(I)
151   DELZ(I)=Z(I)+Z(L)
      Q(I)=DELH(I)/DELZ(I)
      DAQ(I)=(Q(I)**2.)/(4.*T*F**2.)
      S=S+Q(I)
      U=U+DAQ(I)
19    CONTINUE
      P=M-1
      DA=U/P
      WRITE(IOPRT,5007)
5007  FORMAT(1HO,6X,'YF',10X,'AV. DIF. COEFF.1',3X,'AV. DIF. COEFF.2')
      WRITE(IOPRT,5008)YF,DAQY,DA
5008  FORMAT(1H ,3(E15.8))
      WRITE(7,5090)T,FS
5090  FORMAT(F15.8,2X,F15.8)
      DA=DA*(10.**6.)
      RECT=RECT*100.
      WRITE(7,5010)RECT,DA
```

```
5010 FORMAT(F15.8,2X,F15.8)
10   IF(NPTNS-NP)12,12,11
12   STOP
     END
        SIZE OF COMMON  00000     PROGRAM  12076
COMPILATION  MAIN
```

APPENDIX IV

EQUILIBRIUM ADSORPTION DATA

Table IX summarizes the data relating to the effect of pH on equilibrium adsorption behavior. These results are plotted in Fig. 15, 16, and 17.

The data required to prepare equilibrium isotherms are listed in Table X. The calculation of the specific adsorption and Langmuir parameters is shown in Table XI. The symbols have the same meanings as before, i.e., $\underline{C}_o$ is the initial polymer concentration, $\underline{C}_e$ is the concentration of polymer in solution at equilibrium, $\underline{C}^*_e$ is the concentration of adsorbed polymer at equilibrium, $\underline{W}_f$ is the weight (O.D.) of fibers, and Γ is the specific adsorption. These results are given in graphical form in Fig. 18 through 22.

TABLE IX

EFFECT OF pH ON ADSORPTION AT INITIAL POLYMER CONCENTRATION OF 96.0 MG./LITER

Sample Number	Run Number	C_{OH^-},[a] mM	pH[b]	A_s[c]	A_t[d]	C_{PEI},[e] mg./liter	Eff.,[f] %
63-6	E-24	0	9.26	1.44	1.56	91.6	4.6
		0.89	11.08	1.64	1.39	71.5	25.5
		1.78	11.45	2.13	2.03	81.0	15.6
		3.56	11.78	2.90	3.00	88.5	7.8
	E-26	0	9.24	1.44	1.53	91.9	4.3
		0.08	9.61	1.48	1.49	87.0	9.4
		0.18	10.09	1.52	1.41	80.1	16.6
		0.36	10.58	1.54	1.32	74.0	22.9
		0.54	10.81	1.57	1.30	71.6	25.6
63-2	E-28	0	7.06	1.55	1.53	94.8	1.2
		0.20	8.23	1.58	1.55	94.4	1.7
		0.40	9.12	1.59	1.53	92.6	3.6
		0.60	9.79	1.60	1.52	91.2	5.0
		0.80	10.13	1.61	1.49	88.9	7.4
		1.20	10.59	1.65	1.49	86.8	9.6
		2.00	11.04	1.75	1.59	87.5	8.9
63-8	E-29	0	9.09	1.48	1.31	85.2	11.2
		0.40	10.55	1.54	0.79	49.4	48.5
		0.60	10.80	1.59	0.76	45.9	52.0
		0.80	10.97	1.58	0.76	46.1	51.8
		1.20	11.20	1.62	0.87	52.3	45.6
		2.00	11.44	1.71	1.04	58.5	39.0
PEI-63	E-30	0	9.81	1.55	1.15	71.2	25.8
		0.40	10.58	1.58	0.97	58.9	38.6
		0.60	10.83	1.60	0.97	58.2	39.4
		0.80	10.99	1.63	0.99	58.4	39.2
		1.20	11.19	1.67	1.05	60.4	37.0
		2.00	11.46	1.76	1.22	66.5	30.8
PEI-63	E-31[g]	0	8.71	1.49	1.29	83.0	13.5
		0.40	8.92	1.55	1.29	79.7	17.0
		0.60	9.91	1.56	1.22	75.0	21.8
		0.80	10.28	1.60	1.20	72.0	25.0
		1.20	10.71	1.63	1.30	76.7	20.1
		2.00	11.13	1.74	1.68	92.8	3.3

[a] Concentration of sodium hydroxide.
[b] pH of solution after adsorption.
[c] Absorbance of standard.
[d] Absorbance of test solution.
[e] Concentration of PEI in solution.
[f] Efficiency, ratio of polymer adsorbed to polymer added.
[g] The substrate for E-31 was oxidized RD-101 fibers, all other tests on regular RD-101.

TABLE X

EQUILIBRIUM ISOTHERM MEASUREMENTS

Fraction Number	Run Number	C_o, mg./liter	Absorbance	Dilution Factor	C_e, mg./liter	C_e^*, mg./liter
63-8[a]	E-33	33.4	0.092	1	8.2	25.2
		66.7	0.176	1	15.8	50.9
		133	0.79	1	70	63
		167	1.027	1	92	75
		200	1.093	0.8	122	78
		334	1.654	0.6	247	87
		334	1.69	0.6	252	82
		467	1.74	0.4	390	77
		STD.	1.342		120	
63-7[a]	E-36	24.0	0.172	1	10.8	13.2
		48.0	0.343	1	21.5	26.5
		72.0	0.599	1	37.6	34.4
		120	1.164	1	73.0	47
		240	1.732	0.6	181	59
		480	1.327	0.2	416	64
		STD.	1.378		86.4	
63-6[a]	E-34	26.4	0.302	1	19.3	7.1
		52.9	0.542	1	34.7	18.2
		79.4	0.842	1	53.9	25.5
		132	1.502	1	96	36
		264	1.99	0.6	212	52
		529	1.465	0.2	469	60
		STD.	1.488		95.2	
63-5[a]	E-37	24.8	0.318	1	19.5	5.3
		49.6	0.638	1	39.1	10.5
		74.4	1.004	1	61.5	12.9
		124	1.658	1	102	22
		248	2.14	0.6	218	30
		496	1.516	0.2	464	32
		STD.	1.456		89.2	
63-4[a]	E-35	24.0	0.382	1	22.4	1.6
		48.0	0.735	1	43.0	5.0
		72.0	1.047	1	61.2	10.8
		120	1.80	1	105	15
		240	2.28	0.6	223	17
		480	1.58	0.2	462	18
		STD.	1.500		86.4	
63-7[b]	E-38	22.9	0.295	1	18.9	4.0
		48.0	0.630	1	40.4	7.6
		72.0	0.958	1	62	10
		144	1.88	1	120	14
		240	2.00	0.6	213	27
		STD.	1.353		86.6	

[a] 8.0×10^{-4} N NaOH.

[b] 8.0×10^{-5} N NaOH.

TABLE XI

LANGMUIR ISOTHERM CALCULATIONS

Fraction Number	Run Number	C_o, mg./liter	W_f, mg.	Γ, g./100 g.	C_e/C^*_e
63-8[a]	E-33	33.4	130	0.87	0.33
		66.7	130	1.76	0.31
		133	130	2.18	1.11
		167	131	2.58	1.23
		200	131	2.68	1.56
		334	132	2.97	2.84
		334	131	2.82	3.08
		467	131	2.64	5.08
63-7[a]	E-36	24.0	131	0.45	0.82
		48.0	131	0.91	0.84
		72.0	130	1.19	1.09
		120	131	1.62	1.55
		240	131	2.03	3.06
		480	130	2.21	6.50
63-6[a]	E-34	26.4	131	0.24	2.72
		52.9	130	0.63	1.92
		79.4	130	0.88	2.11
		132	132	1.23	2.67
		264	131	1.78	4.08
		529	131	2.06	7.80
63-5[a]	E-37	24.8	131	0.18	3.68
		49.6	132	0.36	3.72
		74.4	131	0.44	4.76
		124	131	0.76	4.64
		248	132	1.02	7.3
		496	130	1.11	14.5
63-4[a]	E-35	24.0	130	0.06	14.0
		48.0	130	0.17	8.6
		72.0	130	0.38	5.7
		120	130	0.52	7.0
		240	130	0.59	13.1
		480	130	0.62	25.6
63-7[b]	E-38	22.9	130	0.14	4.7
		48.0	131	0.26	5.3
		72.0	131	0.35	6.2
		144	130	0.48	8.6
		240	131	0.93	7.9

[a] 8.0×10^{-4} N NaOH.
[b] 8.0×10^{-5} N NaOH.

APPENDIX V

ADSORPTION RATE DATA

Table XII lists the rate data used to prepare Fig. 25 through 43. The initial polymer concentration is given by C_o, C_s is the solution-phase concentration at time t, and C^* is the adsorbed polymer at time t. For every case, 131 ± 1 mg. of RD-101 fiber was used. The sorption temperature was controlled at 25.0 ± 0.2°C.

TABLE XII

ADSORPTION RATE DATA

Fraction Number	Run Number	C_o, mg./liter	Time, min.	Absorbance	C_s, mg./liter	C^*, mg./liter	Solvent
63-8	K-15[a]	133	468	0.79	70	63	8.0×10^{-4} N NaOH
			372	0.78	69	64	
			245	0.82	73	60	
			120	0.89	79	54	
			91	0.94	84	49	
			60	1.05	93	40	
			45	1.07	95	38	
			29	1.14	102	31	
			20	1.20	107	24	
			STD.	1.34	120		
	K-9	133	1260	0.72	62	71	8.0×10^{-4} N NaOH
			480	0.79	68	65	
			350	0.80	69	64	
			240	0.86	74	59	
			180	0.90	76	57	
			120	0.98	83	50	
			105	1.00	85	48	
			90	1.02	87	46	
			75	1.05	89	44	
			60	1.08	92	41	
			45	1.11	94	39	
			30	1.17	99	34	
			15	1.29	110	23	
			10.2	1.48	127	6	
			4.9	1.51	129	4	
			2.8	1.52	130	3	
			STD.	1.40	120		

[a]See end of table for footnote.

TABLE XII (Continued)

ADSORPTION RATE DATA

Fraction Number	Run Number	C_o, mg./liter	Time, min.	Absorbance	C_s, mg./liter	C^*, mg./liter	Solvent
63-8	K-13	133	480	0.97	86	47	8.0×10^{-4} N NaOH
			360	0.96	85	48	+ 2.0 mM NaCl
			240	1.02	90	43	
			119	1.07	95	38	
			104	1.11	98	35	
			60	1.18	104	29	
			45	1.21	107	26	
			30	1.27	112	21	
			16	1.29	114	19	
			STD.	1.36	120		
63-8	K-14	133	1493	1.04	91	42	8.0×10^{-4} N NaOH
			820	1.07	93	40	+ 5.0 mM NaCl
			576	1.11	97	36	
			480	1.07	92	41	
			360	1.15	99	34	
			311	1.12	98	35	
			240	1.18	102	31	
			202	1.15	100	33	
			132	1.19	103	30	
			90	1.24	107	26	
			60	1.27	110	23	
			30	1.32	114	19	
			20	1.37	119	14	
			15	1.39	120	13	
			10	1.46	127	6	
			STD.	1.38	120		
63-7	K-19	191	484	1.30	146	45	8.0×10^{-4} N NaOH
			377	1.27	142	49	
			296	1.27	142	49	
			112	1.36	152	39	
			50	1.44	161	30	
			30	1.50	168	23	
			20	1.54	173	18	
			10	1.64	184	7	
			STD.	1.29	138		

[a]See end of table for footnote.

TABLE XII (Continued)

ADSORPTION RATE DATA

Fraction Number	Run Number	C_o, mg./liter	Time, min.	Absorbance	C_s, mg./liter	C^*, mg./liter	Solvent
63-7	K-18	137	736	1.60	95	42	8.0×10^{-4} N NaOH
			381	1.60	95	42	
			261	1.63	97	40	
			124	1.74	104	33	
			53	1.88	112	25	
			30	1.96	117	20	
			20	2.06	123	14	
			10	2.20	131	6	
			5	2.21	132	5	
			STD.	1.65	98.4		
63-7	K-12	96	480	1.01	61	35	8.0×10^{-4} N NaOH
			360	1.03	63	33	
			240	1.09	66	30	
			120	1.17	71	25	
			90	1.20	73	23	
			59	1.25	76	20	
			45	1.30	79	17	
			30	1.31	80	16	
			15	1.47	90	6	
			STD.	1.38	86.4		
63-7	K-17	54.7	564	0.490	29.0	25.7	8.0×10^{-4} N NaOH
			360	0.518	30.6	24.1	
			283	0.528	31.2	23.5	
			145	0.602	35.7	19.0	
			88	0.662	39.2	15.5	
			59	0.744	44.0	10.7	
			47	0.740	43.9	10.8	
			45	0.718	42.6	12.1	
			30	0.790	47.0	7.7	
			20	0.805	47.9	6.8	
			10	0.842	49.9	4.8	
			5	0.870	51.5	3.2	
			STD.	0.662	39.4		
63-7	K-20	27.4	770	0.213	13.2	14.2	8.0×10^{-4} N NaOH
			360	0.251	15.6	11.8	
			232	0.262	16.3	11.1	
			122	0.304	18.9	8.5	
			50	0.345	21.4	6.0	

[a]See end of table for footnote.

TABLE XII (Continued)

ADSORPTION RATE DATA

Fraction Number	Run Number	C_o, mg./liter	Time, min.	Absorbance	C_s, mg./liter	C^*, mg./liter	Solvent
63-7	K-20	27.4	30	0.375	23.3	4.1	8.0 x 10^{-4} N NaOH
			20	0.384	23.8	3.6	
			10	0.387	24.1	3.3	
			5	0.410	25.5	1.9	
			STD.	0.317	19.7		
63-7	K-22	96.2	2213	1.291	82.7	13.5	8.0 x 10^{-5} N NaOH
			1140	1.319	84.4	11.8	
			765	1.808	83.6	12.6	
			480	1.330	85.2	11.0	
			243	1.379	88.2	8.0	
			120	1.420	90.8	5.4	
			94	1.434	91.8	4.4	
			60	1.442	92.3	3.9	
			45	1.450	92.8	3.4	
			30	1.450	92.8	3.4	
			15	1.465	93.6	2.6	
			6	1.485	95.0	1.2	
			STD.	1.353	86.6		
63-6	K-5; 6 and 16	106	480	1.26	83	23	8.0 x 10^{-4} N NaOH
			240	1.28	84	22	
			120	1.35	88	18	
			91	1.38	90	16	
			60	1.43	94	12	
			45	1.47	96	10	
			16	1.56	102	4	
			12	1.58	104	2	
			4.4	1.60	105	1	
			STD.	1.48	97		
63-5	K-8	99	479	1.38	85	14	8.0 x 10^{-4} N NaOH
			366	1.38	85	14	
			245	1.39	86	13	
			120	1.46	90	9	
			90	1.48	91	8	
			60	1.49	92	7	
			44	1.52	94	5	
			30	1.54	95	4	
			15	1.57	97	2	
			STD.	1.44	89		

[a] See end of table for footnote.

TABLE XII (Continued)

ADSORPTION RATE DATA

Fraction Number	Run Number	C_o, mg./liter	Time, min.	Absorbance	C_s, mg./liter	C^*, mg./liter	Solvent
63-4	K-10	96.0	480	1.50	86.4	9.6	8.0×10^{-4} N NaOH
			362	1.51	87.0	9.0	
			208	1.54	88.8	7.2	
			182	1.54	88.8	7.2	
			125	1.55	89.3	6.7	
			91	1.57	90.4	5.6	
			62	1.60	92.2	3.8	
			50	1.61	92.7	3.3	
			30	1.63	93.8	2.2	
			15	1.65	95.0	1.0	
			STD.	1.50	86.4		

[a]Agitation rate: 45 r.p.m. at 30°, all others at 4.5 r.p.m. and 15°.

APPENDIX VI

RELIABILITY OF RESULTS

The 95% confidence limits on the diffusion coefficient values are about $\pm$ 0.05 x 10^{-6} cm.^{2}/sec. except for those determined at very low concentrations. At concentrations of less than five fringes, the error limits at the 95% level are as high as 0.1 to 0.2 x 10^{-6} cm.^{2}/sec.

The molecular weight values at infinite dilution are good to about $\pm$ 4%.

The spectrophotometric analysis yields results which are reproducible to less than $\pm$ 2%. Since the amount of polymer adsorbed is calculated from the decrease in solution concentration, the error in $\underline{C}^*$ depends on the adsorption efficiency. Some of the equilibrium measurements taken at high initial polymer concentrations (greater than about 400 mg./liter) are only known to within about 6 mg./liter. For the rest of the equilibrium data and for all of the rate data the uncertainty in the adsorption values is only 1 to 2 mg./liter.

The initial rates can only be estimated to about $\pm$ 10%.

APPENDIX VII

ELECTRON MICROSCOPY

Samples were prepared for electron microscopy by soaking 0.13 g. of RD-101 fibers in 45 ml. of 200 mg./liter PEI solution at pH 10.9 for 24 hours. A similar sample was treated the same way omitting the polymer. After treatment both samples were dewatered and washed thoroughly with distilled water. The two samples were then treated with 0.1M cupric acetate for eight hours, filtered, and washed thoroughly with distilled water.

The samples were prepared for cross sectioning by first exchanging the occluded water with ethanol. The ethanol was replaced with butyl methacrylate with accelerator for the imbedding process. After the resin had cured, several cross sections were prepared by microtoming. These sections were approximately one-thirtieth of a micron thick. The butyl methacrylate was removed from the cross sections with chloroform and the remaining material was shadowed with palladium.

A representative micrograph of the PEI-treated sample is shown in Fig. 44. For comparison, Fig. 45 is a micrograph of the fibers which were not treated with PEI but were identical in all other respects. It is apparent that the PEI lessens the definition of the internal porous structure of the fiber. This effect can be observed across the entire section of the fiber.

The actual cause of the polymer-induced structure change is not clear at the present. One could conjecture that this observation is related to the ability of amines to act as swelling agents for cellulose. Many amines are more effective swelling agents than water. A more clear elucidation of this phenomena could contribute significantly to a better understanding of the wet-strengthening process.

Figure 44. Electron Micrograph of Cross Section from Wall of RD-101 Fiber Treated with PEI

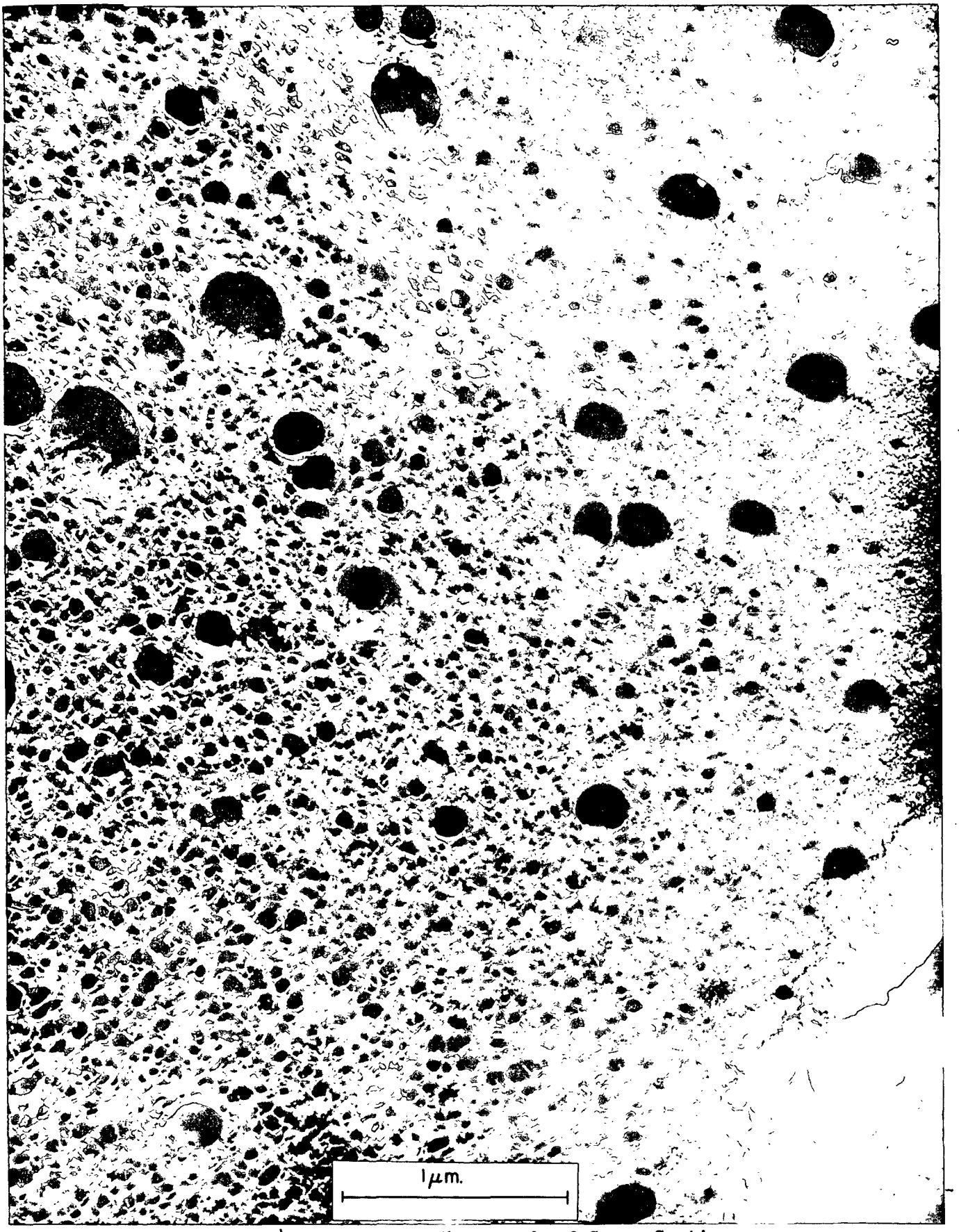

Figure 45. Electron Micrograph of Cross Section from Wall of Untreated RD-101 Fiber